DEPARTMENT OF THE ARMY
U.S. ARMY CHEMICAL AND BIOLOGICAL DEFENSE COMMAND
5232 FLEMING ROAD
ABERDEEN PROVING GROUND, MARYLAND 21010-5423

REPLY TO
ATTENTION OF

August 10, 1998

Freedom of Information and Privacy Act Office

Mr. John Greenewald, Jr.
[redacted]

Dear Mr. Greenewald:

In response to your June 4, 1998, Freedom of Information Act (FOIA) request, enclosed is a copy of "Test Report for Agent BZ Detonation Tests". This report has been reviewed and approved for release under the FOIA.

Fees in the amount of $25.50, incurred while processing this request, have been waived.

Sincerely,

Cheryl S. Fields

Cheryl S. Fields
Freedom of Information and Privacy Act Officer

Enclosure

REPORT NO. DRXTH-IS-CR-82128

ENGINEERING AND TECHNICAL SUPPORT OF AGENT BZ DISPOSAL

ARO Scientific Services Program TCN-81-220
Test Report For Agent BZ
Detonation Tests

B. D. Trott

BATTELLE
COLUMBUS LABORATORIES
505 KING AVENUE
COLUMBUS, OHIO 43201

JANUARY, 1982

FINAL REPORT

Prepared for:

U.S. ARMY TOXIC AND HAZARDOUS MATERIALS AGENCY
ABERDEEN PROVING GROUND, MARYLAND 21010

BZ

DISCLAIMER

The views, opinions and/or findings contained in this report are those of the authors and should not be construed as an official Department of the Army position, policy, or decision, unless so designated by other documents.

Unclassified

SECURITY CLASSIFICATION OF THIS PAGE (When Data Entered)

REPORT DOCUMENTATION PAGE

READ INSTRUCTIONS BEFORE COMPLETING FORM

1. REPORT NUMBER: DRXTH-IS-CR- 82128

2. GOVT ACCESSION NO.

3. RECIPIENT'S CATALOG NUMBER

4. TITLE (and Subtitle): Test Report for Agent BZ Detonation Tests

5. TYPE OF REPORT & PERIOD COVERED: Final Report June-Nov. 1981

6. PERFORMING ORG. REPORT NUMBER

7. AUTHOR(s): B. D. Trott

8. CONTRACT OR GRANT NUMBER(s): ARO Scientific Services Program TCN-81-220

9. PERFORMING ORGANIZATION NAME AND ADDRESS: Battelle Columbus Laboratories, 505 King Avenue, Columbus, Ohio 43201

10. PROGRAM ELEMENT, PROJECT, TASK AREA & WORK UNIT NUMBERS

11. CONTROLLING OFFICE NAME AND ADDRESS: U.S. Army Toxic & Hazardous Materials Agency, Aberdeen Proving Ground, Maryland 21010

12. REPORT DATE: January 22, 1982

13. NUMBER OF PAGES

14. MONITORING AGENCY NAME & ADDRESS (if different from Controlling Office)

15. SECURITY CLASS. (of this report): Unclassified

15a. DECLASSIFICATION/ DOWNGRADING SCHEDULE

16. DISTRIBUTION STATEMENT (of this Report)

Distribution limited to U.S. Government Agencies only because of test and evaluation, December, 1981. Other requests for this document must be referred to: Commander, USATHAMA, Attn: DRXTH-IS, APG, MD. 21010

17. DISTRIBUTION STATEMENT (of the abstract entered in Block 20, if different from Report)

18. SUPPLEMENTARY NOTES

19. KEY WORDS (Continue on reverse side if necessary and identify by block number)

Detonability Tests
Agent BZ
Pyrotechnics

20. ABSTRACT (Continue on reverse side if necessary and identify by block number)

BZ-Pyrotechnic mixture as it exists in the current U.S. Inventory of munitions was shown to be non-detonable at 22 C and at 80 C. The test configuration was an M138 BZ-Pyromix munition additionally confined by a 2.3 mm-wall close-fitting steel tube the full length of the munition. The 0.59-Kg donor charge was a full munition diameter composition C-4 charge. The tested munitions were drawn from 8 different manufacturing lots. Seven tests were conducted at ambient temperature and 7 after preheating to 80 C. Four of the ambient temperature tests were on munitions (continued)

DD FORM 1 JAN 73 1473 EDITION OF 1 NOV 65 IS OBSOLETE

Unclassified

SECURITY CLASSIFICATION OF THIS PAGE (When Data Entered)

20. Abstract

"inerted" by immersion in a water plus 0.01% Avirol-113 wetting agent. The BZ-pyrotechnic mixture was ignited in most tests, although one or more of the 0.1 meter long M7 canisters remained intact in half of the tests. (Four M7s are in each M138.)

The shock wave travelling down the length of the munition was monitored in real time by a resistance probe technique. There was no significant difference in the observed shock velocity decay between ambient live, ambient inerted, preheated live, and a special test on a mockup containing no reactive ingredients. These results, together with the recovery of intact portions of the munitions in many tests, are conclusive evidence for non-detonability of the munitions.

SUMMARY

The U.S. Army Toxic and Hazardous Materials Agency is preparing to demilitarize the U.S. inventory of agent BZ-filled munitions. As employed in the munitions, BZ is blended with an energetic pyrotechnic mixture. In normal functioning, this mixture is ignited along central core holes in the munitions and reacts over a few tens of seconds to produce an aerosol cloud of BZ. However, upper limit theoretical calculations suggested that this mixture could potentially be detonable. To facilitate selection from among the five candidate demilitarization concepts it was desirable that the detonability of the munitions be established. To this end, a series of experimental tests was conducted. These tests gave conclusive evidence of non-detonability.

The potentially most detonable item in the BZ inventory was selected for detonability tests. This is the bomblet with the largest continuous diameter, 72 mm of BZ-pyrotechnic mix, the M138. This bomblet also has the thickest steel walls, ~ 3 mm, for radial confinement. An individual M138 bomblet is one of 57 packed in each M43 cluster munition. As such, adjacent M138s in the close-packed array could provide an additional 3-mm steel radial confinement along 6 line contacts with the M138. Therefore, the M138, fitted inside an additional close-fitting steel tube with 2.3 mm wall thickness (nearest to 3 mm thickness available), was selected as the configuration for detonability tests. Proof of non-detonability of this item would constitute proof of non-detonability of the entire BZ-containing munition inventory.

The test configuration included a full munition diameter donor explosive charge of composition C-4 in firm contact with one end of the munition. The primary indication of detonability was from dynamic instrumentation, epoxy potted into the entire length of the core hole, which showed the steady decay of the input shock velocity to sonic values as the shock progressed down the munition. Examination of the munition remains provided a secondary indication.

The tests were conducted in a sealed blast containment chamber inside an igloo at Pine Bluff Arsenal. A pilot plant incinerator, previously qualified for destruction of BZ, was used to dispose of the BZ released during the tests.

Of 17 tests attempted, 14 tests provided detonability data. In two tests the munitions self-ignited during heating to the original target preheat temperature of 105 C. This self-ignition resulted in lowering the preheat temperature to 80 C on remaining tests. Data from the third test were lost due to an equipment malfunction. To provide the broadest possible sampling base, the tested munitions were drawn from all of the eight manufacturing lots from which M138s had been downloaded from the original M43 cluster configuration. These lots were judged to be reasonably representative of the total inventory on the basis of available lot characterization data. Seven tests were conducted at ambient temperature and seven were conducted after preheating the munitions to 80 C. Four of the ambient temperature tests were conducted on munitions "inerted" by immersion in a water-plus 0.01% Avirol-113 wetting agent. The BZ-pyrotechnic mixture was ignited by the shock wave in most tests, although one or more of the 0.1-m M7 canisters remained intact in half of the tests.

There was no significant difference in the observed shock decay between inerted, ambient live, and preheated live munitions. The average shock wave travel, above the apparent sonic velocity of 2.0 mm/microsec, was 115.1 ±8.5 mm through the munitions for all tests. A shock travel of 130 mm above 2.0 mm/microsec was observed in a similiar detonability test on a mockup which contained no reactive ingredients. These results, together with the recovery of intact portions of the munitions in many tests, are conclusive evidence for non-detonability of the munitions.

ACKNOWLEDGEMENTS

This program was conducted under the able direction of the USATHAMA project manager for BZ demilitarization, Mr. Richard Roux, with assistance from Mr. Edward Meseke. Their support and insistance on the achievement of high technical standards are gratefully acknowledged. A large number of people contributed to the successful conduct of the detonability tests. The specialized apparatus used in these tests was designed, constructed and proof-tested at Battelle Columbus Laboratories prior to shipment to Pine Bluff Arsenal where the tests were conducted. The contributions of the following members of the Battelle staff are acknowledged in the areas noted.

Overall Program Management	Wayne E. Ballantyne
BZ Incinerator, Afterburner	Albert E. Weller David R. Hopper
Proof Tests of Blast Containment Sphere	William F. Schola
Installation at Pine Bluff Arsenal	David R. Hopper
Qualification of Potting Resins	Eugene J. Mezey
Construction of Detonation Probes	Harvey N. Ebersole
Operation of the Detonation Tests Data Acquisition System	Harvey N. Ebersole David W. Carpenter
Reduction of the Detonability Data	Harvey N. Ebersole

The test director at Pine Bluff Arsenal was Mr. James C. Stuart who had overall responsibility for the tests at Pine Bluff Arsenal. He was responsible for the igloo modifications including the ventilation and cooling systems, power and utilities supplies, the line for input of materials, and change-house for personnel. He arranged all logistic support and staffing for the tests, wrote the Standing Operating Procedures and secured local approvals for them, and personally supervised all the operations of the testing proper, including assurance of testing the correct munition lot numbers and other innumerable details. He was assisted by several members of the Pine Bluff Arsenal staff. The contributions of Mr. Huey Desoto in the area of electrical controls and instrumentation, and of Mr. Floyd Hickerson and Alvin Wooten in leading and directing the technicians who conducted the munition preparations and performed the testing inside the igloo are particularly acknowledged.

TABLE OF CONTENTS

LIST OF TABLES

LIST OF FIGURES

LIST OF FIGURES (Continued)

LIST OF FIGURES (Continued)

LIST OF FIGURES (Continued)

FINAL REPORT

on

ARO SCIENTIFIC SERVICES PROGRAM TCN-81-220

TEST REPORT FOR AGENT BZ DETONATION TESTS

to

DEPARTMENT OF THE ARMY

TOXIC AND HAZARDOUS MATERIALS AGENCY

BATTELLE

Columbus Laboratories

January 18, 1982

1. INTRODUCTION

The U.S. Army Toxic and Hazardous Materials Agency is preparing for demilitarization of the current U.S. inventory of munitions containing the incapacitating agent BZ. The agent BZ is blended with a pyrotechnic mixture in the munition inventory. These munitions normally function in a manner similar to the familiar smoke grenades, producing a fine aerosol smoke of BZ agent. However, it was not known whether the BZ-pyromix containing 50% BZ, 23% $KClO_3$, 9% S, and 18% $NaHCO_3$ could detonate.

Five major system concepts have been proposed for demilitarizing the BZ item/munition inventory[1]. Selection from among these concepts and details of the plant design can more confidently be determined if the detonable characteristics of the BZ munitions are established. Proven non-detonability of the BZ munitions is expected to lead to major savings in full-scale plant equipment and operating costs. This report documents a series of tests conducted to determine the detonability of the BZ munition inventory.

The body of the report is organized into four major sections following this introduction. Section 2 describes the technical approach, the background for selection of the detonability test configuration, the basis for selection of test conditions, and the basis for interpretation of the results obtained. Section 3 describes the specialized experimental apparatus used for these tests. Section 4 presents the experimental procedures used and the results obtained. Section 5 lists conclusions and recommendations.

2. TECHNICAL APPROACH

2.1 Background

The process of detonation can be conceptualized as a supersonic compressive shock wave driven through a reactive material by the energy released in the Chapman-Jouguet (C-J) reaction zone immediately behind the shock wave. The adiabatic heating associated with the shock compression of the material triggers the chemical reaction(s) responsible for the energy release. Immediately behind the shock wave, the particle or mass velocity is in the same direction as the shock wave velocity. The mass velocity, pressure, and internal energy decay behind the shock wave front. The energy released behind the shock wave front can contribute to driving the shock front only in the zone in which the energy transfer speed (the sum of the local sonic velocity plus the mass velocity) is equal to or greater than the shock velocity. As the mass velocity, pressure, and temperature decay behind the shock front, a limiting boundary is reached where the energy transfer speed drops below the shock velocity. The shock wave and this boundary define the C-J reaction zone. Chemical reaction may continue behind this boundary and can contribute to the total energy released during explosion but cannot influence the detonation (or shock wave) velocity. In a uniform charge of constant cross sectional area and confinement along its length, a steady detonation velocity is normally achieved in which the energy released in the reaction zone is equal to the energy required to drive the shock wave (the energy required to shock compress the unreacted material).

However, at the lateral surfaces of the charge, the energy released in the reaction zone may also be expended in the production of lateral mass velocity components and resultant lateral expansion of the charge. This energy is lost for the

purpose of driving the detonation front, but must be included in the energy balance which determines the detonation velocity. Because the ratio of lateral surface area to reaction zone volume increases as the charge diameter decreases, the fraction of energy lost laterally increases with decreasing charge diameter. This effect leads to a decreasing detonation velocity with charge diameter because the energy required to drive the shock front decreases with shock velocity. With decreasing shock velocity, the shock pressure and induced temperature rise also decrease. These decreases lead, in turn, to a generally exponential rate of decrease in chemical reaction rate. The detonation velocity does not decrease below a certain level which depends on the detailed characterics of the reactive material. Instead, a minimum diameter (the critical diameter) is reached below which a sustained detonation is not possible.

Because the critical diameter arises due to lateral energy losses from the reaction zone, the critical diameter of a given reactive material also depends on the lateral confinement of the charge. Thus the critical diameter for a charge inside a confinement tube is less, perhaps much less, than for an unconfined charge.

In sufficiently large charge diameters, many energetic materials such as gun and rocket propellants can be detonated. These materials are not commonly referred to as detonable materials because their critical diameters for a sustained detonation are simply larger than are normally prepared and/or no sufficiently large initiating shocks (in magnitude and cross-sectional area) are available to start the detonation process.

2.2 Selection of Test Configuration

The determination of the detonability of the material of interest here, i.e. BZ-pyromix, from a practical viewpoint need not be an absolute determination, but rather a determination of detonability under the combined conditions of maximum existing charge diameter and lateral confinement. For this purpose, three munition configurations were of primary interest, the M16, the M138 and the M43. (For descriptions of the munitions used in these experiments and others referred to in this report, see Appendix A.) In the M16, the 42 individual canisters (M6s) are not arranged in a close-packed array as are the M138s in the M43. Hence, any proof of non-detonability of the M43 cluster would automatically include the M16 as a subset.

The array of 19 M138 bomblets through a cross-section of an M43 cluster might be considered to form an equivalent diameter larger than a single M138 from the standpoint of critical diameter for detonation. However, a deflagration-to-detonation transition (DDT) must occur over a diameter at least equal to the critical diameter to develop a self-sustaining detonation. Thus, if the critical diameter is greater than the diameter of a single M138, but smaller than an M43, a DDT must occur simultaneously in three or more contiguous M138s. A DDT in a single M138, being below the critical diameter, could not occur and an induced detonation wave in a single M138 would be quenched. The likelihood of a DDT occurring simultaneously across the junctures of the M138s so that the resultant detonation wave was contiguous across the junctures of the M138s appears negligibly small under any conceivable real circumstances during demilitarization. Hence, we believe that proof of the critical diameter for detonation of BZ-pyromix being greater than that of a single M138, as confined inside an M43, is sufficient to support an assessment of non-detonability for all of the BZ munitions.

An M138 inside an M43 is confined around its perimeter by line contacts with six adjacent M138s along its length. The combined wall thickness of the M138 case and contained M7 canister cases approximates 3 mm of steel. Hence, a test of an M138 contained inside a steel tube with a 3.2-mm wall thickness would provide an over-test of the confinement provided by the adjacent M138s in an M43 cluster. Thus the munition selected for detonability tests was a single M138 housed inside a close-fitting steel tube with a 2.3-mm wall thickness (the nearest standard size to 3 mm).

From the standpoint of theoretical predictions of detonability, the maximum possible energy release from the reaction of the BZ-pyromix can be calculated with the aid of thermo-chemical data. This value of energy release can be equated to the energy required to drive a shock wave through the unreacted material. This latter value may be calculated as a function of the shock velocity and pressure with aid of Hugoniot equations of state (pressure, volume, internal energy relations) for the unreacted materials. By ignoring lateral energy losses, the problem is simplified and becomes equivalent to mocking up very large or well confined charges. A calculational scheme based on the above premises has been built into a code called TIGER.

It should be noted that this calculation cannot predict whether detonation will or can occur because it cannot be predicted at present whether the hypothesized

reactions will occur, or whether they can occur rapidly enough to take place within the C-J reaction zone. What this calculation can do is predict a theoretical upper limit for the detonation velocity and pressure within the uncertainty of knowledge of the required inputs to the code calculation. The TIGER code was run for the BZ-pyromix composition by Robert Gentner of ARRADCOM[2], Dover Site. The theoretically predicted detonation velocity was 3.3 mm/microsec at a pressure of about 2.5 GPa (25 kbar).

Thus for detonability testing, a donor charge which provides a shock velocity (and pressure) input to a confined M138 over its entire cross sectional area in excess of the predicted upper limit sustained detonation velocity (and pressure) is all that is required. In the absence of a detonation, the input shock would be expected to decay along the length of the M138. The shock pressure would decay from the initial high input pressure from the donor charge to very low levels. Accompanying the pressure decay, the shock velocity would decay from high initial values > 5 mm/microsec down to the sonic velocity in BZ-pyromix. There does not appear to be any sonic velocity data available for BZ-pyromix. However, based on comparisons with other materials it seems unlikely that the sonic velocity will exceed 2.3 mm/microsec, and may be appreciably lower.

2.3 Basis for Interpretation of Results

Historically, and commonly, the occurrence of a detonation is signalled by the perforation of a steel witness plate in close proximity to the charge[3]. However, in the case of BZ-pyromix, the predicted upper limit detonation parameters are sufficiently low that such perforation might not occur even in the presence of a detonation. Instead, a dual basis for the test interpretation was developed. One relies on instrumentation in the core hole to measure the shock front position with time (and hence shock velocity by differentiation) along the length of the M138. The other relies on visual observation of the remaining metal parts after the test. In the event of failure of the real time instrumentation or as confirmation, a post-test examination which shows major parts of the M138 remaining intact, or broken into fairly large pieces, constitutes evidence for non-detonation. A measured sustained shock velocity in the M138 near 3 mm/microsec coupled with fragmentation of the metal parts would constitute evidence for detonation. On the other hand, a decaying shock velocity to

2.3 mm/microsec which remains below this value together with some metal parts remaining intact, or only fractured in relatively large pieces, would constitute a non-detonation. In this context, "relatively large" pieces means fragments approximate to the length of an M7 canister and wide enough to span about one-half the M138 circumference.

2.4 Test Conditions and Lot Selection

Processes being evaluated for application to the demilitarization of the BZ munition inventory involve handling of the munitions in both inventory condition and after inerting by submersion in an inerting liquid. Destruction is expected to occur by burning off the BZ-pyromix in a heating chamber or rotary kiln, with subsequent incineration of the evolved BZ vapor or aerosol. Thus it is desirable to obtain data on the detonability of munitions at ambient temperatures in (1) the inventory condition, (2) after short (5-minute) inerting liquid submersion, and (3) after normal (2-hour) inerting liquid submersion, for a plant design to withstand detonation effects, if shown to be necessary. Since heating of munitions is also contemplated, it is desirable to obtain detonability data on preheated munitions as an aid in assessing the requirements for the heating-functioning furnace or kiln.

Bomblets which had been downloaded from M43s were available for testing from several different lots of production. Production testing showed the burning (normal functioning) rates to vary appreciably from lot to lot. Although there is no known correlation between detonability and burning rate in the normal functioning mode, the burning rate data seemed likely to be the most significant data available. Thus M138 munitions were selected for test from all available lots, but with replications of the fastest burning and near the slowest burning time munitions available. The numerical values of this parameter are reported in Section 4.1 on test conditions and lot selection.

3. EXPERIMENTAL APPARATUS

To conduct the planned series of detonability tests, two major items of equipment were required:

- An explosive and gas containment vessel capable of containing the detonation of at least 3.3 lb TNT-equivalent high explosive and retaining the gases and aerosol without significant leakage
- A vapor incinerator, afterburner, and water quench system capable of reducing the BZ content and temperature of gases resulting from the detonability tests to a level allowable for discharge into the igloo environment.

The vapor incinerator, afterburner, and water quench system was constructed to obtain preliminary plant design information as well as to destroy the BZ vapor/aerosol generated during these tests. The incinerator system was extensively tested and qualified for the destruction of BZ prior to the conduct of these tests. It has been described in detail elsewhere.[4]

3.1 Blast Containment Sphere

The blast containment vessel was modified from a previously constructed, 1.07-m- diameter spherical chamber with an average wall thickness of 22.9 mm. As originally constructed and qualified for blast containment, the chamber design included a single large port with a captive door inside which overlapped the inside of the port reinforcing ring over the full circumference. This design provided a good blast seal but was never intended to be gas tight. In this configuration, other vessels of the same design demonstrated the capability to contain the blast from 4.54 Kg of composition C-4 on a repetitive basis and 9.08 Kg in a single trial[5]. For this application, the original port reinforcing ring and door were replaced by an O-ring-sealed door externally mounted and secured by a double row of bolts. This port design was patterned after similar closures which had been qualified for blast containment at Los Alamos National Laboratory. Additional penetrations were a high-pressure, 28-pin electrical lead-through manufactured by D.G. O'Brien, incorporated for heater and instrumentation connections, and two Swagelok® high voltage lead-throughs for the exploding bridgewire detonators. Piping connections for the pressure transducer and for gas purging were made through the door. After modification, the sphere was requalified by the test firing of a 1.82 Kg spherical composition C-4 test charge, as well as static gas pressure tests at 2.27 MPa. These tests are described in detail in a previous report[6].

3.2 Fragment Restraint Assembly

Figure 1 shows a schematic of a hot detonability test assembly arranged inside the containment sphere. To provide protection for the sphere interior from fragment damage, a 0.46-m-length of 0.41-m O.D. pipe with near 25.4-mm wall thickness was hung, as shown, on the sphere horizontal centerline. This pipe was specially constructed of high toughness steel alloy. It was fitted with a replaceable, mild steel liner rolled from 9.61-mm-thickness plate. The pipe provided the structural strength to absorb the fragment momentum while the liner absorbed the fragment craters. About midway through the test series, the liner was replaced to prevent penetration of the accumulated fragment craters through the liner. This was a planned operation.

3.3 Detonability Assemblies

Inside the fragment restraint pipe, the detonability assembly was supported on the sphere centerline by a steel tubing and sheet metal cradle. The assembly shown schematically in Figure 1 is for a preheated detonability test. At the heart of the assembly is a specially instrumented M138 bomblet which is described in the following section (Section 3.4). The bomblet is secured inside a 13-gage steel tube over its full length to provide the desired additional confinement. This tube in turn was fitted with fiberglass-insulated electrical heating tapes. Two separate heaters were provided, a main heater and an end compensating heater. The end heater, only 25.4 mm long, served to compensate for the additional heat losses at the end of the munition. Each heater was controlled by a thermocouple, hard-soldered to the confinement tube. The two control thermocouples were connected to strip chart recorder-controllers. The heaters were powered through variable autotransformers which were adjusted during heating to maintain the center and end thermocouple at near the same temperature and to maintain good temperature control once the heating jacket reached the desired temperature.

The 1.3-lb composition C-4 donor charge was designed to provide a charge length at full diameter equal to the charge diameter plus a conical lead-in to insure near-planar, axial symmetry of the detonation shock entering the munition. For the pre-heated tests, it was supported inside a fiberglass-reinforced silicone plastic tube,

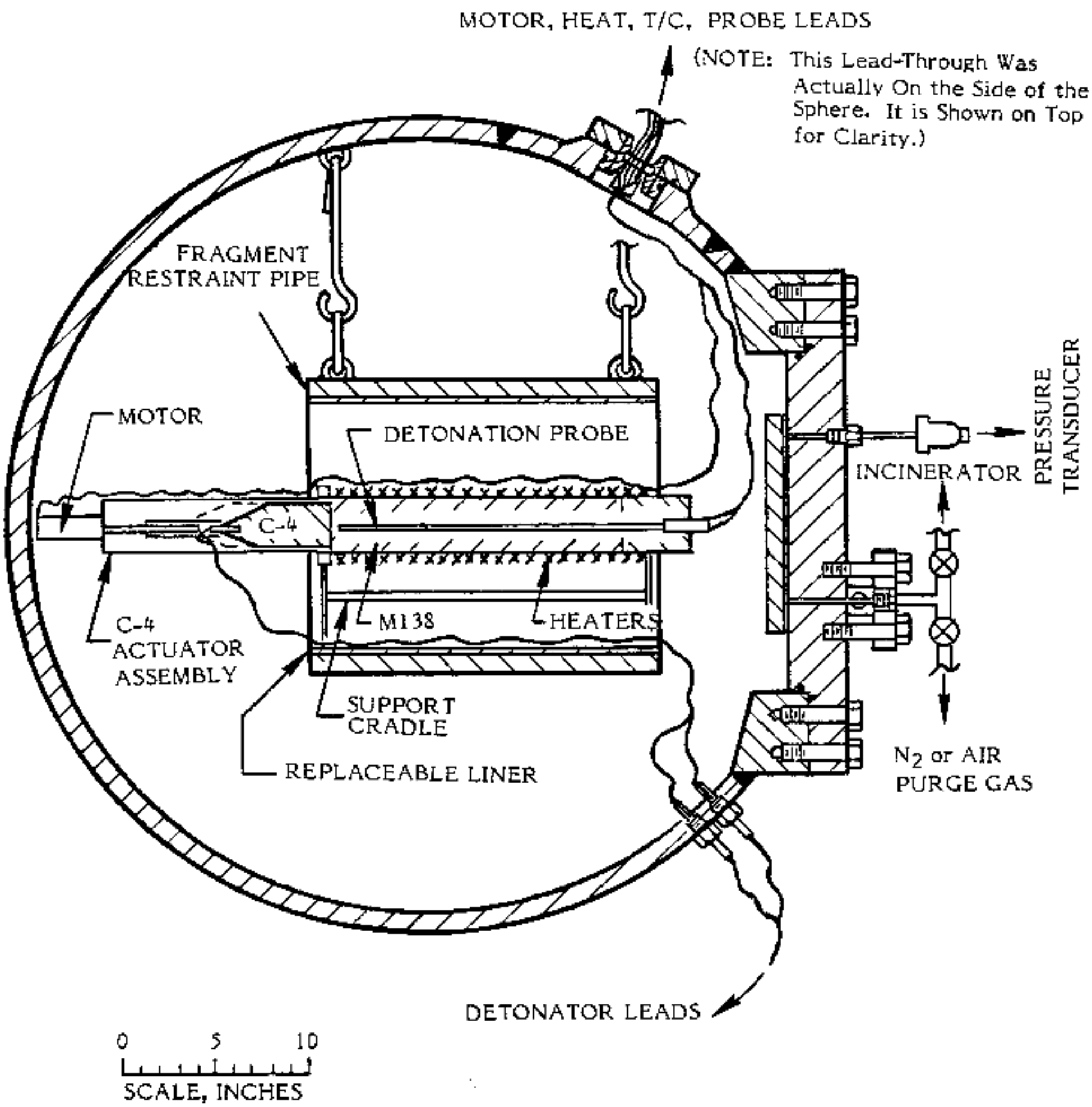

FIGURE 1. SPHERE ASSEMBLY

separated from the M138 by a 51-mm air space during heating to minimize preheating of the C-4. After the desired preheat, a specially-designed electric gearmotor actuator moved the charge into firm contact with the M138 just before detonation. The C-4 charge was contained inside a 0.20- to 0.46-mm thick vacu-formed PVC container. This container was supported by a strong, wooden mold during packing of the C-4 plastic explosive to allow the production of a fully densified charge of the correct dimensions. After packing, the thin plastic container provided sufficient support to allow easy handling of the explosive charge.

The C-4 charge was detonated by an RP-83 exploding bridgewire detonator. This detonation was selected to provide safety from stray electrical currents during loading operations. The exploding bridgewires were fired by a Model FS-10 firing unit manufactured by Reynolds Products, Inc.

The confinement tube for the unheated M138 munitions was identical to that for the heated munitions. For these tests, the composition C-4 charges were secured in firm contact with the munitions by the force of several strong rubber bands between the M138 and a specially shaped, wooden block across the base of the C-4 charge.

3.4 Instrumented M138 Assembly

The M138 itself was fitted with a special detonation probe assembly inserted into the core hole of the munition. Figure 2 shows the detonation probe assembly. As shown, the assembly was comprised of two 28 ga type K (Chromel-Alumel) thermocouples and two detonation probes potted inside a low-density polyethylene tube. The header assembly served to protect the otherwise extremely fragile connection between the detonation probes and the coaxial cables used to connect the probes to the exterior instrumentation.

Two detonation probes were used in each assembly to provide redundant information on the position of the shock front (Figure 2). Each probe was comprised of a 0.51-mm-diameter aluminum tube (0.038-mm wall thickness) containing an 0.025-mm-diameter Moleculloy® resistance wire (0.33 ohms/mm resistance). The resistance wire was insulated by skip-wound nylon. The resistance wire was soldered to the aluminum tube at one end and connected to the center wire of the coaxial signal cable at the other. The aluminum tube was connected to the coaxial cable shield.

In operation, a high pressure shock wave travelling up the M138 and probe from the originally shorted end progressively shorted out more of the resistance wire by crushing the aluminum tubing against the wire. Of course, if the pressure in the shock wave dropped below that required to crush the tube, the probe would cease to provide position data; at pressure levels near the threshold, the crushing of the tube could be expected to be somewhat erratic. The circuitry associated with each probe consisted of a battery-powered, constant current source and a high-impedance measurement of the variation in voltage across the probe with time. With appropriate calibrations, the measured voltage could be related to the position of the shock front (as described in detail in Appendix B). The constant current supply was adjusted to provide ~ 74 MA through the probe resistance of ~ 121 ohms, giving an initial voltage ~ 9V. This represents a power dissipation of ~ 2/3 Watt so that neglible heating was produced by the probe exitation current.

The probe voltages were recorded using a digital processing oscilloscope manufactured by T. G. Branden, Inc. The data reduction steps described in Appendix B were carried out with the aid of a pre-recorded data reduction program within the oscilloscope. The plots shown in this report were produced semi-automatically directly from the processed data by a direct-connected digital plotter.

The detonation probe assemblies for the ambient temperature tests were identical to those shown in Figure 2 except the thermocouples were not installed.

The detonation probe assemblies used represent a re-design of a previous probe which had an outside diameter of 9.5 mm. This diameter had proved to be too large to insert into the M138 core holes without interference with the starter mix. To insure that no interference would be encountered during assembly of the 6.35-mm probes into the M138 munition, each core hole was optically gaged with the aid of a small (2 mW) He-Ne laser fitted with a beam expander which provided a 12-mm diameter parallel light beam. If the light beam was unobstructed over a 6.35-mm diameter after passing through the core hole of the munition, the probe could be safely inserted. This optical gaging technique showed that all munitions were safe to insert the 6.35-mm probe.

One detonation probe assembly was potted inside the core-hole of each M138 bomblet tested. To do this, the core hole opposite the fuze end was sealed with tape and the bottom M7 canister sealed with epoxy putty, after bending out the retaining tabs on the M138 case. The core hole was filled with a low viscosity epoxy

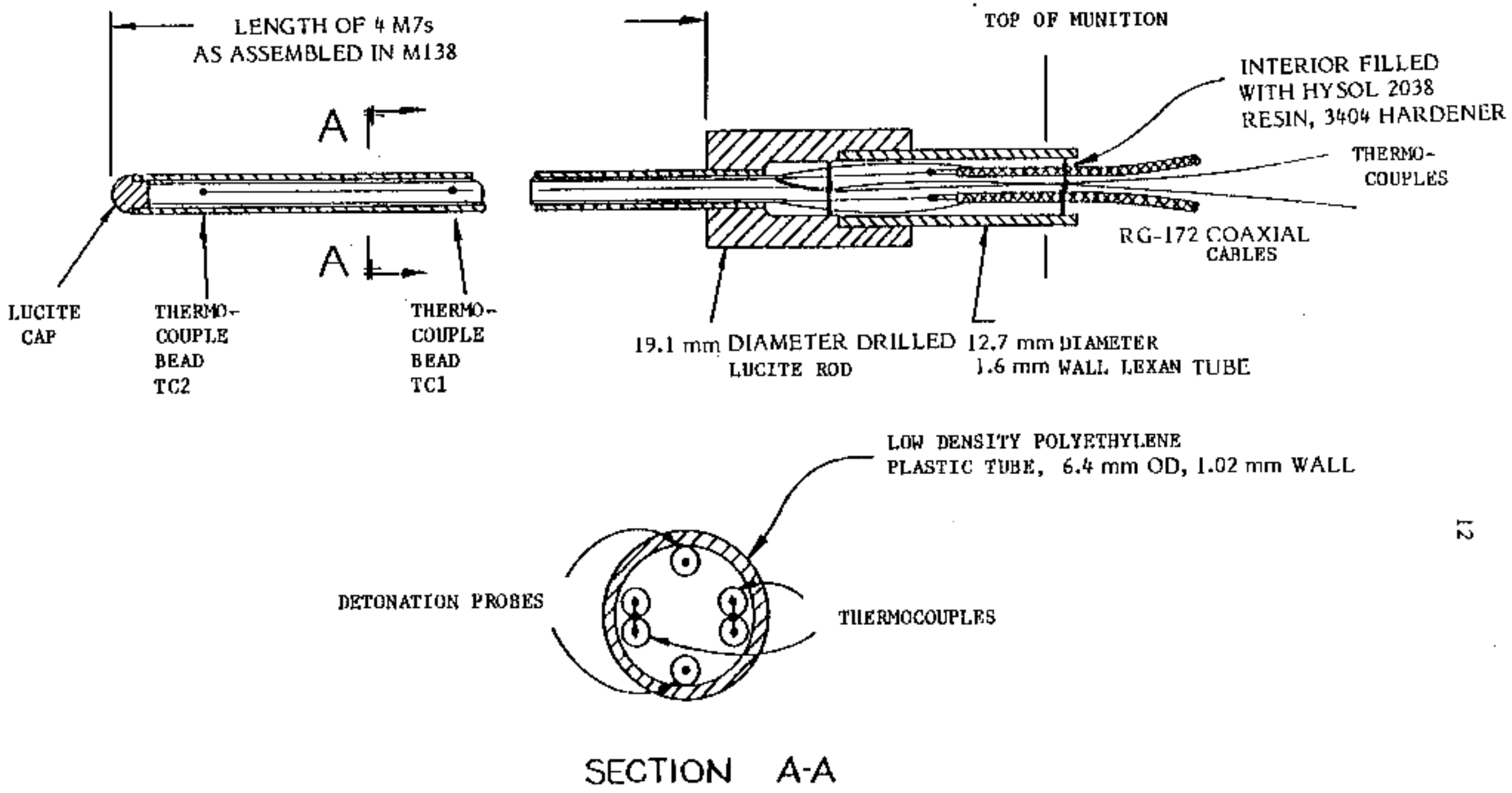

FIGURE 2. DETONATION PROBE ASSEMBLY

resin (Hysol® resin R8-2038 with HD-3404 hardner) and the detonation probe assembly inserted through the fuze opening of the bomblet all the way to the tape. Thus the active end of the actual detonation probes were approximately 1/4-inch, or 6.3 mm, from the end of the bottom M7 canister. No correction for this 6 mm difference was applied in the calculated shock positions which are reported on the basis of shock progress along the detonation probes.

Following insertion of the probe assembly, which submerged the probe header assembly into the M138 fuze cavity, the fuze cavity was filled with another epoxy potting compound (Hysol® C8-4143 resin with HD-3404 hardener) to the top of the fuze well. This resin contained 50% silica filler to reduce shrinkage during curing. Both epoxy resins were checked for temperature rise during curing in the configurations used and found to be satisfactory. The munition was maintained in a vertical position until all the epoxy potting had cured. The resultant instrumented M138 was mechanically quite strong to allow handling and installation into the blast containment sphere for testing. All instrumentation and heater leads were pre-connected and potted into a large, 28-pin plug which mated with the lead-through mounted in the blast containment wall. The motor actuator leads were also pre-connected to and potted into the multi-pin connector plug. They were fitted with a separate in-line plug-together connector which allowed connection of the motor after final assembly of the complete test item. Thus it was possible for operating personnel in Level B protective clothing (gas masks, rubber aprons, boots and gloves) to assemble and install these highly instrumented assemblies into the blast containment sphere without recourse to soldering operations.

It should be noted that the coaxial cables used for the detonation probe leads had connections at the probe end and at the plug end which were entirely sealed by immersion in expoxy potting. In addition, the plug O-ring sealed into the containment lead-through socket. Thus the entire probe circuits were protected from the immediate short-circuiting effects of the high pressure, ionized air-shock wave generated by detonation of the C-4 charge. Calculations showed that this shock wave could pass over the probe circuits prior to completion of passage of the shock wave through the M138 munition. This precaution insured against premature loss of the detonation probe signal from this source.

Another result of installation of the detonation probe assembly was to provide additional lateral confinement of the M138 by preventing the free expansion of

the reaction products into the core hole, which would normally occur with inventory munitions. This provided an additional degree of overtest which was necessitated by the requirement to provide a continuous shock path through solid material from the BZ-pyromix fill to the detonation probes.

3.5 Electronic Data Acquistion Apparatus

A block diagram of the apparatus used for gathering the sphere pressure and detonation probe data is shown in Figure 3, together with the detonator firing circuit. In operation, the shot was fired by a push button on the FS-10 firing unit. This unit, through the firing module, produced the fast-rising high voltage (4300 V) pulse needed to fire the exploding bridgewire detonator, Reynold's RP-83. At the same time the firing pulse was initiated, a 30-V pulse was generated which served as a trigger signal for the fast data acquisition system.

The fast data acquisition system was comprised of two major parts, the detonation probe and pressure-signal processing subsystems. The detonation probe subsystem consisted of two individual, adjustable, constant current power supplies from which a voltage proportional to the remaining probe resistance was derived. This voltage was recorded for both probes by a Physical Data Inc. Model 523-A2 two-channel transient waveform recorder. This unit provided 4096 digital samples for each channel at 0.1 microsec per sample. After temporary digital storage in the unit, it was subsequently transferred in analog form to the Smartscope® where it was re-digitized and subsequently processed to provide position and velocity versus time information from the probes, as described in Appendix B. The plots shown in this report were generated directly on the Smartscope plotter.

The internal pressure in the sphere was monitored by a Viatran Model 108 pressure transducer which includes an internal shunt calibrating circuit. Pressure data was output as a 5 VDC full scale signal to the Smartscope where it was sampled over a 10-sec period with 1-msec resolution. The appropriate calibrations were input to Smartscope so that its digital plotter produced the pressure time records given in this report.

Temperature data from the two control thermocouples were individually recorded on two Honeywell controlling strip chart recorders which provided a permanent record of the heating histories. Each controlled heater was supplied

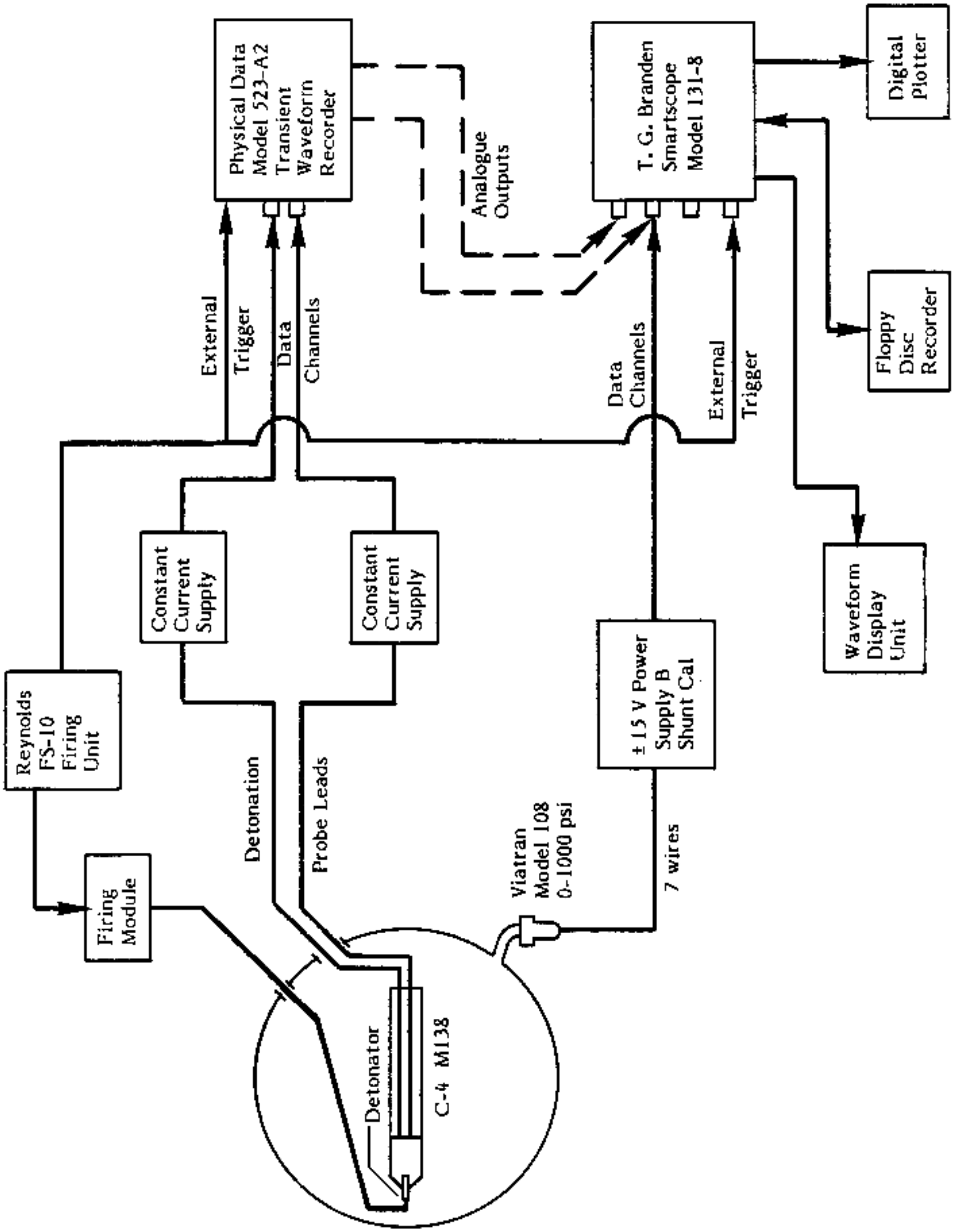

FIGURE 3. DATA ACQUISITION SYSTEM FOR THE DETONATION PROBES AND SPHERE INTERNAL PRESSURE

through a variable autotransformer which allowed adjustment of the power input level to balance the heating rates of the main and end compensating heaters and to obtain good temperature control once the desired temperature was reached. Power levels typically varied from near full power for the main heater to about 55% for the end compensating heater during heating, and somewhat lower levels during the soak period.

The temperature data from the two core thermocouples was recorded for some shots on a Gould multipoint recorder. An instrument failure during the tests required that the core thermocouple data be recorded manually from a digital temperature indicating device for these tests.

4. EXPERIMENTAL PROCEDURES AND RESULTS

The detonability tests were conducted in Igloo 64-250 at Pine Bluff Arsenal, Pine Bluff, Arkansas, under the local supervision of Mr. James Stuart who ably served as the on-site test director and arranged for logistical support of the tests. After initial training, all munition preparations and test operations inside the igloo were conducted by technicians from Pine Bluff Arsenal. Explosive charge preparation, and all handling operations involving explosive and detonators, were performed by members of the 52nd E.O.D. Detachment at Pine Bluff Arsenal.

4.1 Test Conditions and Lot Selection

As described in the technical approach, munitions were selected from all available downloaded lots to provide as broad a sampling base as possible. In addition, where duplicate tests were possible, they were grouped at the extremes of low and high burning times. Testing was planned to include seven ambient temperature tests, followed by up to 10 preheated tests and up to three final ambient temperature tests. However, because it was agreed that the preheated tests were more likely to show detonability, it was decided that if no detonations were observed at completion of the preheated test series, the remaining three ambient temperature tests would be abandoned.

Table 1 shows the test sequence actually followed. As shown, the tests were in four groups. The first two tests were conducted on "inerted" M138 munitions. Inerting was done by immersion in a vertical position in water with 0.01% Avirol-113

Table 1. Test Variables for M138 Detonability Tests

Test No.	Munition Lot No. 1021-	Burning[a] Time Secs.	Test Conditions	
			Preparation	Temperature C
D1	35-153	31.2	inerted	ambient
D2	44-1123	17.0	inerted	ambient
D3	35-153	31.2	short inerted	ambient
D4	44-1123	17.0	short inerted	ambient
D5	35-153	31.2	live inventory	ambient
D6	41-187	26.5	live inventory	ambient
D7	44-1123	17.0	live inventory	ambient
D8	35-153	31.2	live inventory	intended 105[b]
D9	41-1113	30.7	live inventory	intended 105[b]
D10	35-153	31.2	live inventory	74
D11	41-187	26.5	live inventory	81
D12	41-1103	23.3	live inventory	81
D13	36-160	22.5	live inventory	82
D14	44-1123	17.0	live inventory	84
D15	36-181	28.0	live inventory	81
D16	36-157	21.0	live inventory	81
D17	41-1113	30.7	live inventory	80

(a) Of all M43s produced, the shortest burn time measured was 15.3 sec. Only 5 lots had burn times less than 17.0 sec. Some production lots burned considerably slower than the slowest lot available for these tests; five lots had burn times greater than 40 sec.

(b) Munition functioned during heating.

(a wetting agent) added for 2 hours. The sealing tapes were removed manually from the ends of the core holes before immersion. After inerting, the munitions were allowed to drain overnight in a vertical position, before potting the instrumentation into the core hole.

The short inerting on the second two munitions was done the same as for the inerted munitions except the immersion time was 5 minutes.

The third group of three munitions were tested in the inventory condition. All three of these groups were tested at ambient temperature (~ 27 C).

The fourth group of ten munitions was tested in a preheated condition. As shown in Table 1, it was intended to preheat the munitions to a temperature of 105 C. This temperature was chosen to provide a 5 C margin of safety over tests with an inert simulant which caused extrusion of the fill[7]. The preheating protocol was to heat the outer shell to the desired test temperature then maintain this shell temperature until the core temperature reached the approximate shell temperature. During heating of test D8, the BZ-pyromix ignited after the heater shell had been at 106-107 C for 58 minutes and the core thermocouples were indicating 75-77 C. No previous ignition of starter mix or BZ-pyromix at this low temperature had been observed. Hence a second attempt to preheat to 105 C was made in test D9. Again, ignition occurred before the test temperature was reached. This time ignition occurred 74 minutes after the outer shell reached 105-106 C and at an indicated core temperature of 88 C. Ignition of the pyromix caused the Composition C-4 to burn as well, so that no safety problem occurred. No detonability data were obtained from these two tests and it was decided to reduce the test temperature to 80 C.

Table 2 shows the thermal histories of the preheated tests. When the outer shell temperature was restricted to 80 C, the heating time was too long to allow the core to reach 80 C. Thus test D10 was fired at a core temperature of 74 C after heating for 2.4 hours after the shell reached 80 C.

In subsequent tests, the shell temperature was raised to 90-93 C to provide an increased thermal gradient to drive the core temperature up to 80 C. Slightly before the test, the shell temperature was allowed to cool to near 80 C, so that near isothermal conditions were established.

In test D11, the actuator motor to move the Composition C-4 donor charge into contact with the M138 was found to be jammed in an attempt to operate the motor after preheating. Due to possible safety problems in handling a previously preheated device, the donor charge was fired, aborting test D11.

Table 2. Preheated Test Thermal Histories

Test No.	Shell					Core Final	
	Main		End				
	Time min	Hold Temp C	Time min	Hold Temp C	Main Temp C	End Temp C	Total Time min
D8	21	106	21	107	75	77	79[a]
D9	21	105	19	106	88	-	94[a]
D10	14	80	14	80	74	-	158
D11	18	92	14	91			
	51	83	51	83			
	65	78	65	82			
	78	91	80	91			
	118	Cooling	125	Cooling		80	125[b]
	143	71	151	68	-	81	144[c]
D12	15	92	15	91	81	-	68-71[d]
D13	17	88	20	83			75
	30	91	27	91			
	62	Cooling	62	Cooling	75	82	
	70	75	70	74	85	81	75
D14	12	93	11	92			
	58	Cooling	57	Cooling			
	62	80	62	80	80	84	63
D15	12	91	11	92			
	69	Cooling	70	Cooling			
	70	83	76	82	81	81	81
D16	10	90	9	91			
	59	Cooling	59	Cooling			
	62	85	62	85	81	81	76
D17	15	92	114	92			
	56	Cooling	56	Cooling			
	60	82	60	82	81	80	60

Notes:

(a) Munition ignited and functioned during heating at this time without other stimulus

(b) Initial attempt to operate actuator motor

(c) Detonator fired with comp. C-4 ~ 50.8 mm from M138

(d) Times disagreed from two strip chart records

All remaining tests provided detonability data for the M138 configuration tested, although several difficulties were experienced. At the outset, one of two output channels of the Physical Data Model 523-A2 transient waveform recorder was inoperative. A replacement instrument flown in from the manufacturer showed an output fault (a voltage discontinuity at about one-half the probe length). It was possible to correct this output mathematically, and, in any event, the discontinuity occurred after the shock velocity had dropped below the cut-off point of 2.0 mm/microsec.

In addition, much of the data obtained was quite noisy, which required the use of special techniques to extract meaningful data from the records. These data reduction techniques were carried out on the data as stored within the Smartscope so that the data plots presented herein were entirely machine-produced.

4.2 Typical Results Obtained

The results obtained from detonation test D7 are fairly representative of the data obtained from each test. In some cases data from only one probe were obtained and the data ranged from somewhat less to somewhat more noisy. In this section all of the intermediate steps in the data reduction of test D7 are shown in graphical form. These steps were performed in each test although not all intermediate hard copy graphics were prepared.

The graphs presented are:

- Original data as recorded and transferred to the Smartscope
- Conversion of the probe voltage data to shock position data after application of the basic data reduction constants
- Velocity determined after application of the data smoothing operations to reduce the noise content
- Comparison of the smoothed position-time data from the two probes
- Stepwise slope (finite-difference differential shock velocity) of the position-time data
- Cross-plots of the shock velocity versus shock position data.

Figure 4 shows the original voltage versus time data recorded from the two probes of test D7. The initial height of the level portion of the curve is not significant. It merely reflects the adjustment of the constant current supply to provide a nearly full scale initial voltage for recording purposes. The initial large amplitude ringing noise shown on this record appeared only after the replacement Physical Data recorder was put in service. The agreement in phase and amplitude of this ringing between the two probe signals suggests that this is an extraneous electrical noise as does the physics of operation of the probe. It was not possible to find and eliminate this noise source during the time frame of these experiments.

Figure 5 shows the probe voltage curves after conversion to position-time data. This step is described in detail in Appendix B. Briefly, the constant current value is obtained from an auxiliary measurement of the voltage through a known resistance. With the current known, changes in voltage can be related to changes in probe resistance. Likewise, with the resistance change known, and the probe resistance per unit length known, the shock position can be derived as shown. These steps were carried out point by point by the signal processing capability of the Smartscope. The deviation between the two curves at long (>200 mm) shock travel distances arises because the low pressure which exists in this region is unable to produce precision crushing and shorting of the detonation probes, as it does in regions of higher pressure (smaller travel distances).

Examples of reduction of noisy data by smoothed line construction are shown in Figure 6 and 7. The basis for drawing the smooth line is as follows. In the initial time region where the data curve is dominated by a ringing-type noise, the smoothed line is made up of a number of short straight line segments drawn through the average value of the initial ringing signal period by period. Later, the data was smoothed on the basis of engineering judgment as to the probable average position of the shock pressure front, with the guideline that the actual shock front progress has momentum associated with it and would be expected to follow a smooth line of progress. Of course, the munition itself is not homogeneous along its length, but is made up of four M7 canisters stacked end to end. Each M7 has 1.5-mm steel end closures, separated by a 1.0-mm thick plastic spacer. These discontinuities occur at three places along the munition length, as shown in Table 3, which also gives the total BZ-pyromix length. The detonation probe records frequently stop changing with time before the full length of the munition is reached. This means that the shock pressure had dropped too low to continue crushing the detonation probe tube.

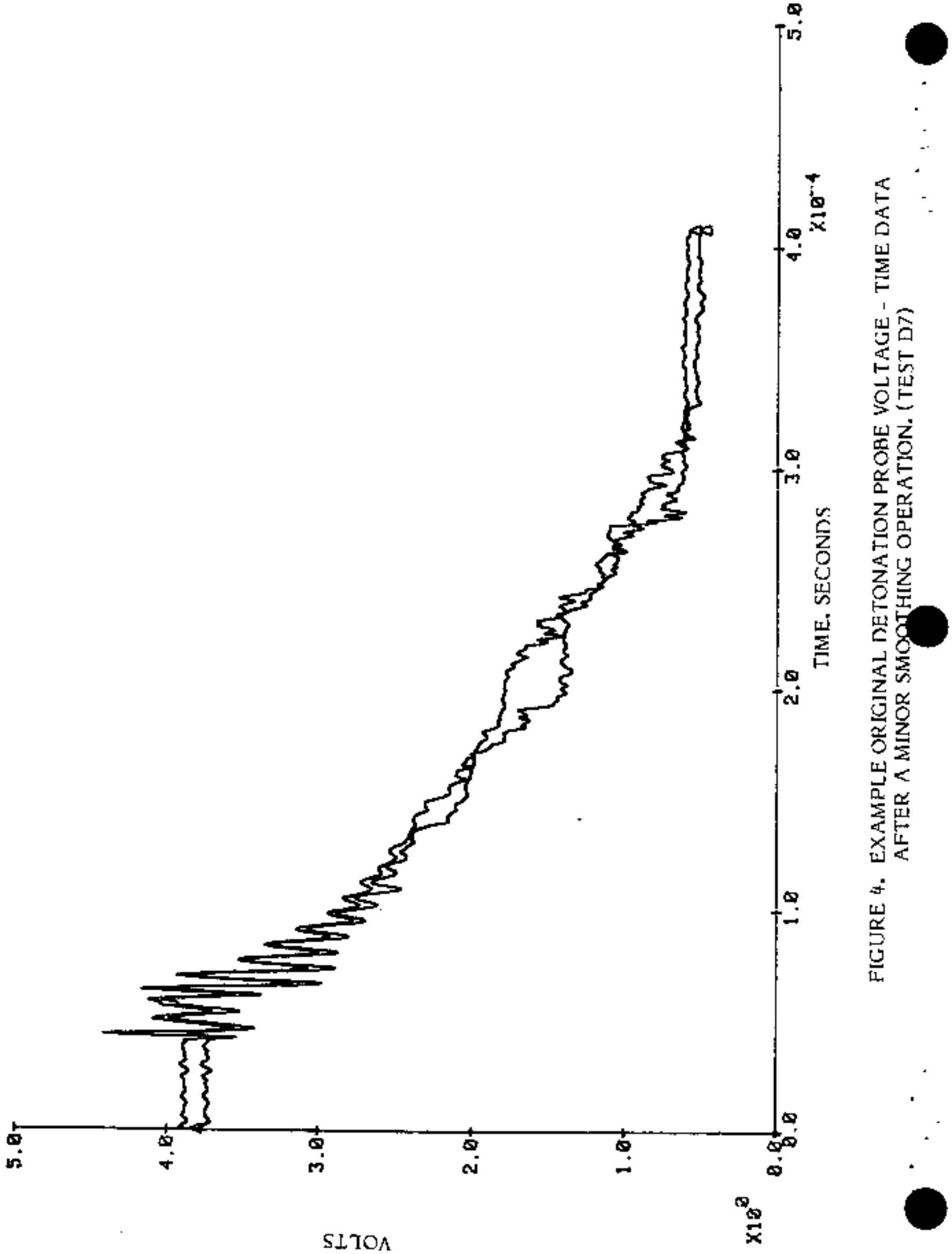

FIGURE 4. EXAMPLE ORIGINAL DETONATION PROBE VOLTAGE - TIME DATA AFTER A MINOR SMOOTHING OPERATION. (TEST D7)

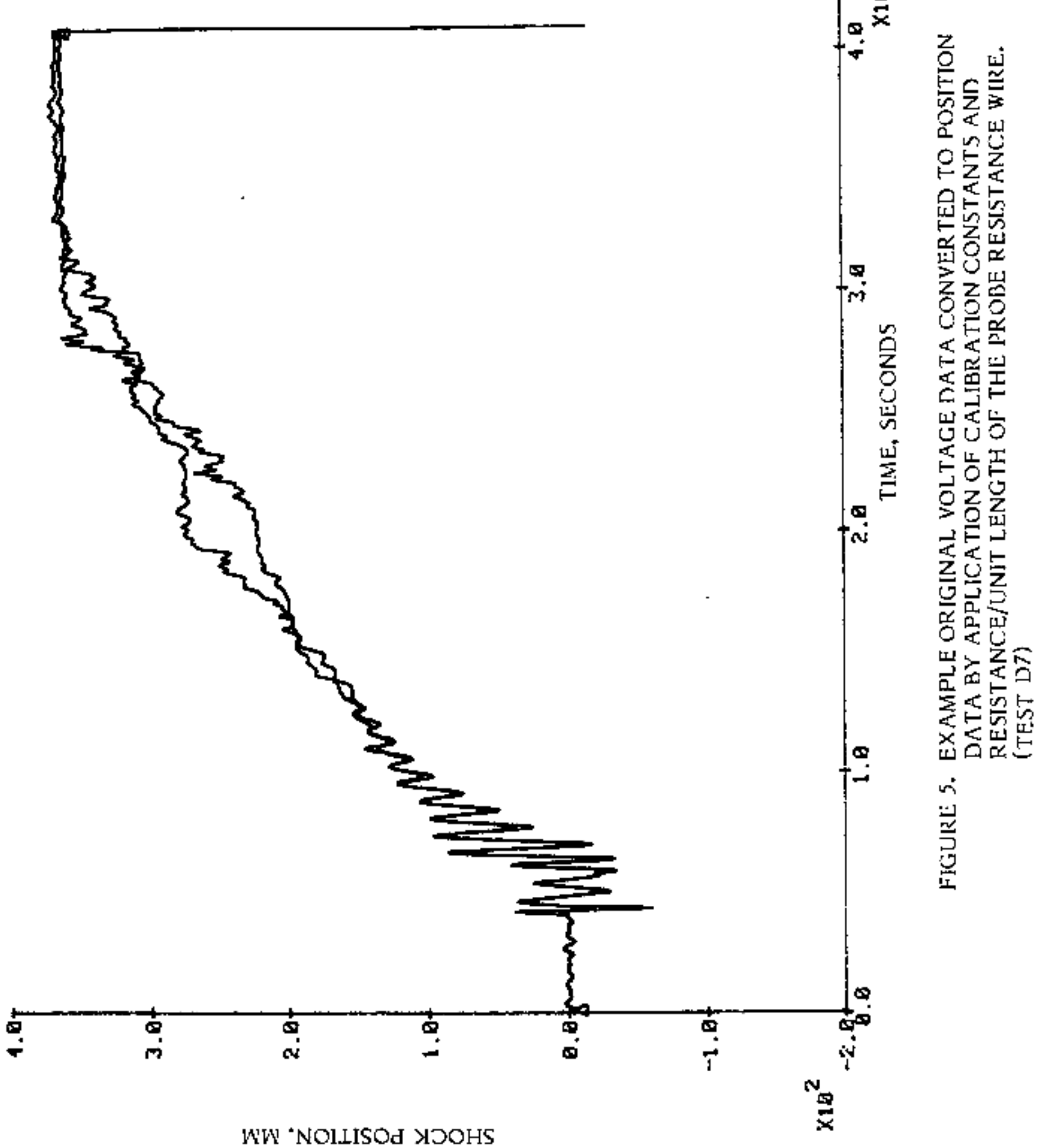

FIGURE 5. EXAMPLE ORIGINAL VOLTAGE DATA CONVERTED TO POSITION DATA BY APPLICATION OF CALIBRATION CONSTANTS AND RESISTANCE/UNIT LENGTH OF THE PROBE RESISTANCE WIRE. (TEST D7)

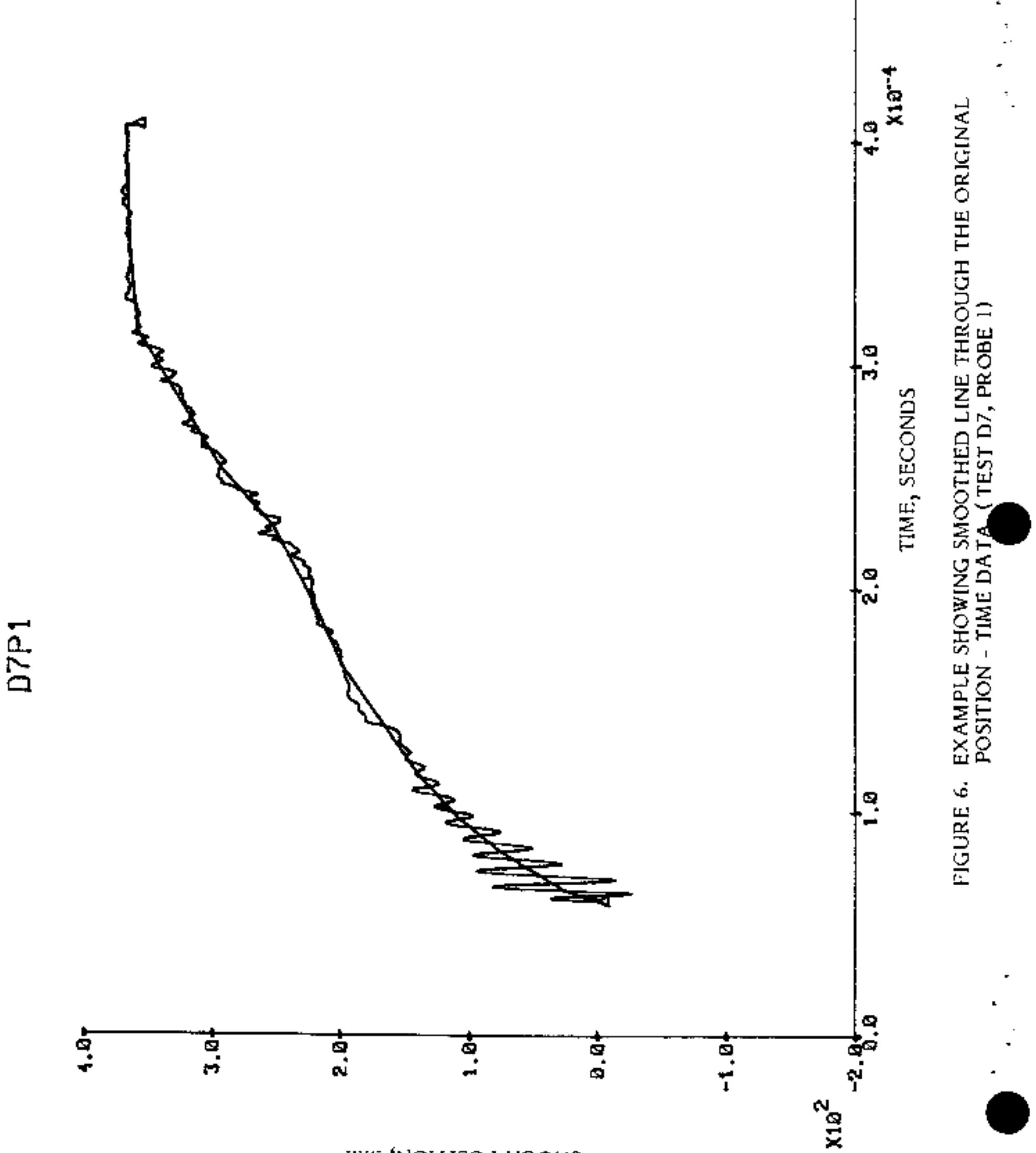

FIGURE 6. EXAMPLE SHOWING SMOOTHED LINE THROUGH THE ORIGINAL POSITION - TIME DATA (TEST D7, PROBE 1)

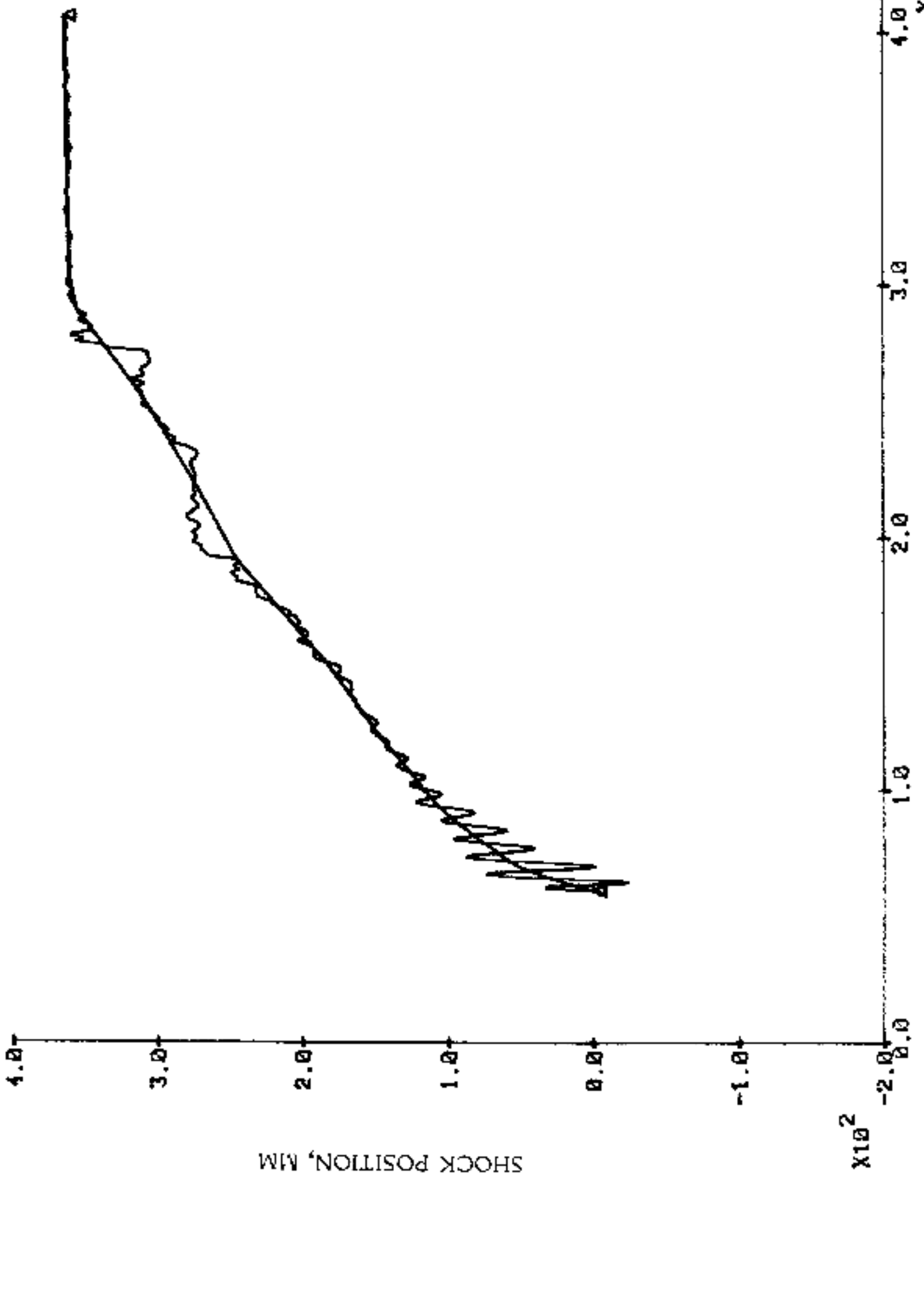

FIGURE 7. EXAMPLE SHOWING SMOOTHED LINE THROUGH THE ORIGINAL POSITION - TIME DATA. (TEST D7, PROBE 2)

Table 3. Locations of Discontinuities for Shock Travel Along M138 Length

Discontinuity	Location, mm	
	From Shock Entrance	As Plotted
Inside Rear of 1st Canister	95.5	89.2
Inside Front of 2nd Canister	101.0	94.7
Inside Rear of 2nd Canister	195.1	188.8
Inside Front of 3rd Canister	200.6	194.3
Inside Rear of 3rd Canister	294.6	288.3
Inside Front of 4th Canister	300.1	293.8
Inside Rear of 4th Canister	396.2	389.9
Outside Rear of 4th Canister (End of BZ-Pyromix Containers)	397.2	390.9

Note: The words "rear" and "front" mean the ends encountered last and first respectively by the shock wave.

Figure 8 shows a comparison of the two smoothed location - time curves from test D7. The curves track very well together until near the 200 mm location. This is after the shock velocity has decayed to the apparent sonic velocity in the material indicating that the pressures are no longer high.

Figures 9 and 10 show the velocity versus time records obtained from the two records by simply taking the slope of the position time curve at 10-microsec intervals along its length, and plotting this velocity as a constant over that time period. Figures 11 and 12 show the final plots of shock velocity versus shock position. These plots are cross plots of the position data from the upper curves of Figures 9 and 10 and velocity data from the lower curves using time as a parameter. From these plots the determination of shock travel at velocities greater than 2.0 mm/microsec was made. The discontinuities near 200 and 300 mm travel are apparent on these plots, coinciding with the ends of the M7 canisters.

4.3 Results

The original data and fully reduced data for each of the tests are provided in Appendix C. From each final plot, the shock travel at a velocity greater than 2.0 mm/microsec was measured and is tabulated in Table 4. Here, the limiting value of 2.0 mm/microsec was chosen over the initially selected 2.3 mm/microsec value after examination of the data which showed that the observed velocities generally fell below this level. (Results using 2.0 mm/microsec versus 2.3 mm/microsec are conservative.) Occasionally, near the end of a record, velocities slightly over 2.0 mm/microsec were observed; this was attributed to the irregular performance of the probes at low pressure levels. This conclusion is supported by the recovery in several tests of intact portions of munitions which came from the same regions where these late velocity excursions were observed. It should be noted that the shock travel at velocities greater than 2.0 mm/microsec for a simulated non-detonable test item[7] was 130 mm, with a very similar velocity decay curve. Improved data reduction techniques from those used in Reference 7 were used on the current data set* so that the difference between the current data and the simulated non-detonable item may be less

---

* The difference arises principally in the use of an additional calibration which eliminates the effect of long term drift in the constant current. It was found after the tests of Reference 7 that the current provided by the constant current supply slowly drifted up with time between pre-calibration measurements and conduct of the test. This drift went undetected in the initial non-agent tests.

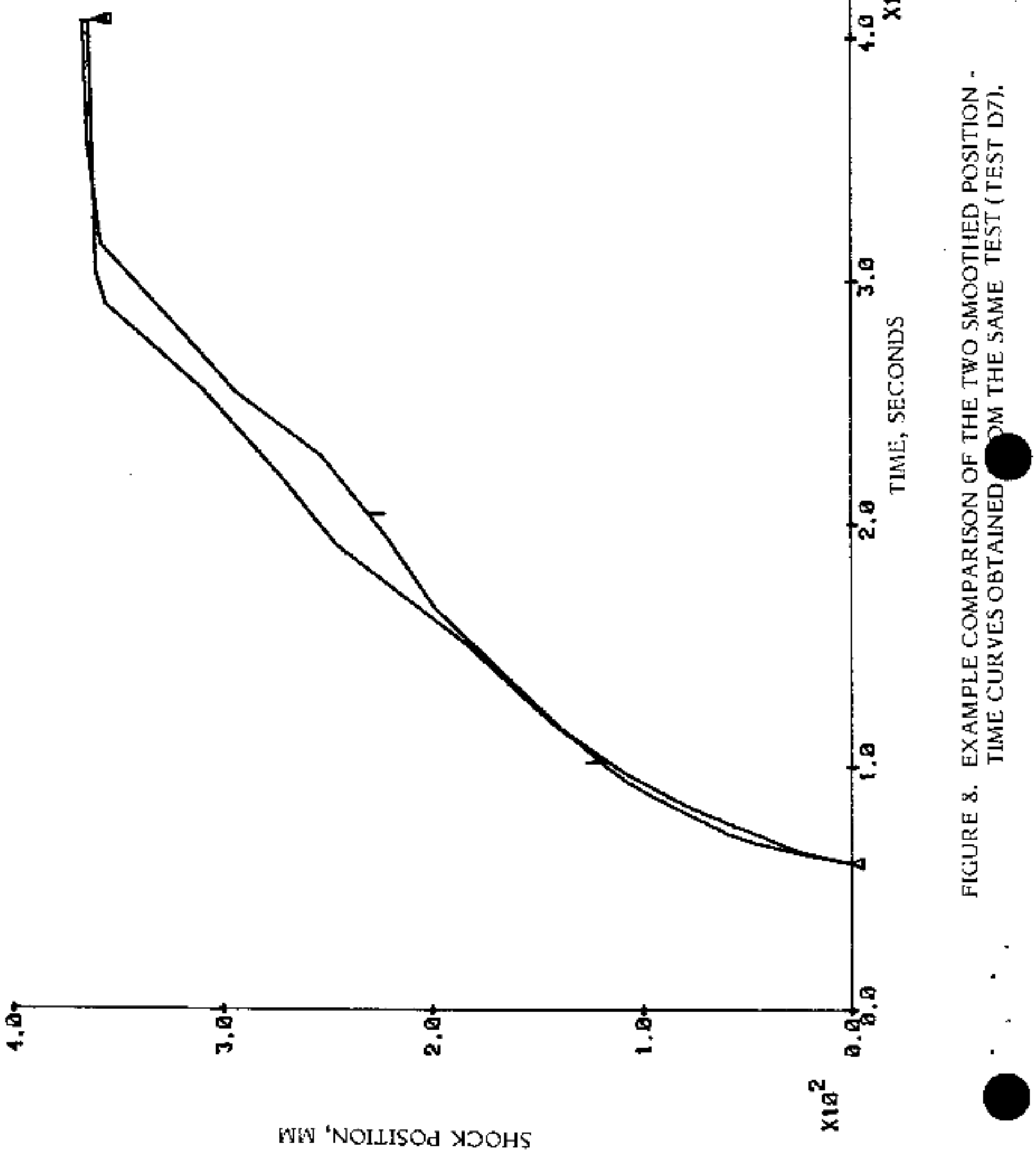

FIGURE 8. EXAMPLE COMPARISON OF THE TWO SMOOTHED POSITION - TIME CURVES OBTAINED FROM THE SAME TEST (TEST D7).

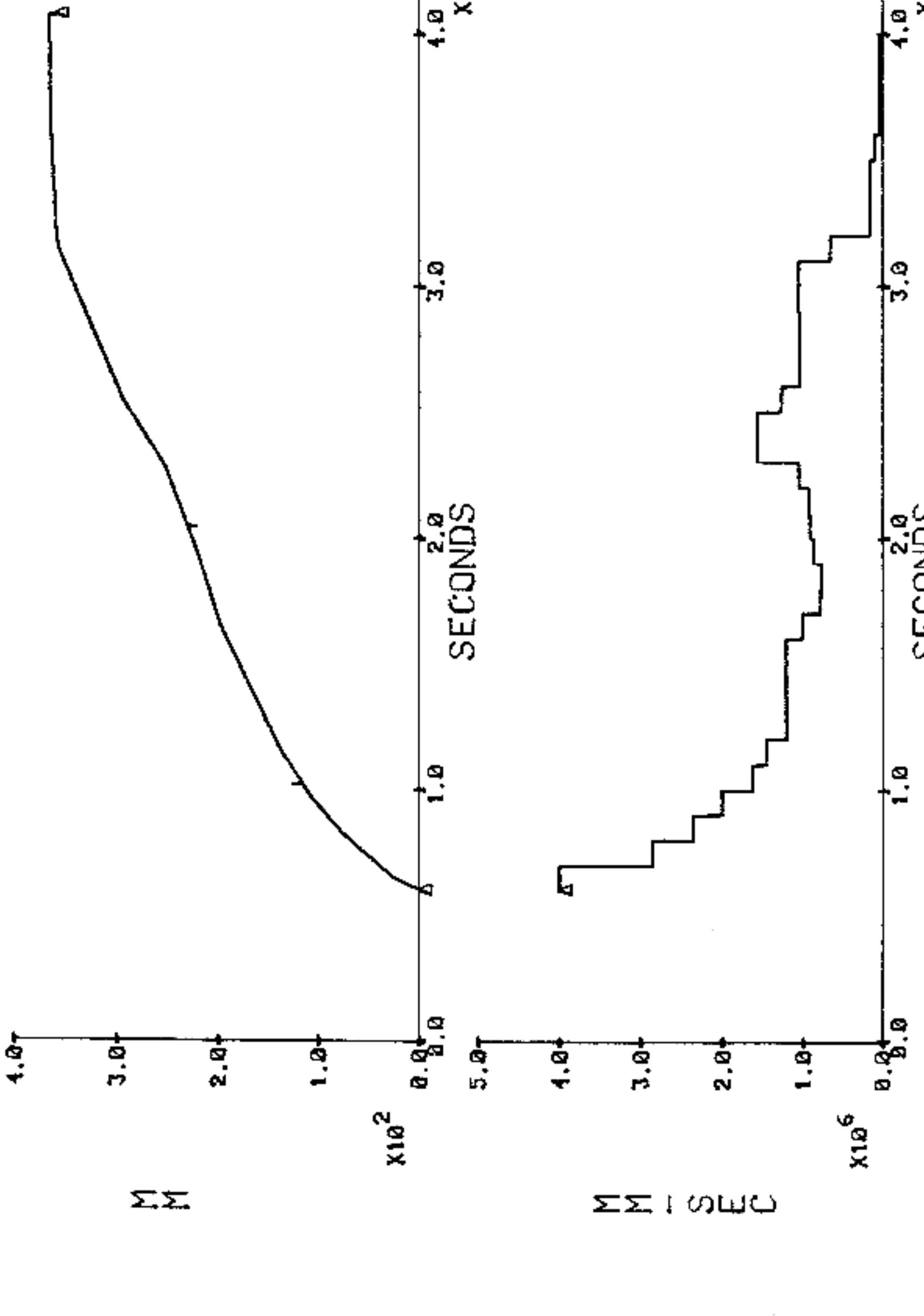

FIGURE 9. UPPER CURVE SMOOTHED POSITION - TIME DATA.
LOWER CURVE STEPWISE VELOCITY DATA FROM UPPER
CURVE (TEST D7 PROBE 1).

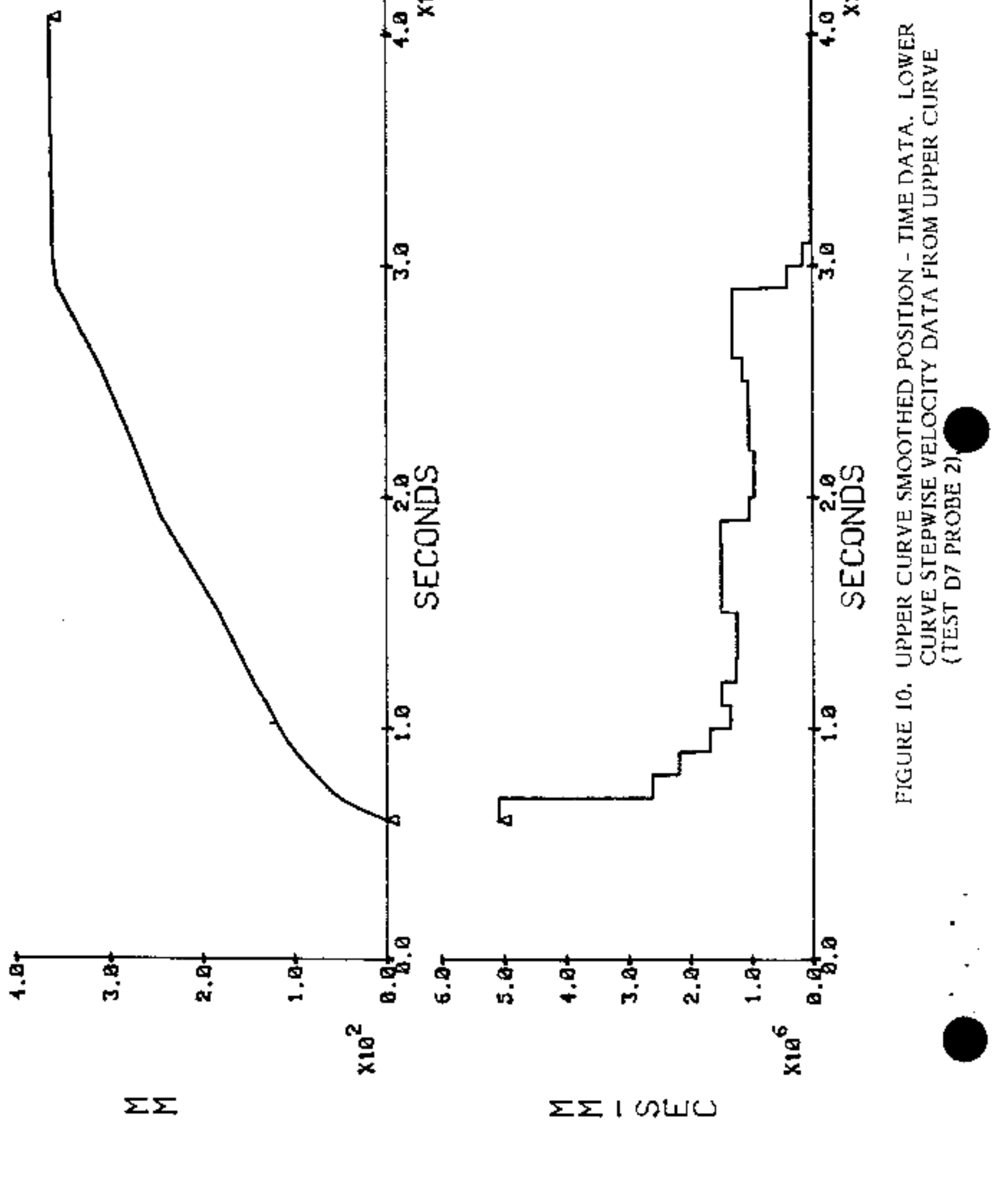

FIGURE 10. UPPER CURVE SMOOTHED POSITION - TIME DATA. LOWER CURVE STEPWISE VELOCITY DATA FROM UPPER CURVE (TEST D7 PROBE 2)

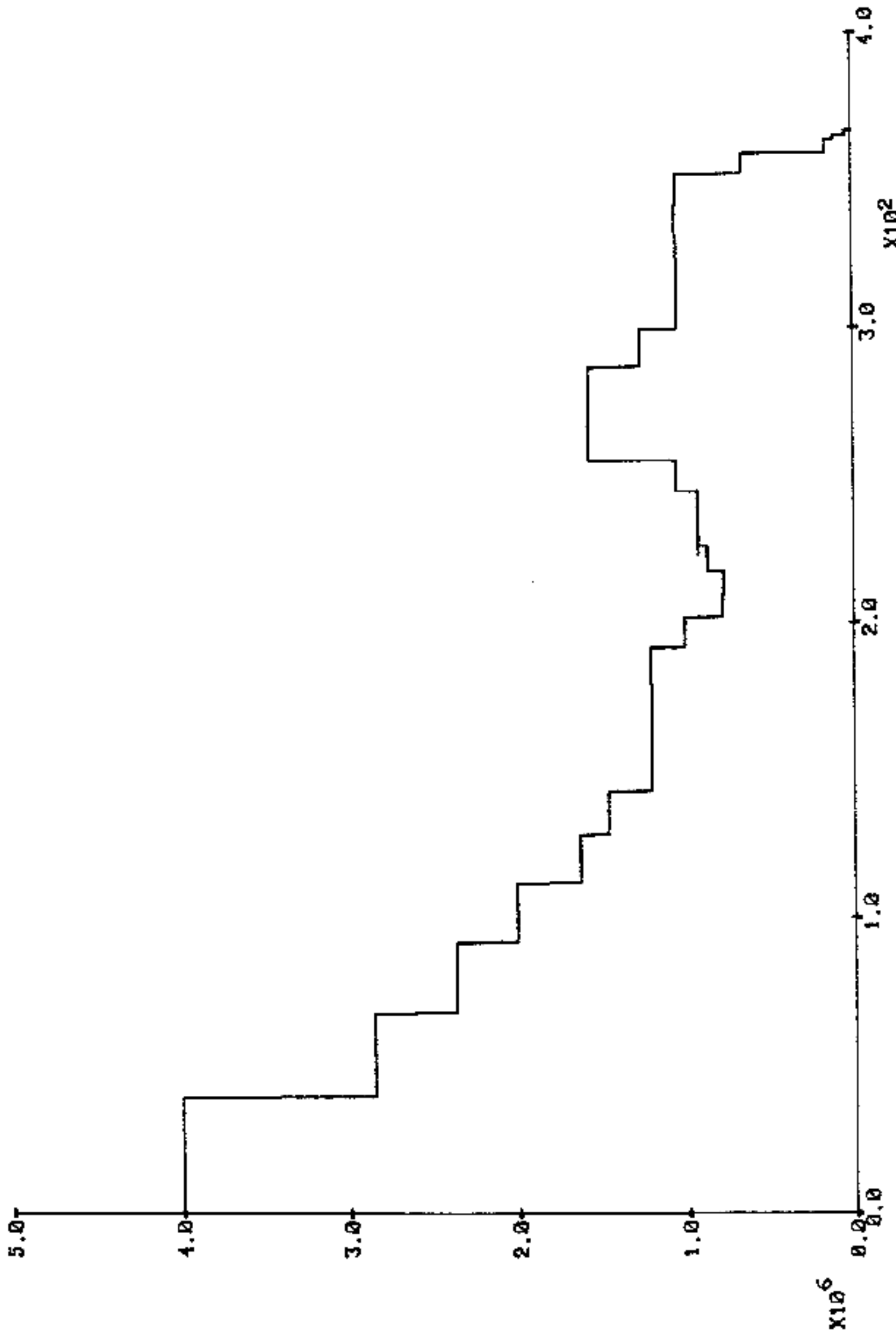

FIGURE 11. CROSS PLOT SHOWING VELOCITY DECAY WITH DISTANCE ALONG THE M138 (TEST D7 PROBE 1).

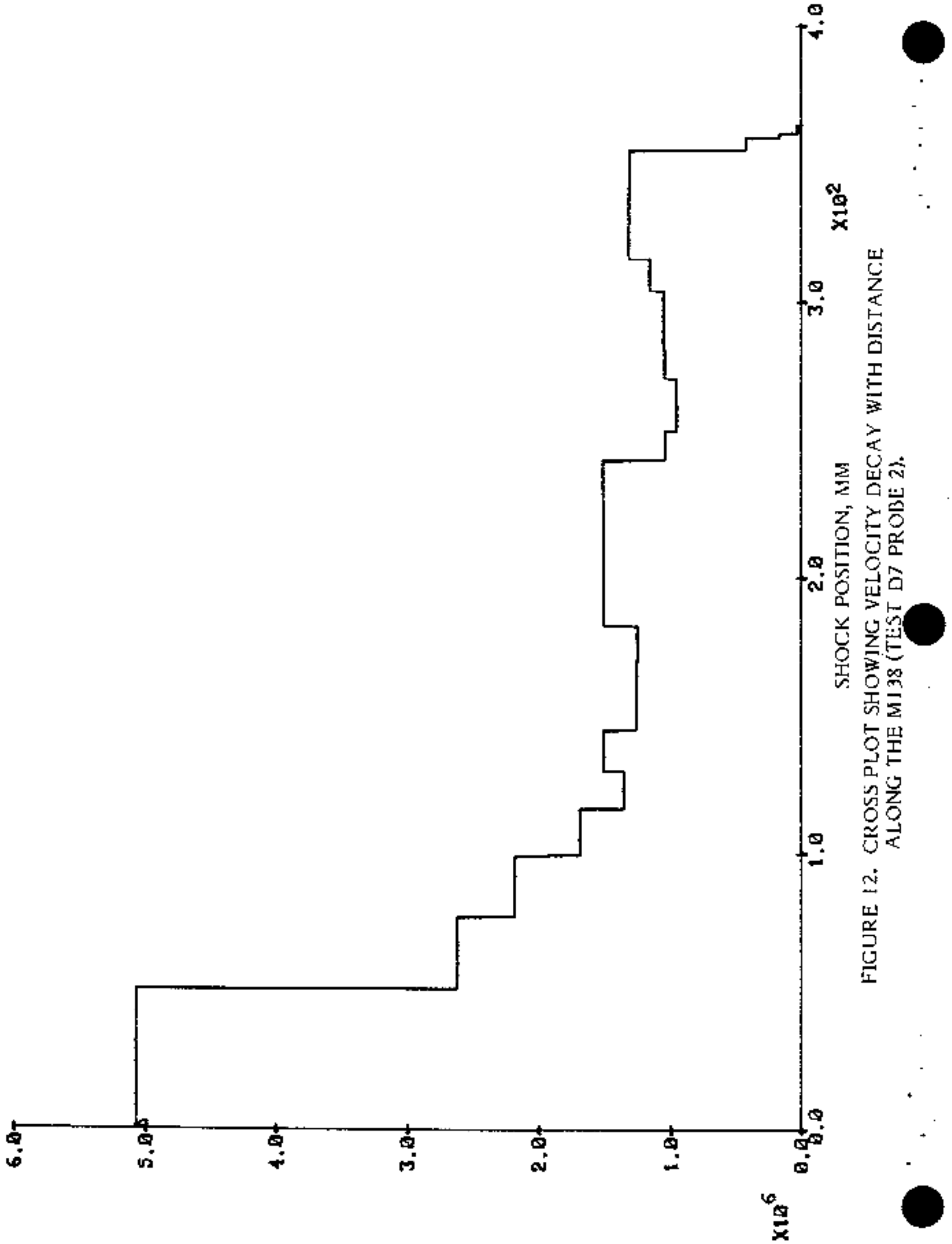

FIGURE 12. CROSS PLOT SHOWING VELOCITY DECAY WITH DISTANCE ALONG THE MI38 (TEST D7 PROBE 2).

Table 4. Shock Travel at Velocity Greater Than 2.0 mm/microsec

Test No.	Probe 1 mm	Probe 2 mm	Average Within Groups mm	Standard Deviation of Group mm
D1	100	-		
D2	107	-	103.5	± 4.9
D3	116	-		
D4	92	92	104	± 17.0
D5	98	116		
D6	115	125		
D7	100	100	109	± 10.1
D9	-	-		
D10	120	130		
D11	58[(a)]	59[(a)]		
D12	108	-		
D13	108	112		
D14	102	110		
D15	115	-		
D16	109	106		
D17	106	113	111.6	± 6.6
	Overall Average		108.8	± 8.5

(a) Not included in averages because of no contact between donor charge and M138 munition.

Note: The total shock travel distance is 6.3 mm greater than the values shown because the end of the active probe was 6.3 mm from the lower end of the munition.

than suggested by the numbers. In any event, the results obtained from the current tests on live BZ-pyromix were quite similar to those obtained on the simulated non-detonable mockup item.

With respect to the munition remains after the test, those from test D4, shown in Figure 13, are representative of the physical appearance of the inerted and short-time inerted munitions tested. About two-thirds of the original munition remained intact, with no burning of the remaining BZ-pyromix-filled canisters. For the non-inerted munitions, a vigorous reaction of most or all the BZ-pyromix occurred. Representative remains are shown in Figure 14 from ambient temperature test D6. Although the entire munition was broken up, many large fragments with areas almost one-half that of a single canister case remained, indicating that the pressures developed prior to canister burst were not appreciably above the minimum pressure required to burst them. Assuming a nominal 60,000 psi for the mild steel strength of the containment including the added tube over the M138, results in a burst pressure of 4300 psi or 0.3 Kbar, far below the predicted detonation pressure of 25 Kbar. In the unheated non-inerted tests and preheated tests D11 and D12, all canisters were destroyed. In the other preheated tests, one distorted but intact M7 canister remained, except in test D17 where two M7s remained intact. In test D17 there also was evidence of unburned BZ-pyromix. The bursting of the M7 canister's M138 sleeve and the added confinement tube in these tests due to the reaction of BZ-pyromix was to be expected because the core hole (which normally vents the generated gases and BZ aerosol) was securely plugged with epoxy resin cast in place.

Both the active instrumentation and the post-shot appearance of the munition remains confirm that no sustained detonation occurred, nor does there appear to be any evidence for a fading detonation as would occur with a material which would support a sustained detonation in a slightly larger charge diameter.

Additional evidence regarding the reaction of the BZ-pyromix was obtained from the measurement of pressure inside the sphere following the detonability tests. The pressure was monitored at 1-msec intervals for 10 sec following each test.

An example pressure measurement record is shown in Figure 15 for test D7. As demonstrated in this example, all records showed an initial spike pressure which rapidly decayed to a more slowly changing pressure, called the initial steady pressure. Ten of the 15 records obtained showed a small increase to a maximum pressure in a small fraction of a second, followed by a steady pressure decay to the last accurately measured pressure at 10 seconds after the test. Copies of all remaining pressure records are provided in Appendix D.

FIGURE 13. REMAINS OF MJ38 FROM AN INERTED DETONATION TEST, TEST D4

FIGURE 14. REMAINS OF M138 FROM AN AMBIENT TEMPERATURE LIVE DETONATION TEST, TEST D6

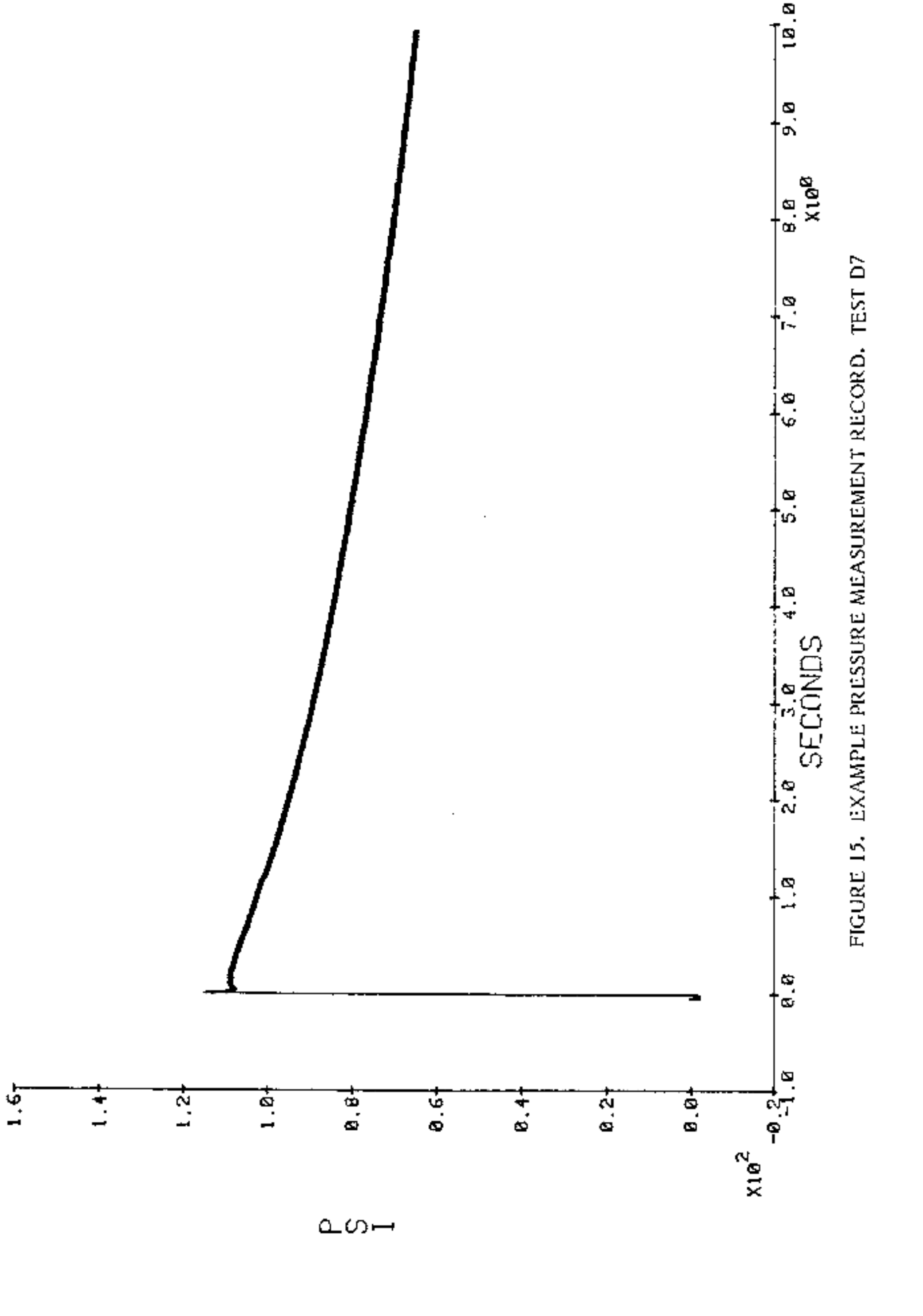

FIGURE 15. EXAMPLE PRESSURE MEASUREMENT RECORD. TEST D7

Table 5 shows a tabulation of the measured pressures from the records as identified in the example above. Examination of this data shows that the initial spike and maximum pressures fall into three groups corresponding to the inerted, short-time inerted, and live munitions. The live munition group includes both the ambient and preheated munitions mixed together. This grouping is shown graphically in Figure 16. The separation of these initial and maximum pressures may be taken as an indication of the fraction of the BZ-pyromix which reacted in the first few tenths of a second. Thus there appears to be no significant difference in the amount of BZ-pyromix reacted during shock wave passage (or detonation if it occurred) between the ambient temperature live munitions and the preheated live munitions.

During the decay of pressure in the first ten seconds, however, the ambient temperature and preheated tests divide into two groups as shown in Figure 16. Significantly less pressure decay occurs in the preheated group than in the ambient temperature group. This shows that the reaction of the BZ-pyromix which remained after initial shock wave passage in the preheated group was taking place faster during the first ten seconds than in the unheated group, but by a gradual and progressive process, not a detonation.

4.4 Analysis of Results

The effects of pre-treatment inerting, short-time inerting, ambient or preheated condition on the shock travel distance at velocities greater than 2.0 mm/microsec was analyzed by comparing the average run distances and standard deviations between groups with different pre-treatments as shown in the two right hand columns of Table 4. The standard deviations of groups generally overlap the means of other groups. It appears that there is no significant difference in shock travel distance between different pre-treatments.

The effect of lot burn time on the shock travel distance at velocities greater than 2.0 mm/microsec observed was analyzed by plotting the shock travel against the observed burn times of the lots tested, as shown in Figure 17. Again no definite correlation is shown, except, perhaps, a very weak correlation with longer burn times and longer shock travel distances. This correlation is the opposite of what might be expected, but is, in any event, too weak to be significant.

The effect of pre-treatment on the pressures developed within the sphere and the subsequent pressure decay has been presented in Figure 16. Analysis for additional correlation of the pressure parameters shown in Table 5 with the measured burn times for each lot showed no correlation between burn time and any of the individual pressure parameters.

Table 5. Sphere Pressure Rise

Test No.	Initial Spike Pressure psi	Initial Steady Pressure psi	Maximum Pressure psi	Maximum Time sec	After 10 Sec Pressure psi
D1	88.2	69.2	70.9	.16	40.1
D2	84.3	75.0	75.0	-	40.7
D3	94.5	80.0	80.0	-	48.8
D4	101.5	90.9	90.9	-	48.5
D5	118.0	108.5	108.5	-	64.2
D6	113.8	107.8	111.6	-	67.4
D7	116.1	108.8	110.0	.11	65.8
D10	119.5	110.4	113.4	.41	83.2
D11	121.4	113.5	114.7	.13	79.4
D12	122.8	112.2	114.5	.18	80.8
D13	123.3	110.8	111.6	.13	77.8
D14	125.4	108.4	109.1	.18	77.6
D15	150.0	109.8	109.8	-	80.1
D16	120.8	112.5	113.8	.07	78.0
D17	115.6	109.8	111.0	.07	74.8

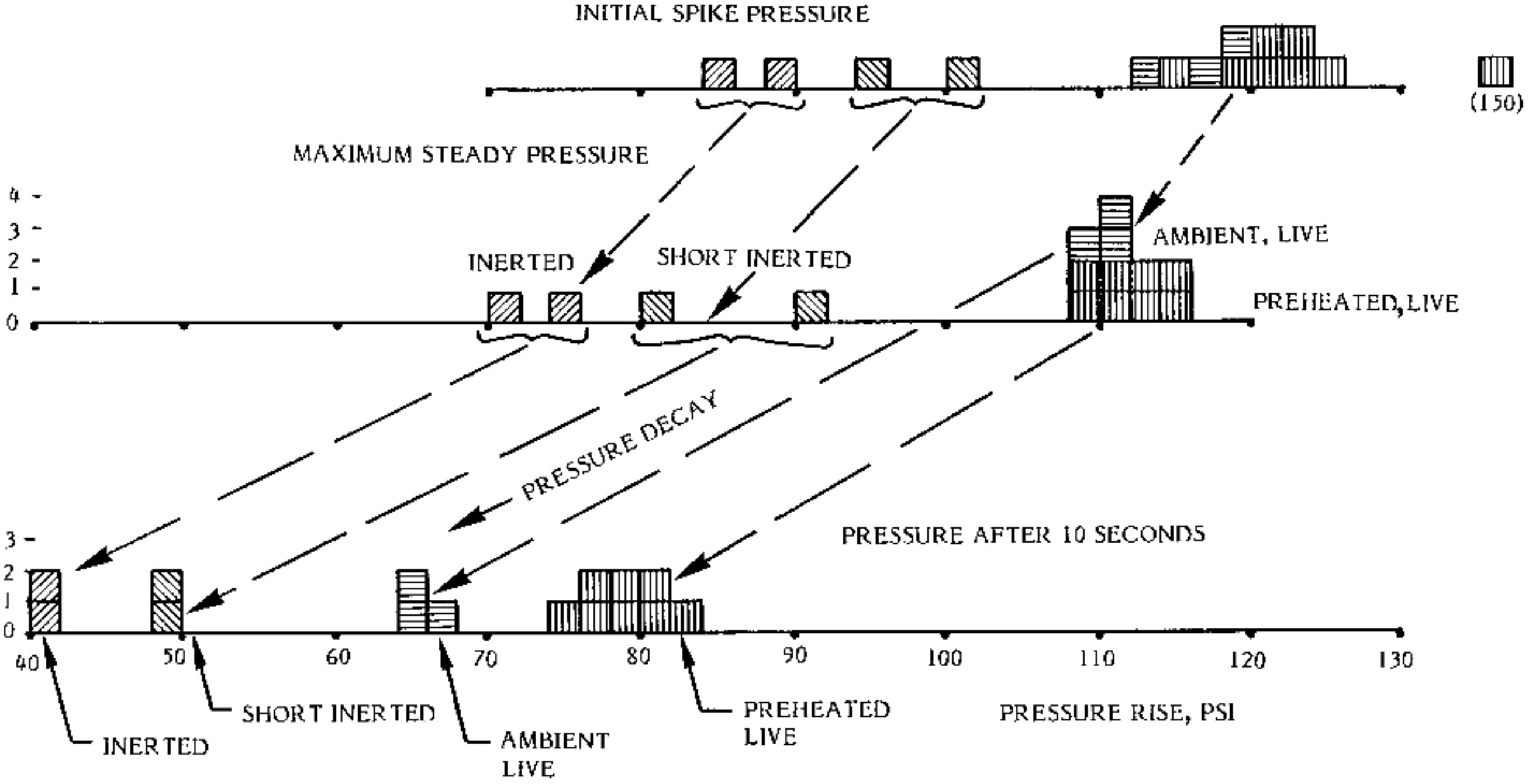

FIGURE 16. PRESSURE DISTRIBUTION HISTOGRAMS, CLASS INTERVAL 2 PSI

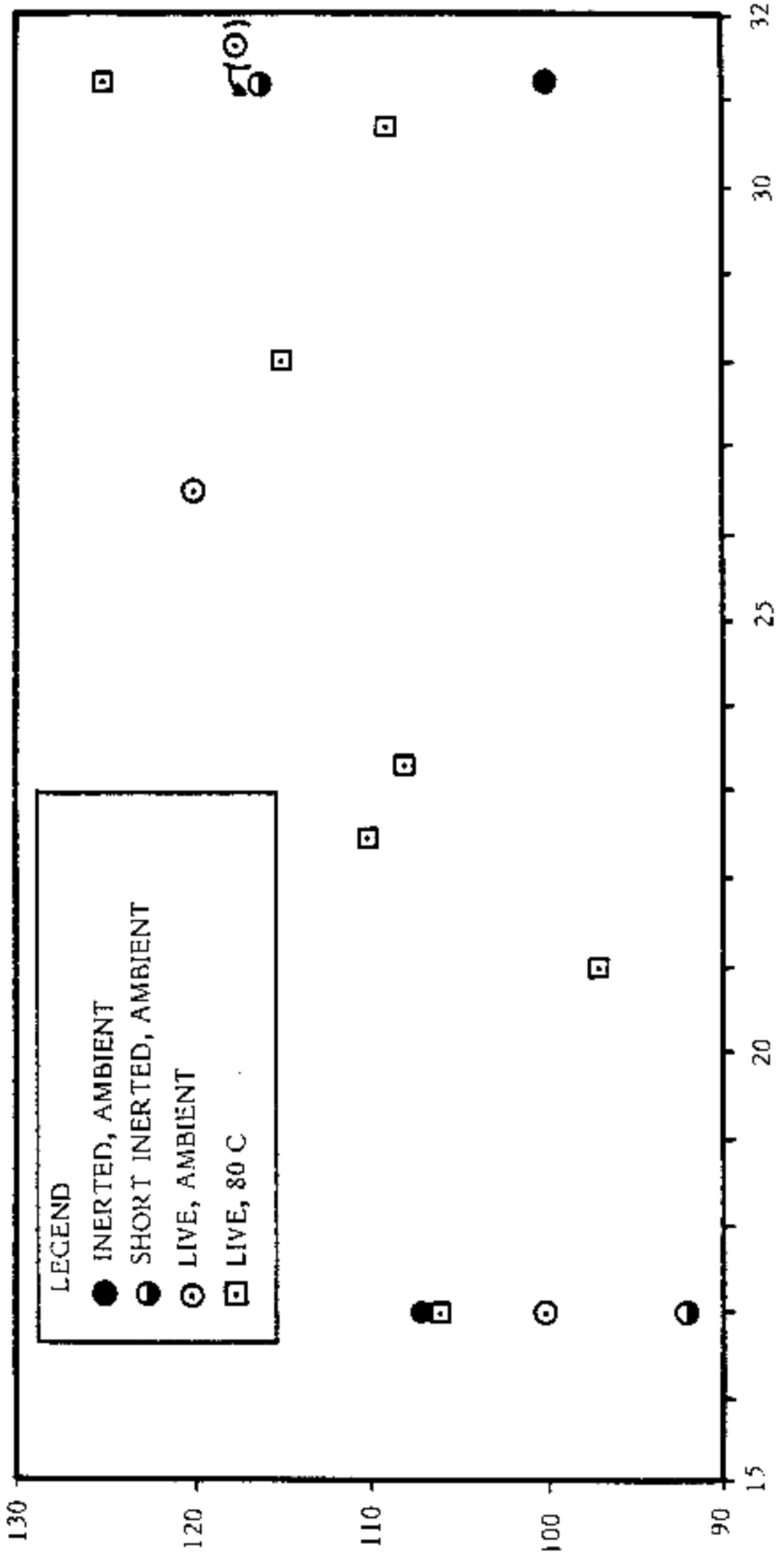

FIGURE 17. CORRELATION OF SHOCK TRAV

CONCLUSIONS AND RECOMMENDATIONS

Based on the results obtained during these tests and their analysis, the following conclusions are drawn:

1. The BZ-pyromix contained in the M138 bomblet configuration is non-detonable.
2. The observed shock wave decay in the munitions from the C-4 donor charge was not affected by pre-treatment inerting by immersion in a water/wetting agent solution, nor by preheating to 80 C.
3. The observed shock wave decay agreed, within experimental error, with the observed shock wave decay in a previous test of an inert mockup munition.
4. No significant correlation exists between a tendency to react during passage of a high pressure shock wave and munition burn time.

As a result of these tests it is recommended that:

1. Subsequent demilitarization plant designs do not include provisions for the containment of accidental BZ detonations because it is believed that the results obtained demonstrate the non-detonability of BZ-pyromix in all configurations contained in the munition inventory.
2. Extreme care must be exercised in any handling operations of non-inerted munitions to prevent premature or accidental ignition. Provisions should be made to protect personnel and contain any released BZ aerosol as a result of premature or accidental ignition.

REFERENCES

1. Ballantyne, W. E., Zeidman, G. G., "Final System Concept Report for Demilitarizing the BZ Item/Munition Inventory", Contract DAAK11-78-C-0096 to the U.S. Army Toxic and Hazardous Materials Agency by Battelle Columbus Laboratories, April 24, 1980.

2. Gentner, Robert of ARRADCOM, Dover Site, reported of a meeting at USATHAMA HQ., Aberdeen Proving Ground, Maryland, February 28, 1979.

3. "Explosives Hazard Classification Procedures" Department of the Army Technical Bulletin DSAR 8220.1, May 19, 1967.

4. Weller, A. E., "Test Report on Incineration Detonation Studies", Contract DAAK-11-78-C-0096 to U.S. Army Toxic and Hazardous Materials Agency by Battelle Columbus Laboratories, June 30, 1981.

5. Trott, B. D. and White, J. J., III, "Design and Evaluation of An Experimental Multipurpose Blast Containment Chamber", NAVEODFAC Technical Report TR-196. Naval Explosive Ordinance Disposal Facility, Indian Head, Md., October, 1978 (AD B033 1266).

6. B.D. Trott, "Test Report for Containment Sphere Leak and Proof Tests", Contract DAAK11-78-C-0096 to U.S. Army Toxic and Hazardous Materials Agency by Battelle Columbus Laboratories, October 15, 1980.

7. Weller, A. E., et al, "Test Report on Non-Agent Tests of Incineration/Detonation Test Equipment", Contract DAAK-11-78-C-0096 to U.S. Army Toxic and Hazardous Materials Agency by Battelle Columbus Laboratories, January 22, 1981.

APPENDIX A

BZ MUNITION DESCRIPTIONS

M43 BOMB CLUSTER

The M43 bomb cluster is an M30 cluster adapter filled with 57 M138 bomblets. The cluster adapter consists of an upper and a lower adapter casing held together by a hinge tube containing a PETN detonating cord (22 ft. long, weighing 2.5 oz.) as a cutting charge. The M138 bomblets are arranged in three stacks of 19 each, separated by fiberboard spacers. Each bomblet, is a thin-walled cylinder equipped on one end with an M150A2 "all-ways" acting impact fuze with an M308 delay element. Upon removal from the cluster adapter, the bomblet immediately becomes armed. The bomblet is composed of four M7 canisters filled with a 50/50 agent-pyrotechnic mixture (pyromix). There is a cylindrical hole through the four canisters that is coated with a starter mixture. Impact of the bomblet will activate the fuze, which, after the 8 to 12 second delay, will ignite the pyromix.

	M7 Canister	M138 Bomblet	M43 Bomb Cluster	BZ-Pyromix, lb[a]	Equivalent Weight of TNT, lb
	1	-	-	0.75	0.375
	4	1	-	3	1.50
	228	57	1	171	85.5
Length - in.	3.88	19.47	65.75		
Diameter - in.	2.75	3.0	16.15		
Weight - lb	(b)	10	750		

(a) Nominal Fill. Actual fill averages 1.04 times nominal.

(b) Approximately 36 ounces

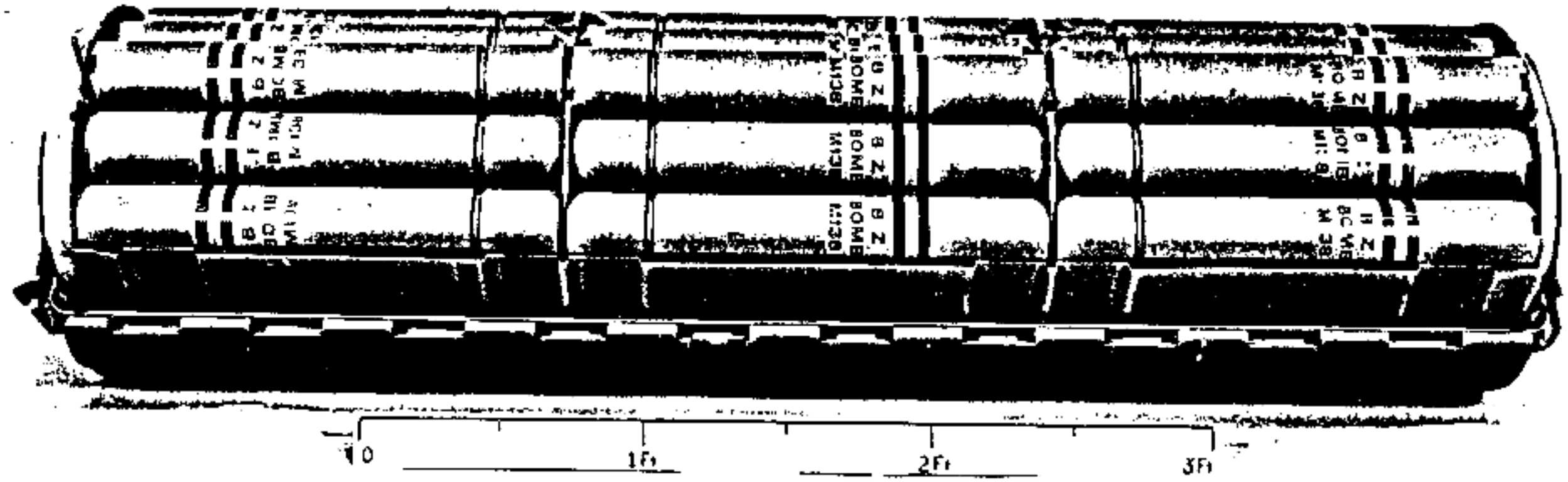

FIGURE A-1. M43 BOMB CLUSTER SHOWING INTERIOR

FIGURE A-2. M138 BZ BOMB

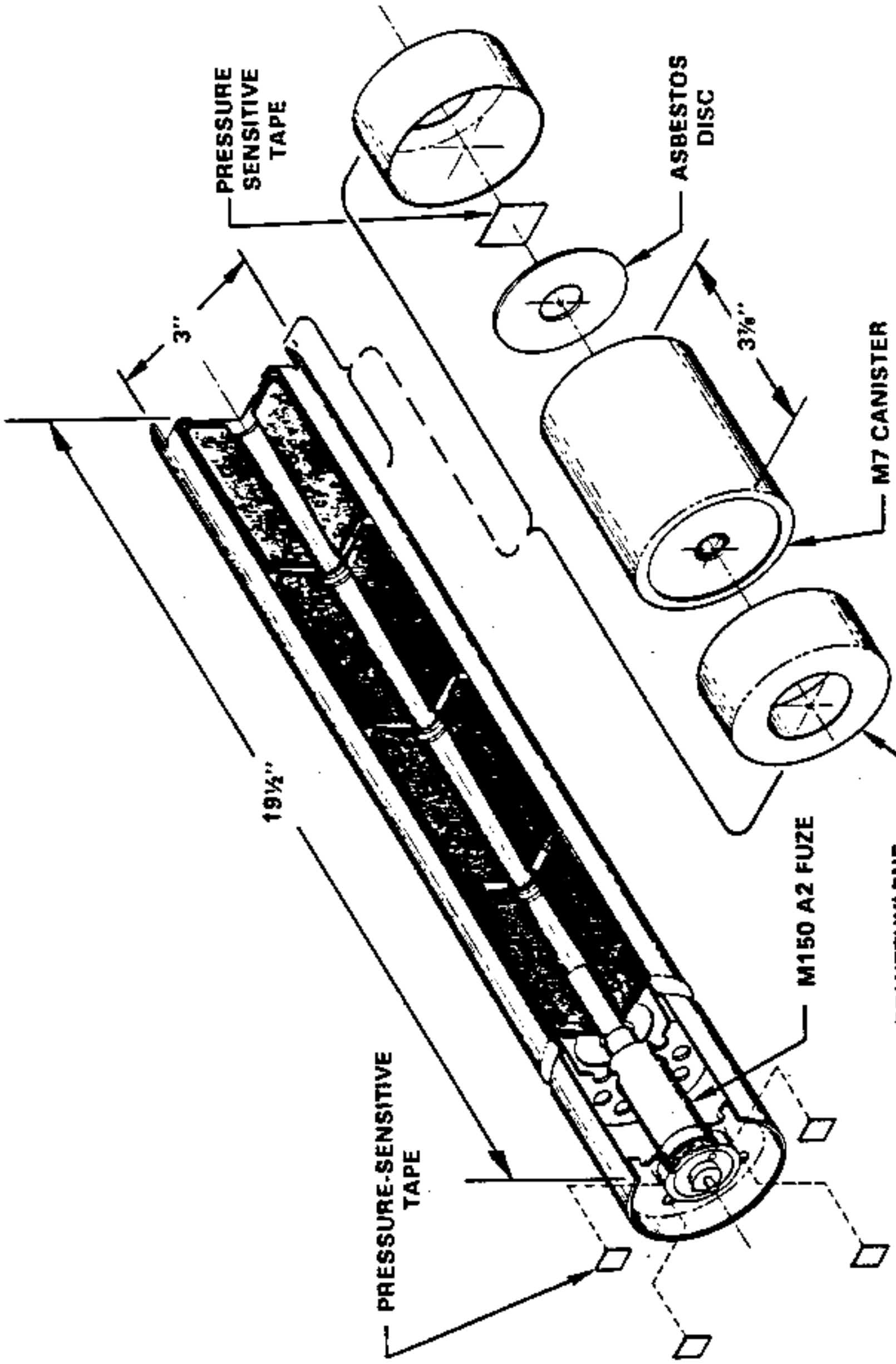

FIGURE A-3. M138 BZ BOMB ASSEMBLY

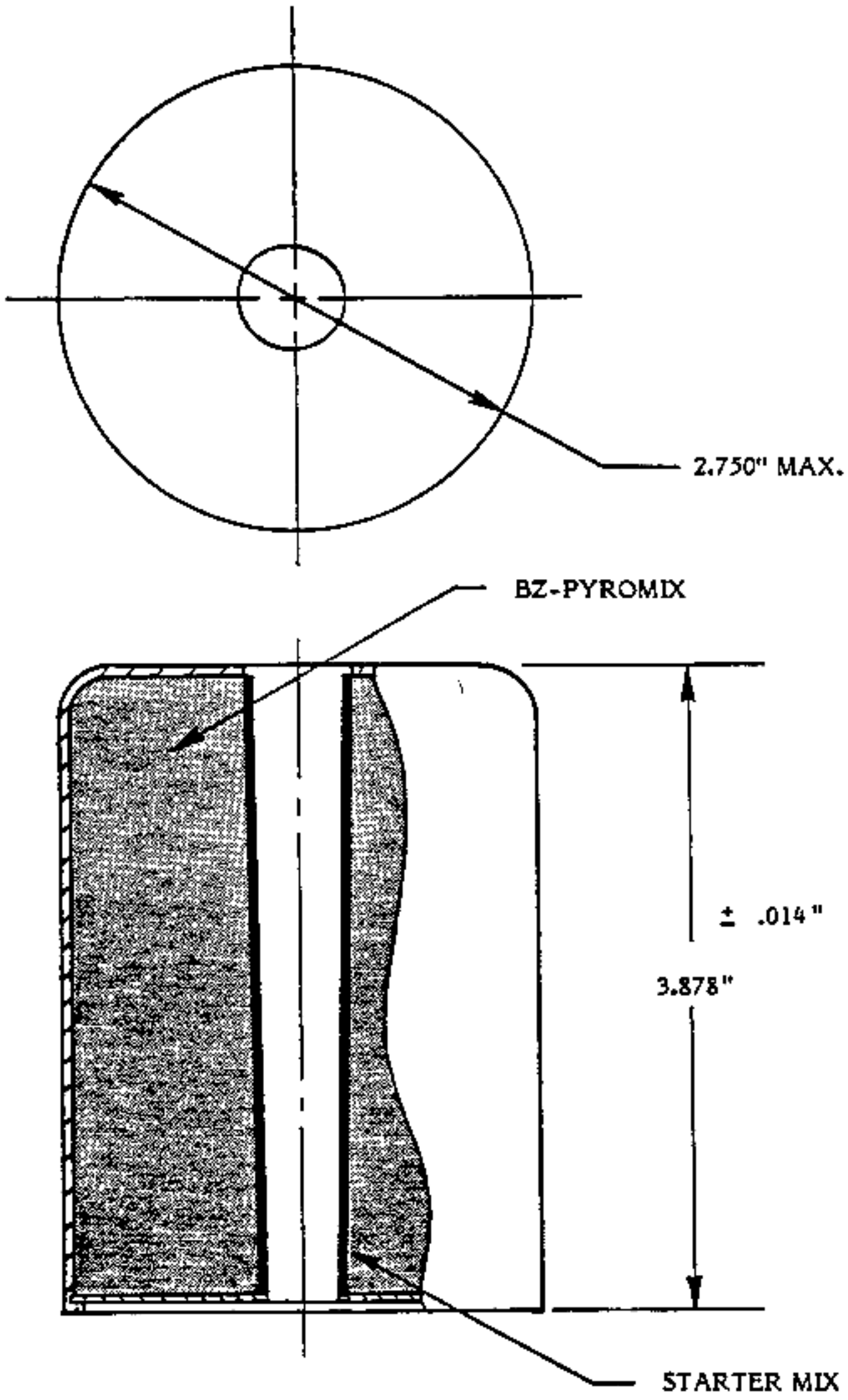

FIGURE A-4. M7 CANISTER FOR M43 MUNITION

M44 GENERATOR CLUSTER

The M44 generator cluster consists of three M16 BZ smoke generators stacked end-to-end in the cluster adapter. Each M16 smoke generator is equipped with an M9 parachute assembly and an M220 time delay fuze. The 12-second delay is activated by a 40-lb pull (approximately) on the fuze lanyard.

Each M16 generator contains three tiers of 14 M6 canisters. The canisters are approximately the size of soup cans. The munition fill has a hollow cylindrical core coated with starter mixture.

	M6 Canister	M16 Generator	M44 Generator Cluster	BZ Pyromix, lb[a]	Equivalent Weight of TNT, lb
	1	-	-	0.625	0.315
	42	1	-	26.25	13.2
	126	3	1	78.75	39.5
Length - in.	4.75	14.87	60		
Diameter-in.	2.5	11.87	15		
Weight-lb	(b)	50	175		

(a) Nominal Fill. Actual fill averages 1.14 times nominal.

(b) Approximately 16 ounces

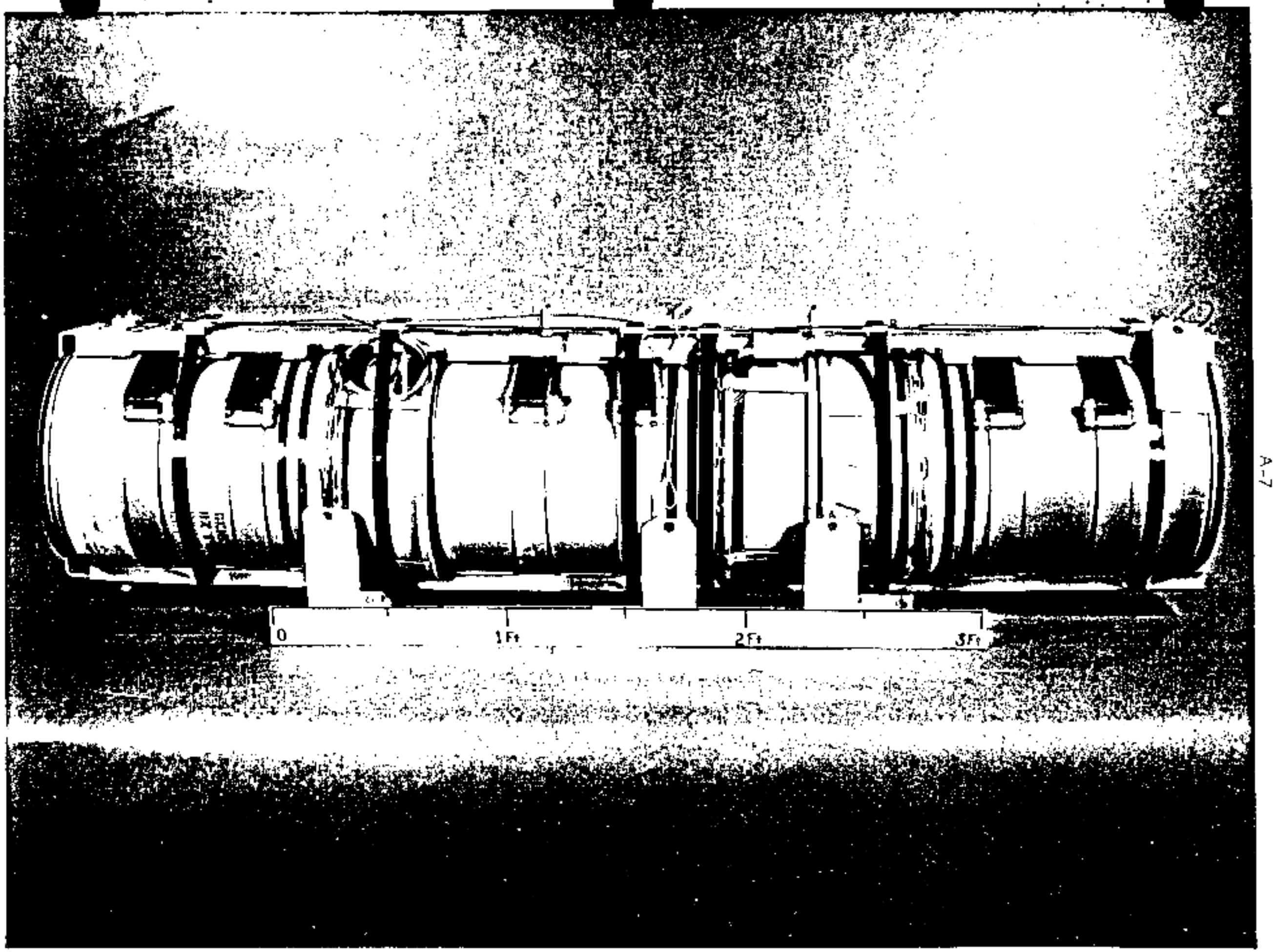

FIGURE A-5. M44 GENERATOR CLUSTER

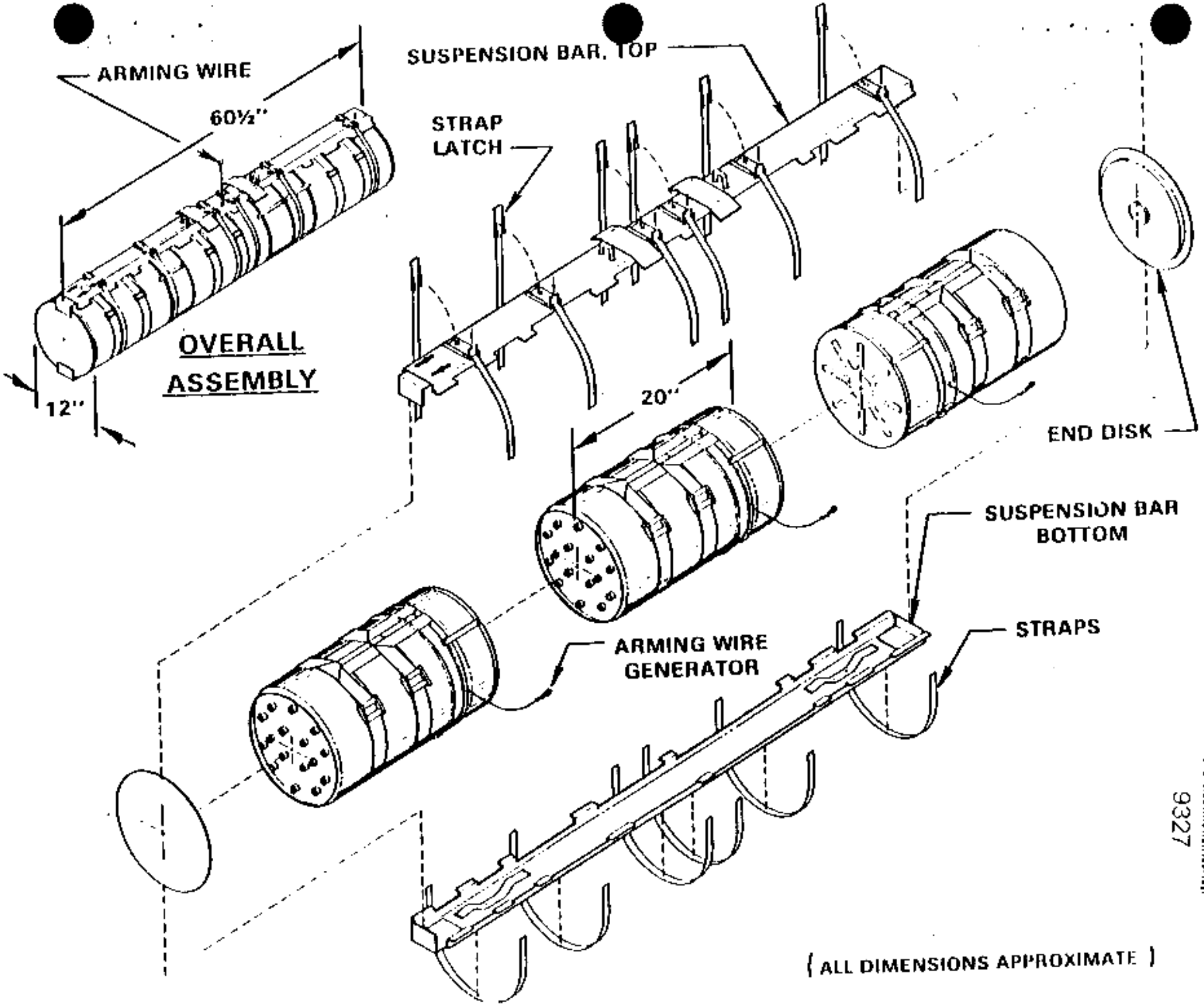

FIGURE A-6. M44 BZ GENERATOR CLUSTER

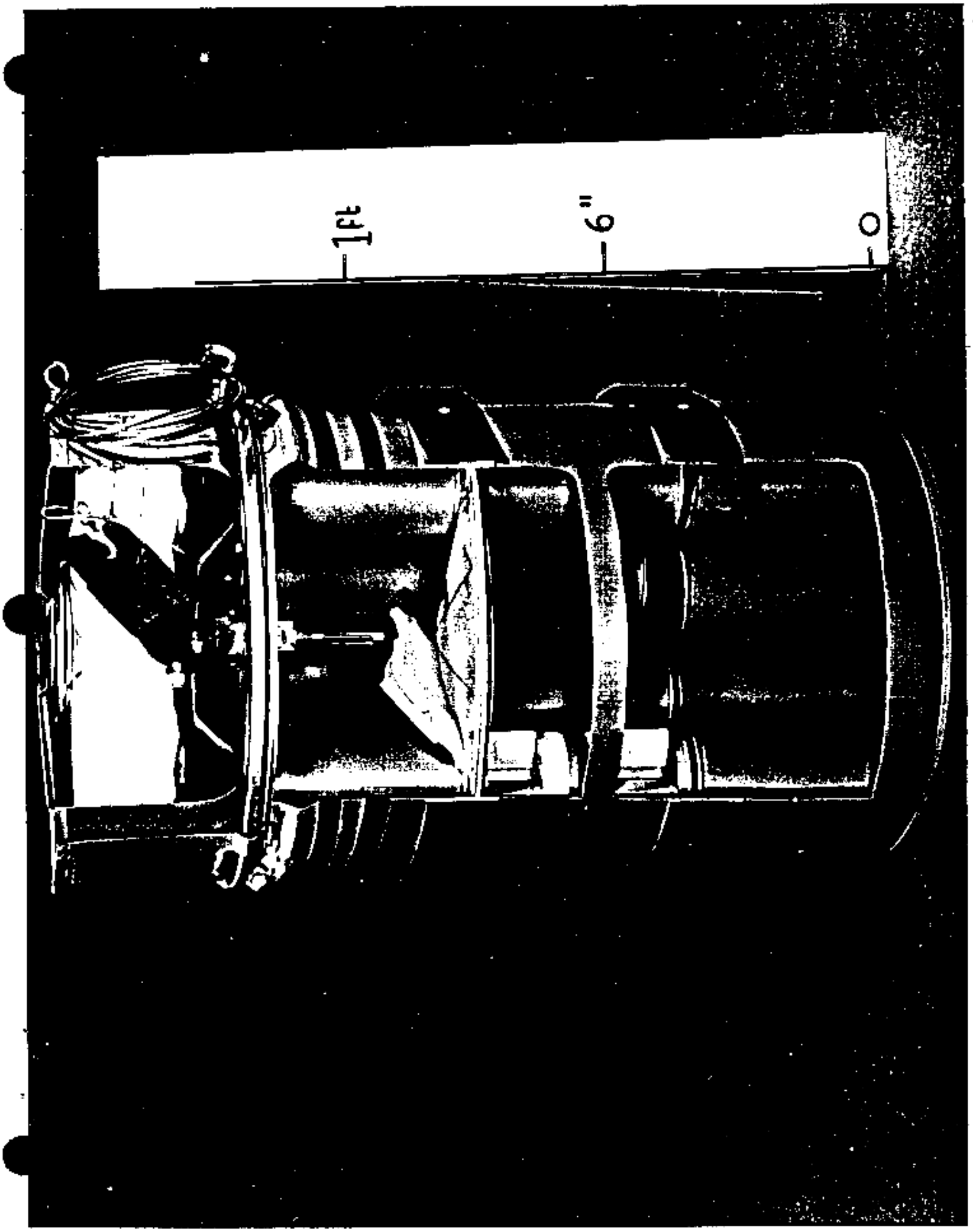

FIGURE A-7. M16 BZ GENERATOR

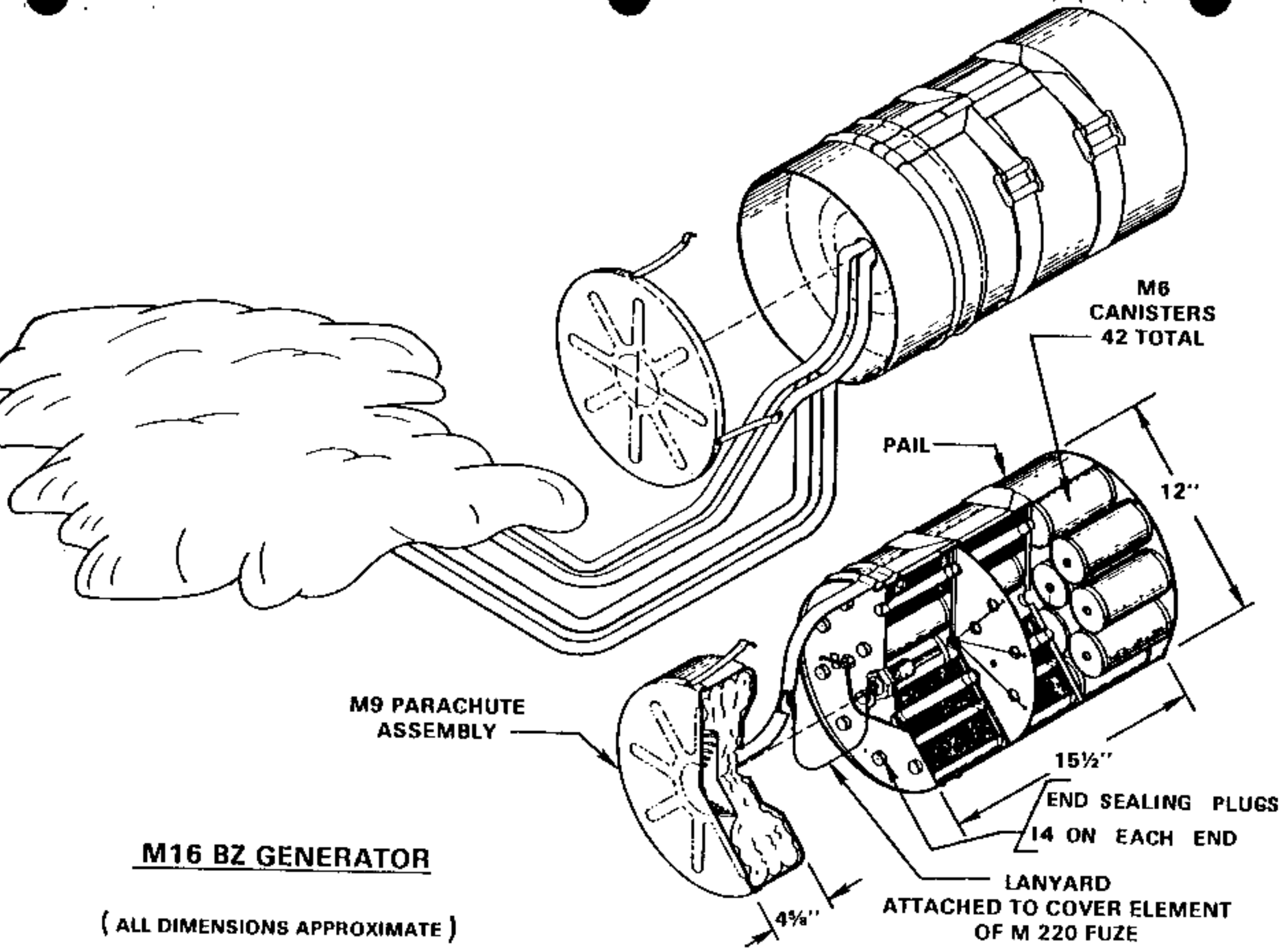

FIGURE A-8. M16 GENERATORS FOR THE M44 MUNITION

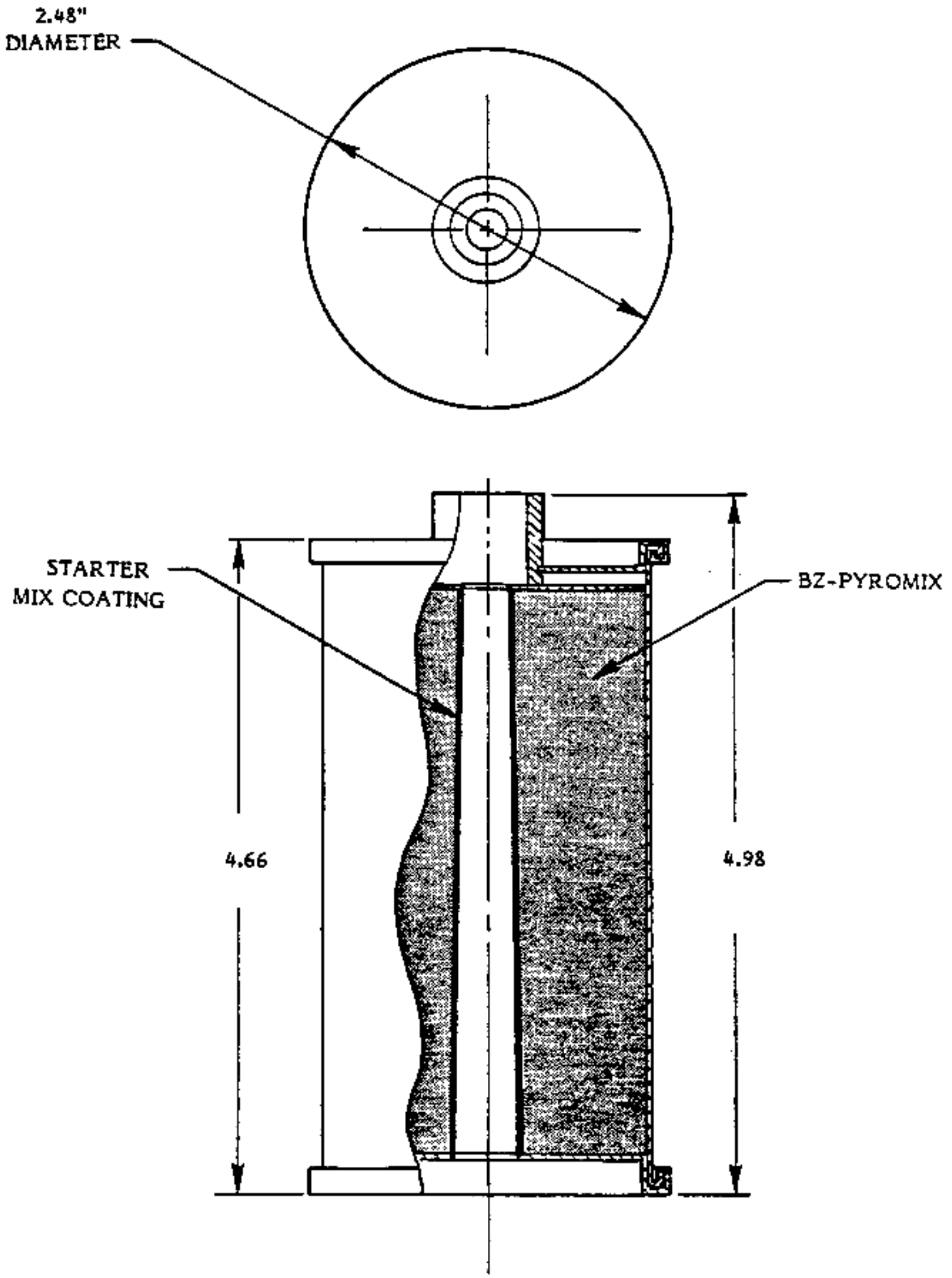

FIGURE A-9. M6 CANISTER FOR M44 MUNITION

APPENDIX B

RESISTANCE PROBE DATA REDUCTION

APPENDIX B

Resistance Probe Data Reduction

The resistance probe circuit is shown in Figure B-1. It consists of the detonation probe supply circuit connected to the detonation probe and to the recording device. The constant current supply makes the output voltage to the recording device proportional to the resistance to ground. In operation, the switch is turned first to "operate" and the output current is adjusted to make the output voltage near the upper limit of the recording scale being used on the recording device to provide optimum resolution of recording. Once the current is adjusted, it is not further changed intentionally. However, in practice the current from the supply remained constant over short time periods, but drifted slowly upwards over longer time periods, such as the time between calibration measurements and shot time. To compensate for this drift, calibration measurements made before the test were adjusted at the time of the experiments with the aid of the pre-detonation baseline voltage measured from the actual detonation probe dynamic voltage record.

Three initial calibration voltage measurements were made at the recording device:

V_{o1} obtained with the switch in the "operate" position,

$V_{cal\ 1}$ obtained with the switch in the "120 ohm cal" position,

and

V_{g1} obtained with the switch in the "short" position.

These three measurements were made over a short time period to insure against current drift in the constant current supply. The measurement of V_{o1} was repeated after measurement of V_{g1}. No change in V_{o1} assured that the initial measuring current I, had indeed remained constant. From Ohms' Law we wrote

$$V_{o1} = I_1 R_p \tag{1}$$

$$V_{cal\ 1} = I_1 (R_{sw} + R_{cal}) \tag{2}$$

$$V_{g1} = I_1 R_{sw} \tag{3}$$

where

R_p = is the total resistance in the probe circuit

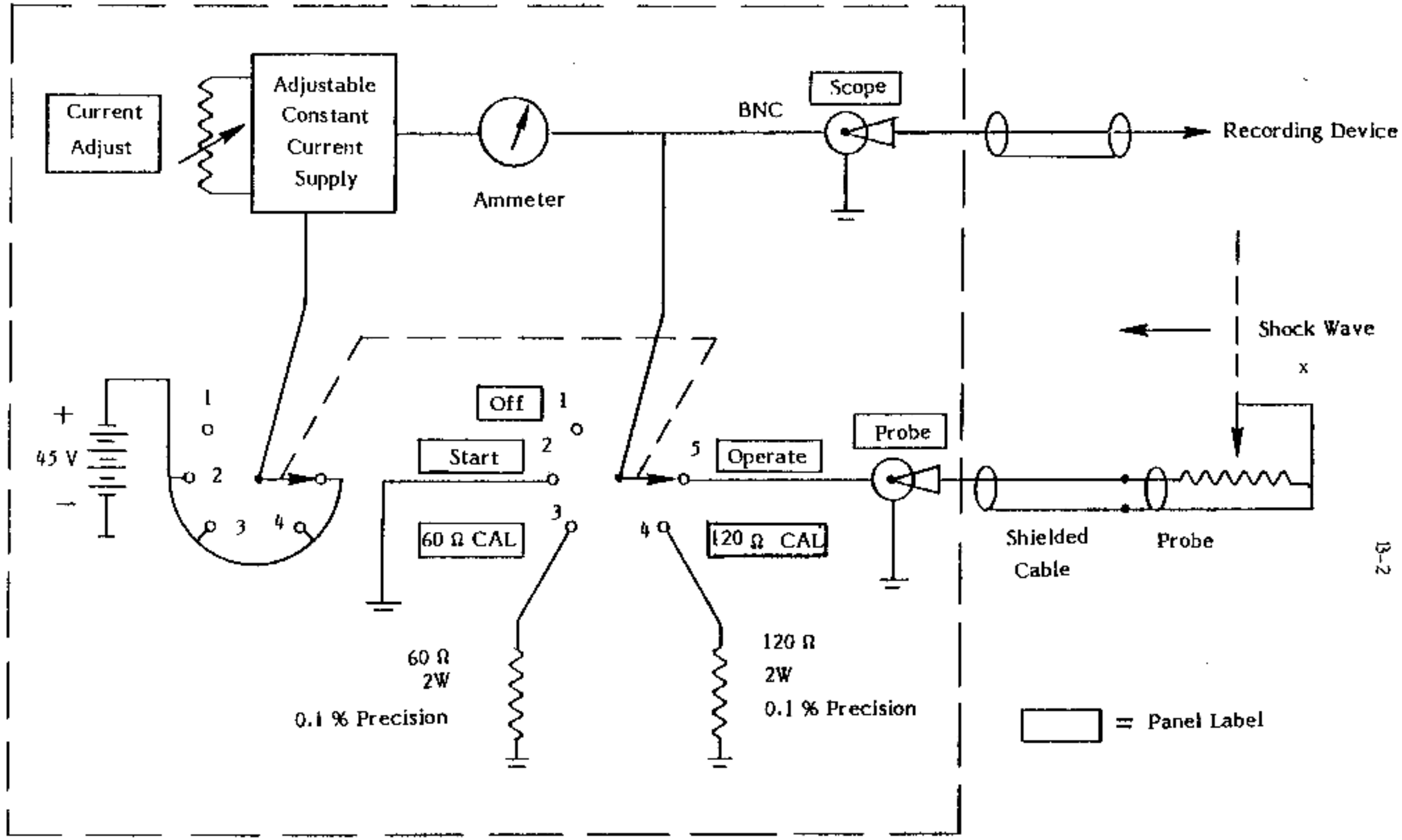

Detonation Probe Supply Circuit

FIGURE B-1. DETONATION PROBE CIRCUIT

R_{sw} = resistance of the switch contacts and directly associated circuitry

R_{cal} = resistance of precision resistance = 120 Ω

By subtracting (3) from (2) the unknown switch contact resistance was eliminated, or at least errors from this source reduced, and an expression for the initial measuring current was obtained:

$$I_1 = (V_{cal\ 1} - V_{g1})/R_{cal} \tag{4}$$

After the shot was fired (switch in operate position), a measurement of the initial, predetonation baseline voltage, say V_{o2} yielded:

$$R_p = V_{o2}/I_2 \tag{5}$$

where I_2 = the measuring current at shot time

This expression for R_p was equated to the value of R_p from equation (1) yielding:

$$\frac{I_1}{I_2} = \frac{V_{o1}}{V_{o2}} \tag{6}$$

Finally the value of the total probe resistance is given by

$$R_p = R_{ld} + r_p (L - x) \tag{7}$$

where

R_{ld} is the resistance of the connecting lead wires to the probe

r_p is the specific resistance of the probe wire (in the present case r_p = 0.2892 Ω/mm or 88.15 Ω/ft).

L is the total length of the probe resistance wire

and

x is the length of probe resistance shorted out by crushing of the surrounding tube by the shock wave pressure. This is taken as the shock wave position which is the value to be determined.

At shot time, V_{o2} from (5) and (7) is given by:

$$V_{o2} = I_2 (R_{id} + r_p L) \tag{8}$$

and V_s the dynamic value of the signal voltage during the shot is given by

$$V_s = I_2 (R_{id} + r_p (L-x)) \tag{9}$$

By subtracting V_s (9) from V_{o2} (8) the unknown probe lead resistance R_{id} and the probe total length were eliminated. The resultant expression solved for x:

$$x = (V_{o2} - V_s)/I_2 r_p. \tag{10}$$

The value for I_2 was found from equations (6) and (4) and substituted into (10) to yield the final expression for x in terms of known constants or measured quantities:

$$x = \frac{R_{cal}}{r_p} \frac{V_{o1}}{V_{o2}} \frac{(V_{o2} - V_s)}{(V_{cal\ 1} - V_{g1})}. \tag{11}$$

In practice, evaluation of (11) merely meant subtracting the time varying signal V_s from the constant V_{o2} and multiplying the difference by the experimentally derived constant for each experiment of $R_{cal}\ V_{o1}/r_p V_{o2}\ (V_{cal\ 1} - V_{g1})$. (12)

The indicated operations were carried out by the signal processing capability of the Smartscope.

APPENDIX C

DETONATION PROBE TEST RECORDS

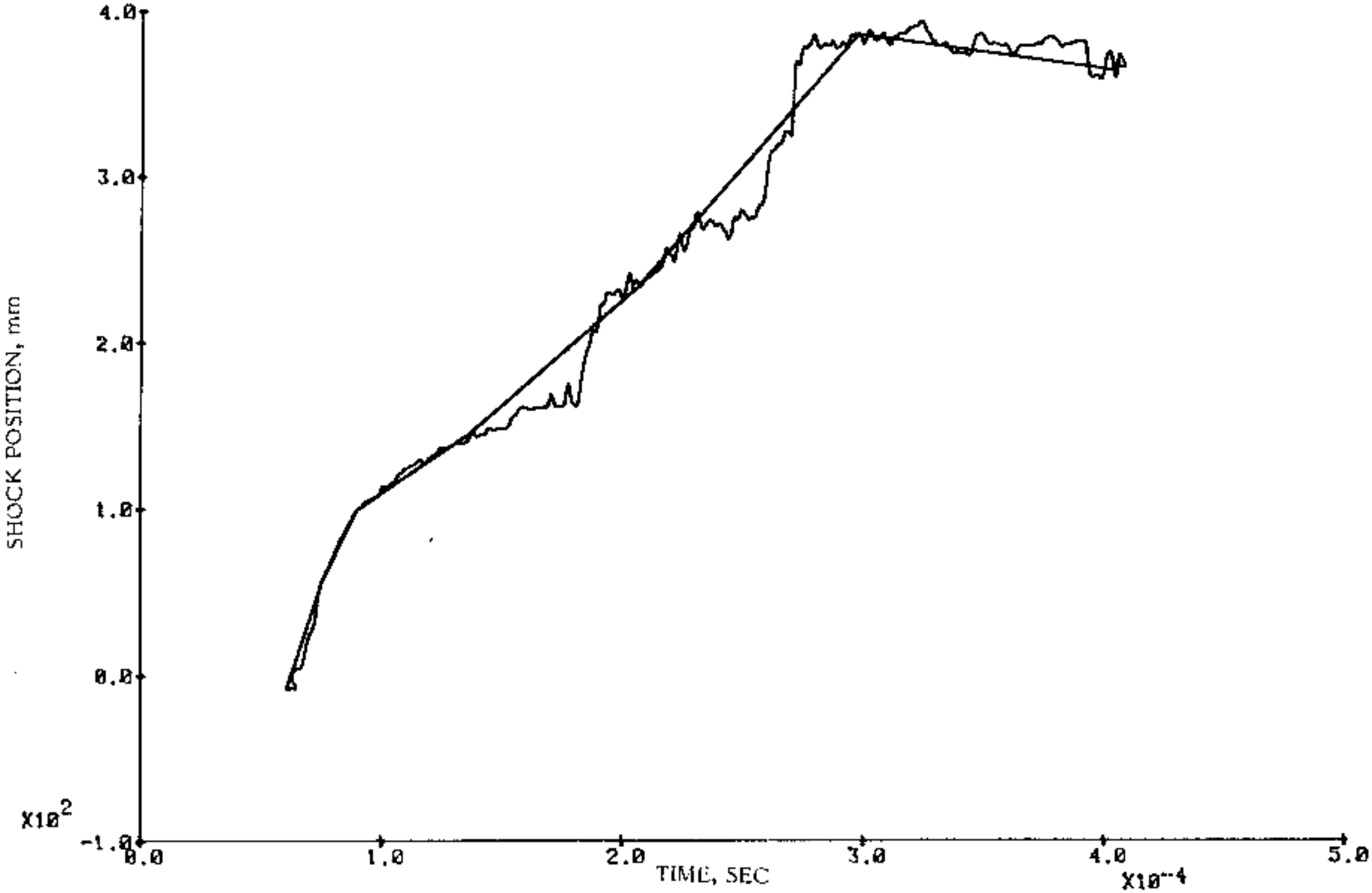

FIGURE C-1. RAW AND FINAL POSITION-TIME RECORD TEST D1

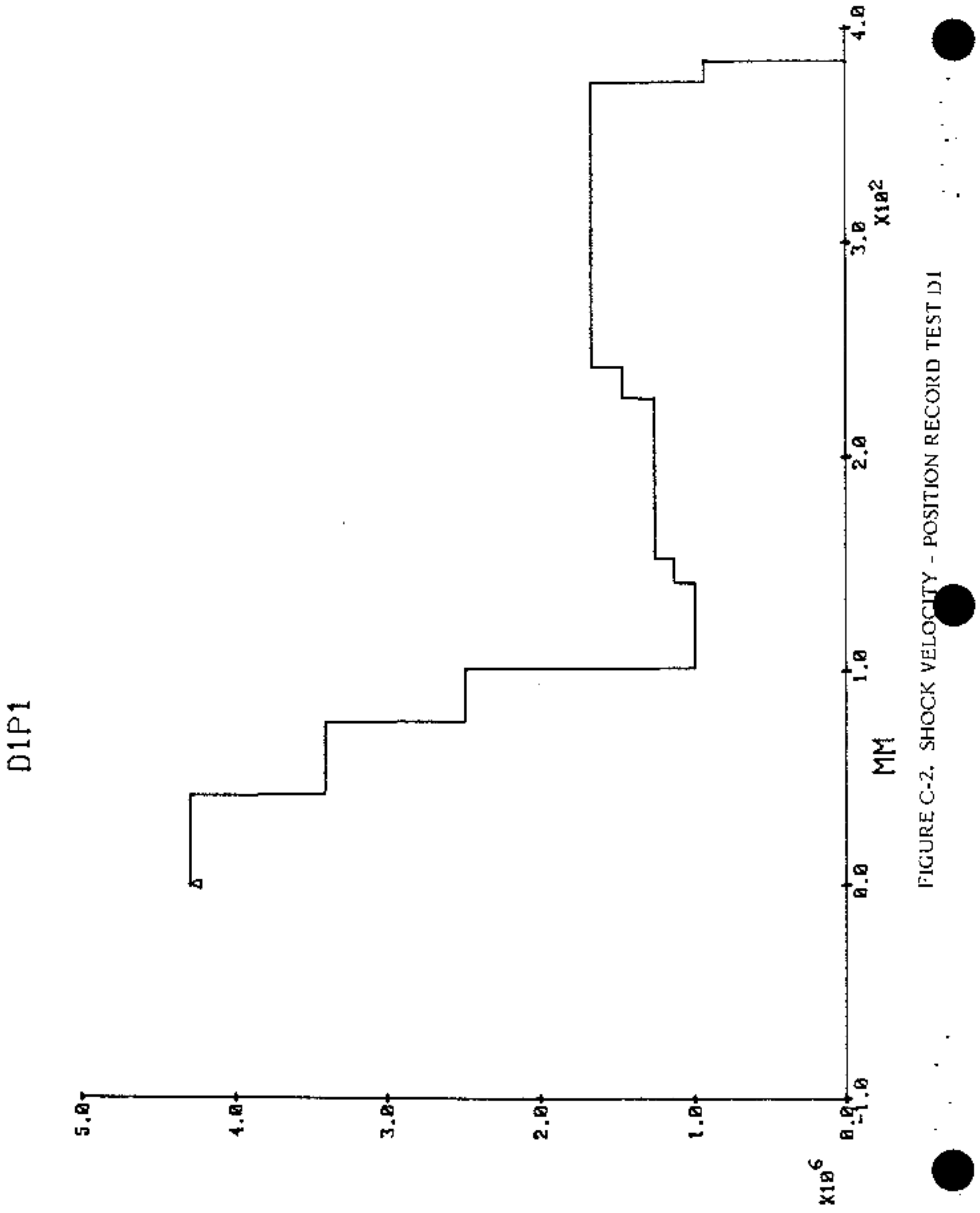

FIGURE C-2. SHOCK VELOCITY - POSITION RECORD TEST D1

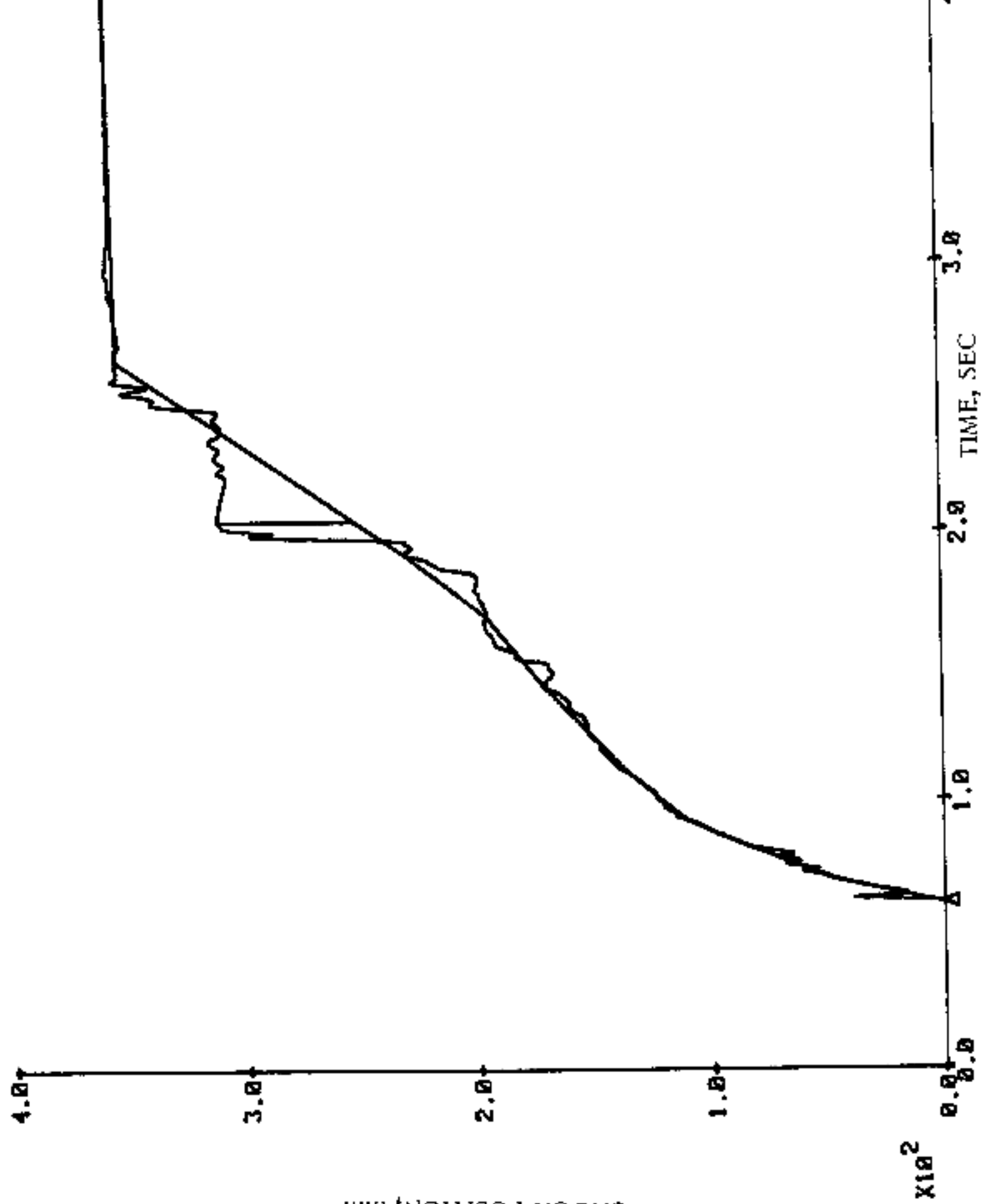

FIGURE C-3. RAW AND FINAL POSITION TIME RECORD TEST D2

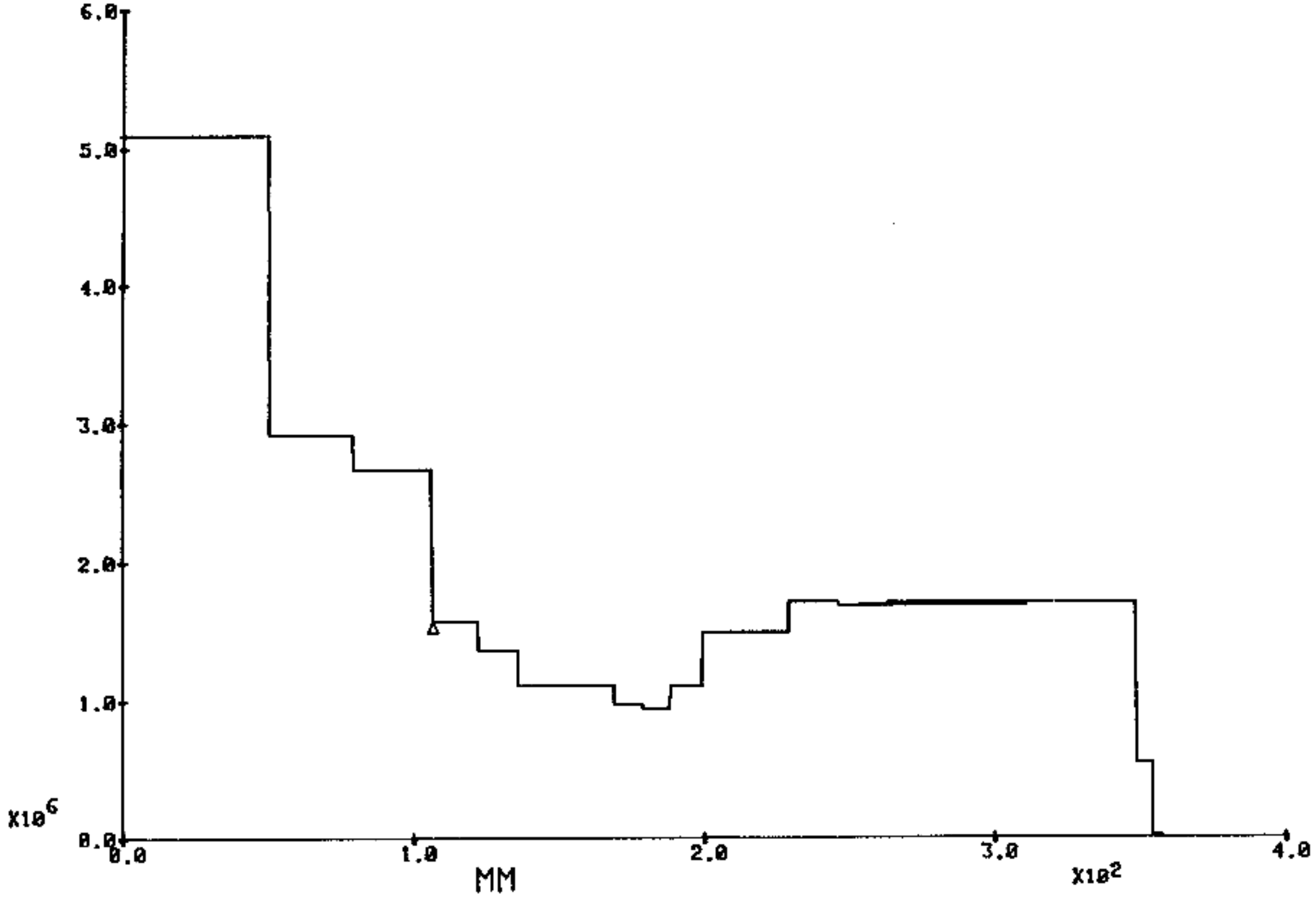

FIGURE C-4. SHOCK VELOCITY - POSITION RECORD TEST D2

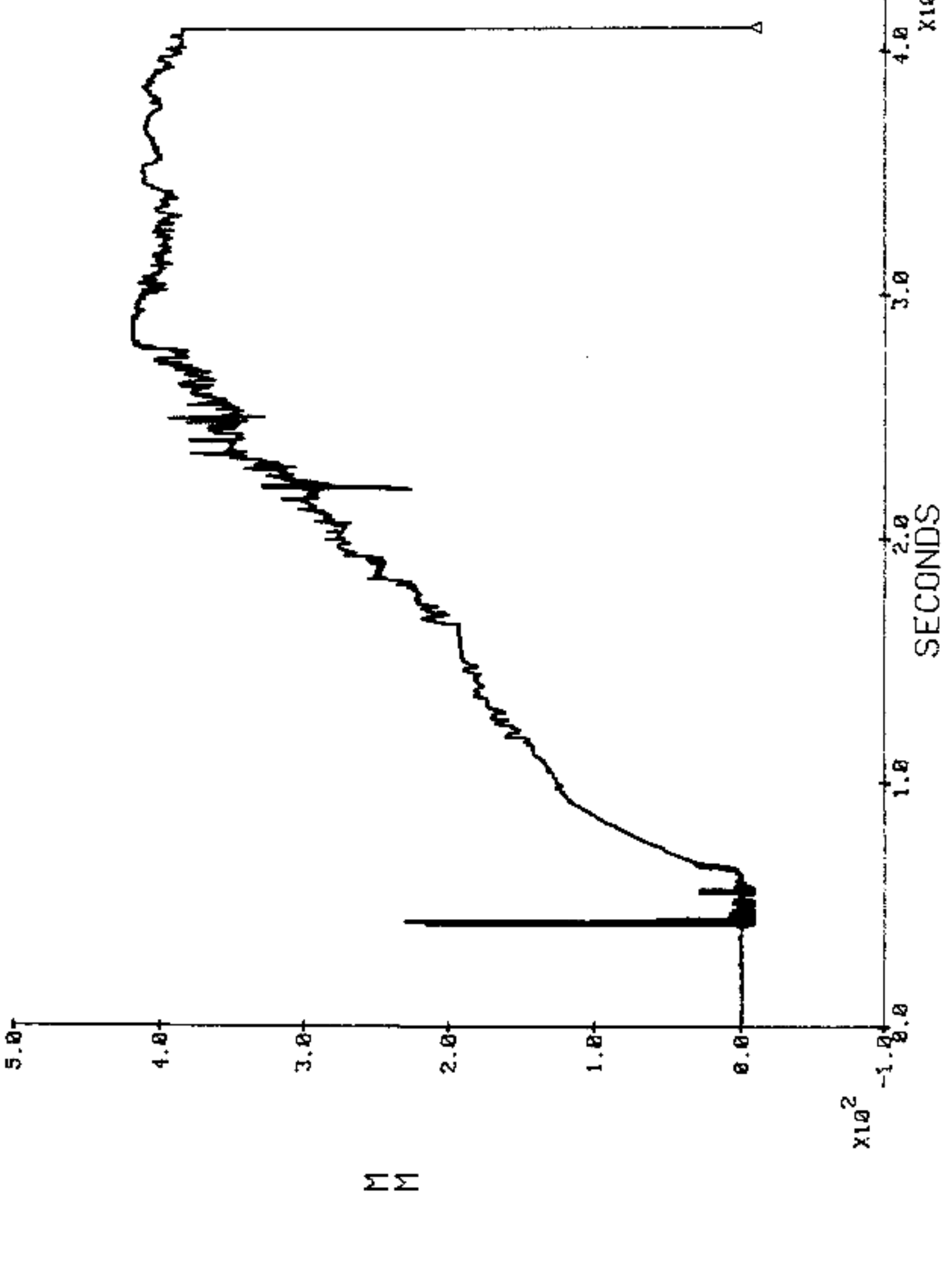

FIGURE C-5. RAW SHOCK POSITION - TIME RECORD TEST D3

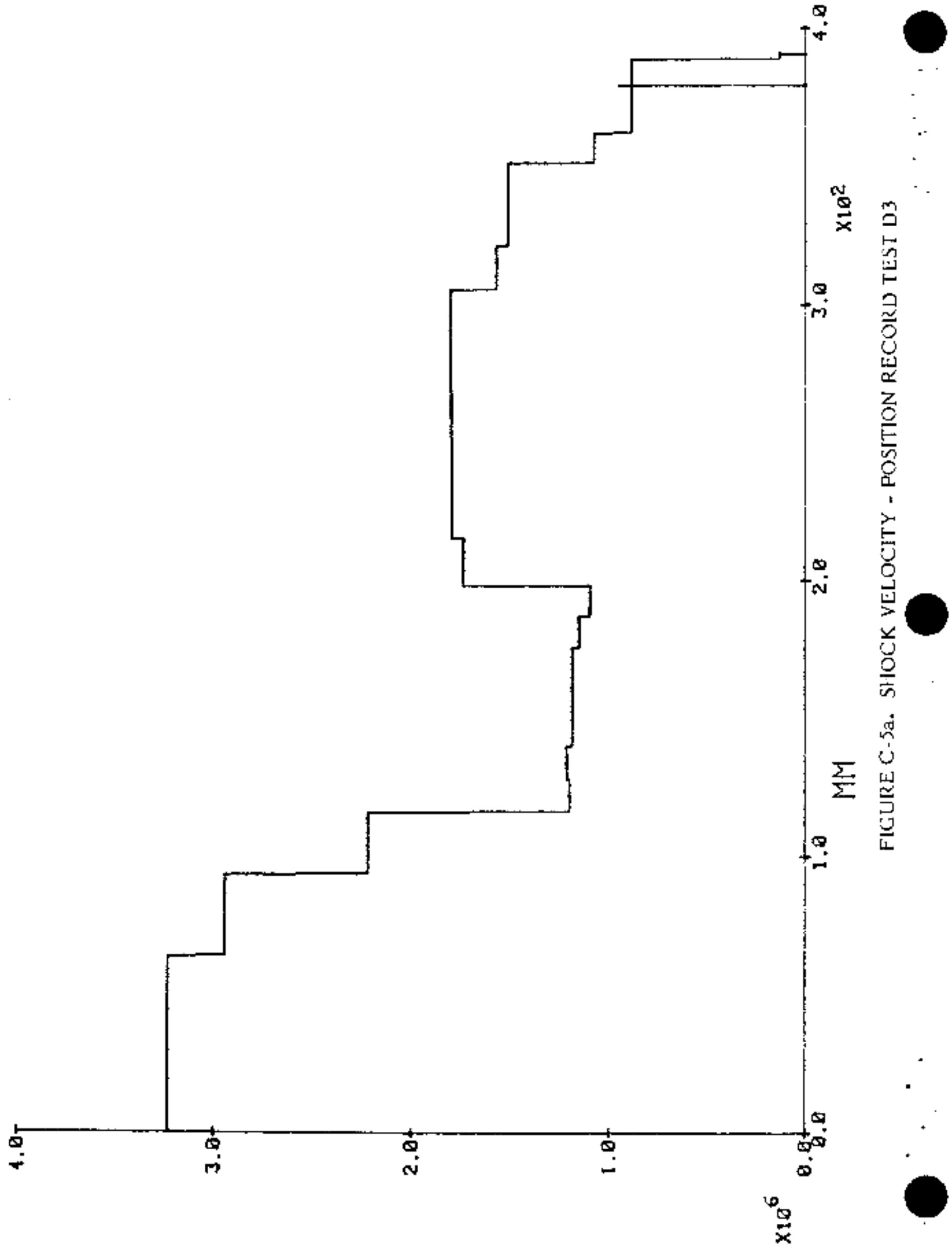

FIGURE C-5a. SHOCK VELOCITY - POSITION RECORD TEST D3

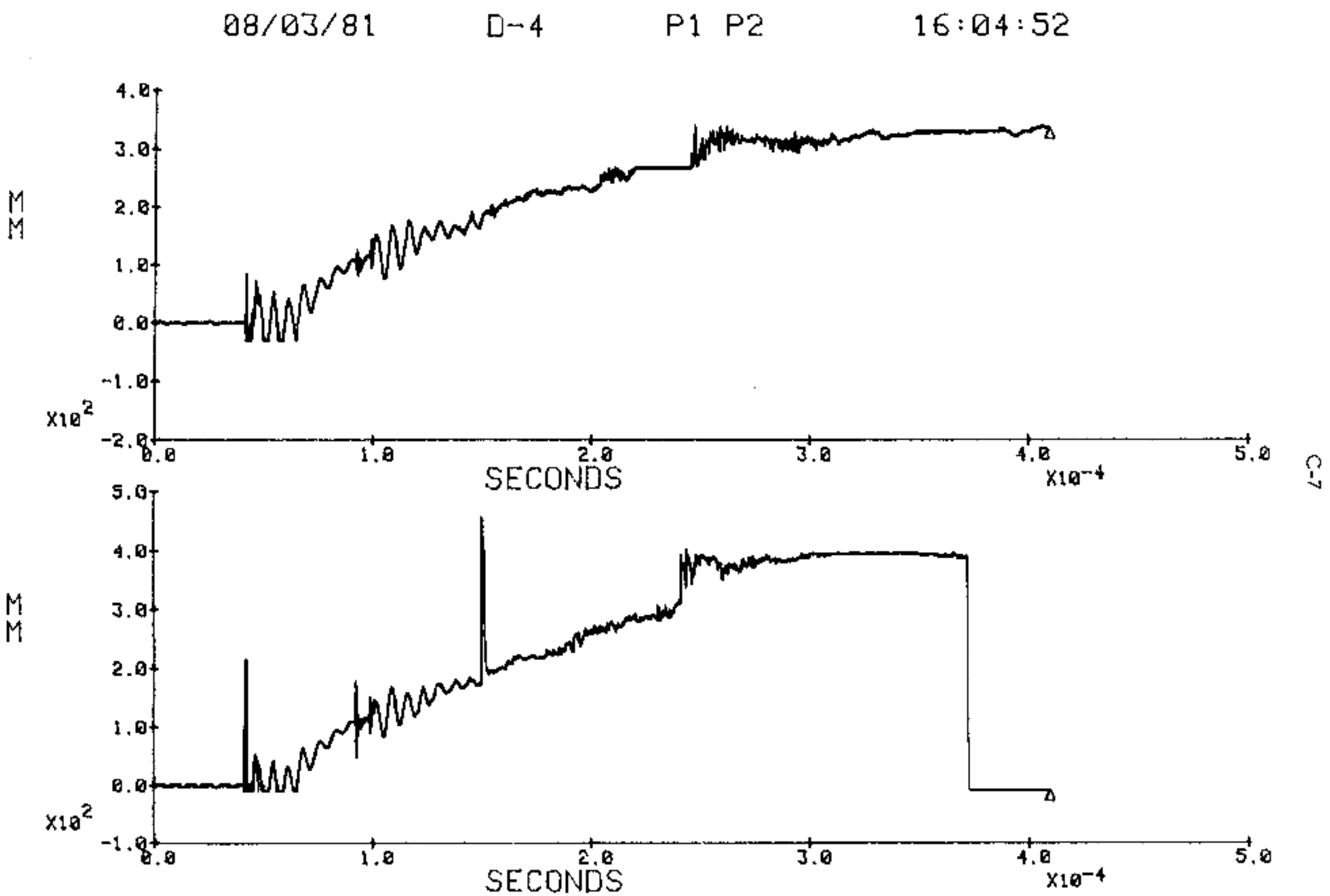

FIGURE C-6. RAW POSITION - TIME RECORDS TEST D4

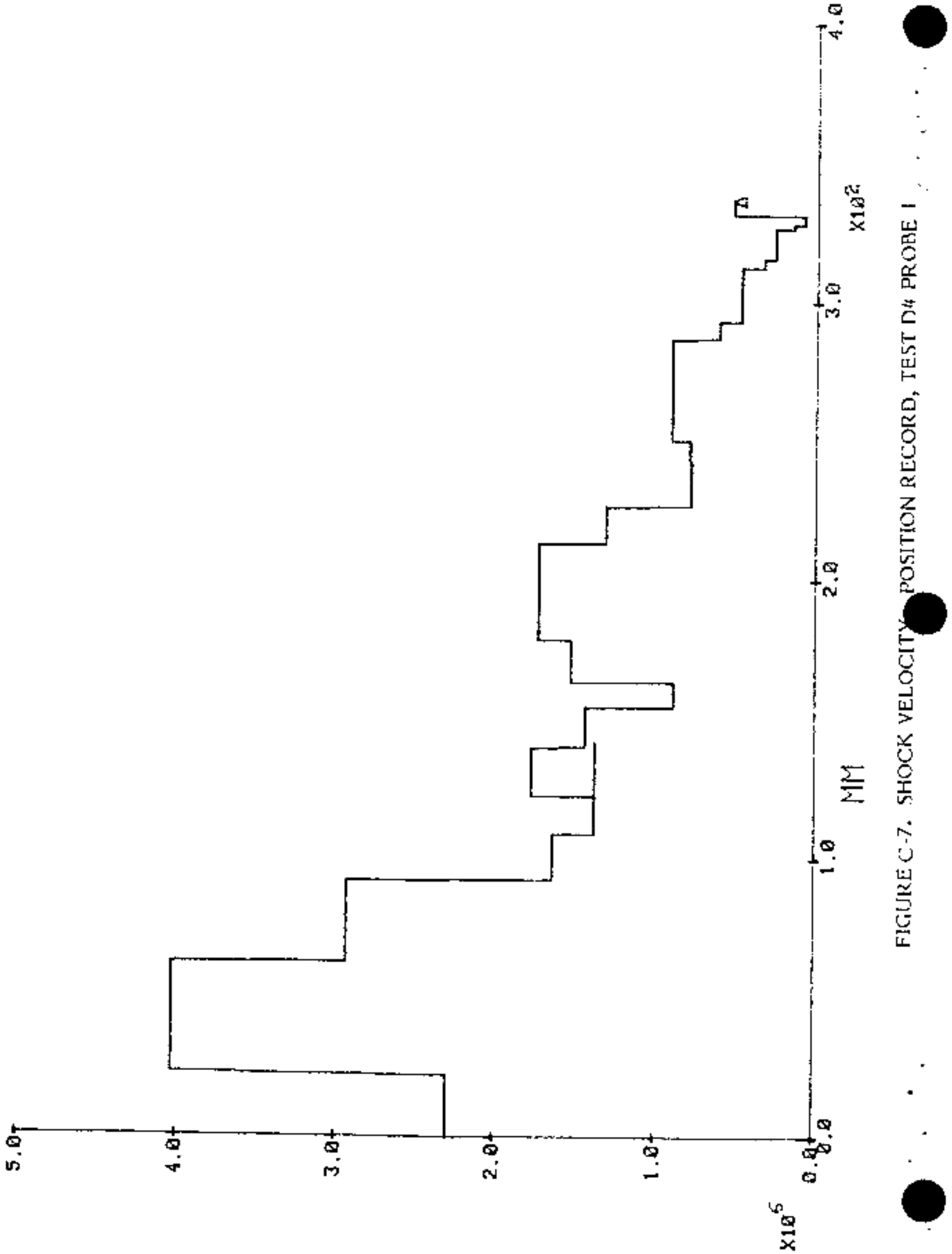

FIGURE C-7. SHOCK VELOCITY - POSITION RECORD, TEST D4 PROBE 1

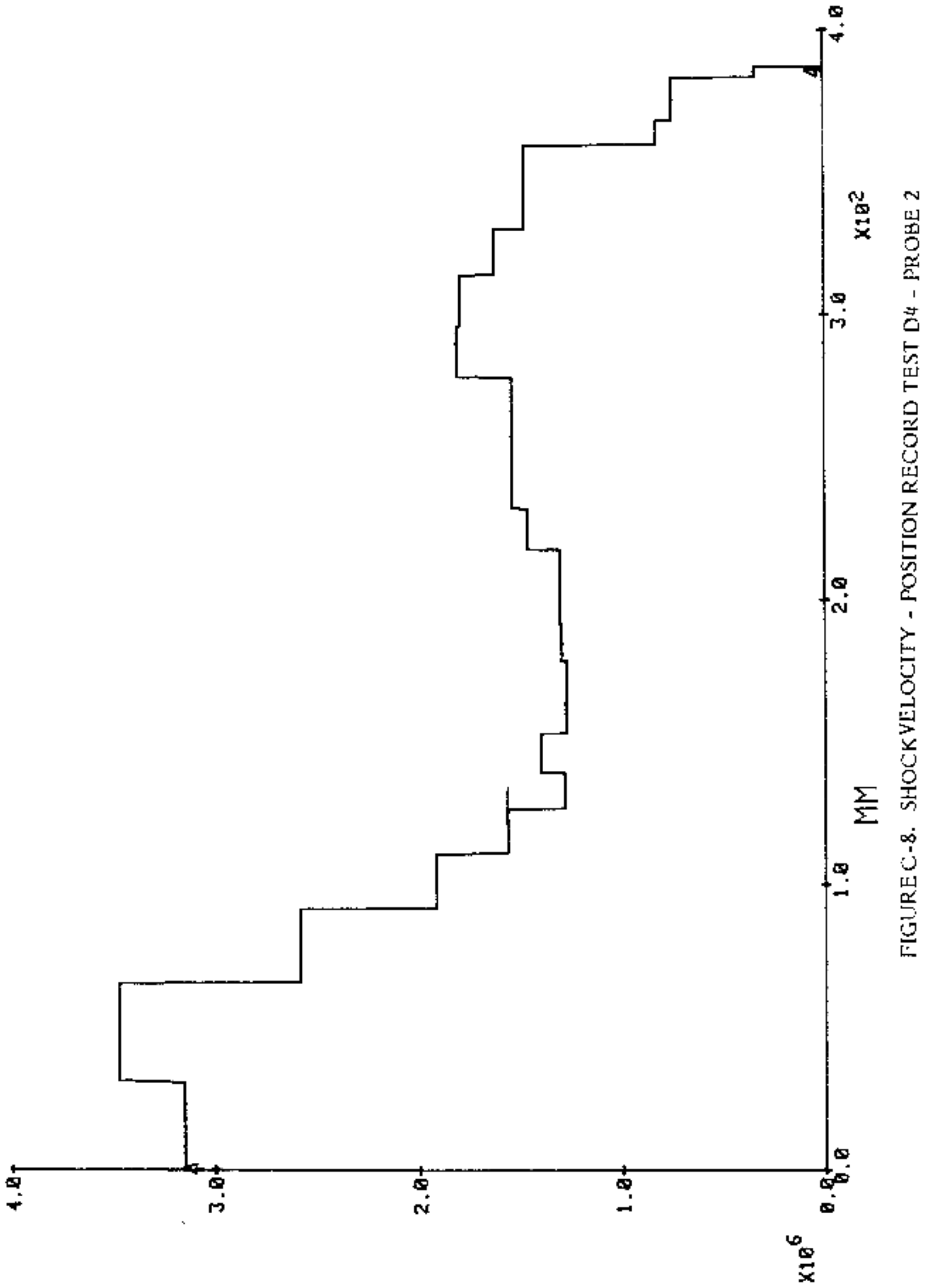

FIGURE C-8. SHOCKVELOCITY - POSITION RECORD TEST D4 - PROBE 2

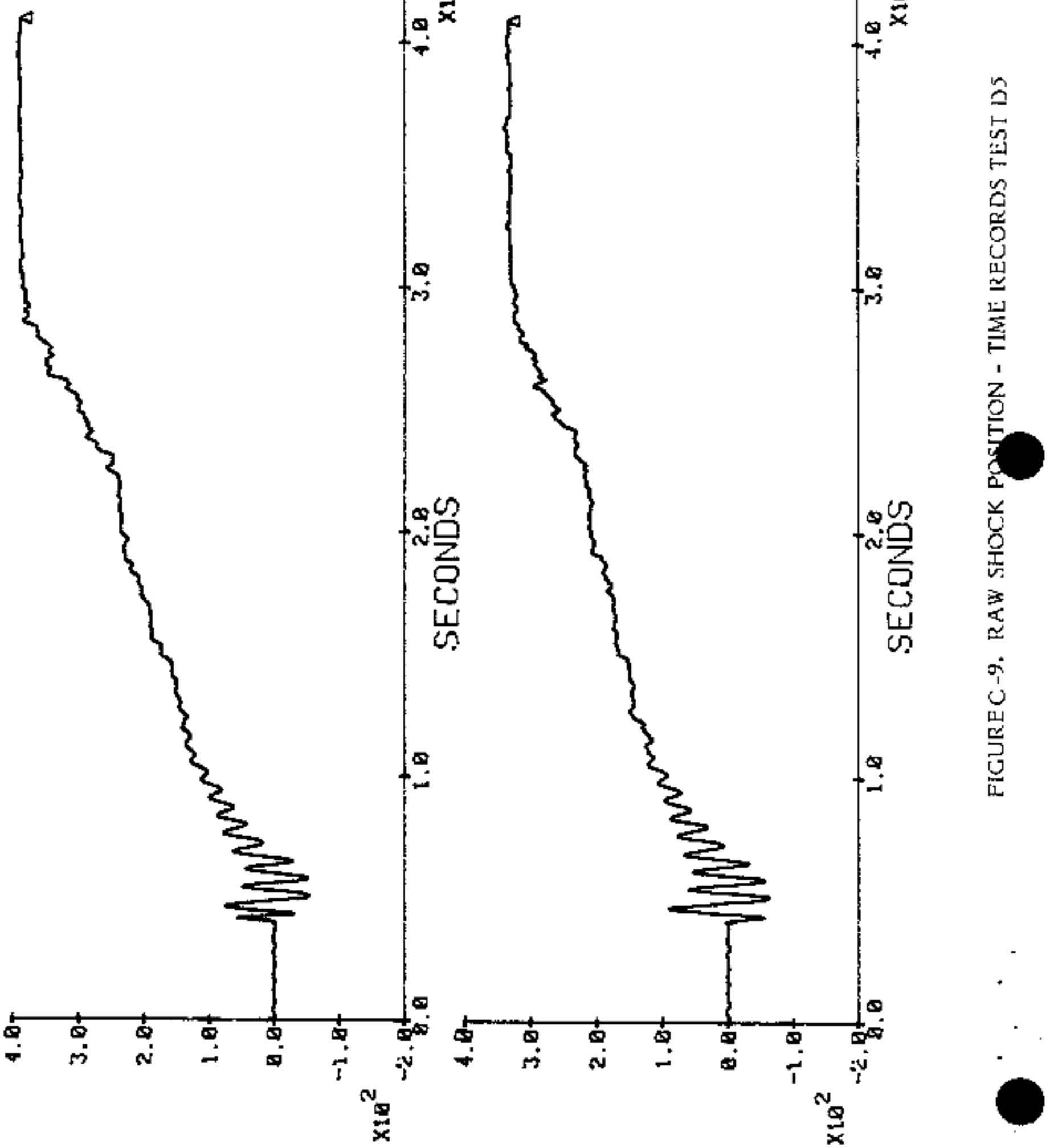

FIGUREC-9. RAW SHOCK POSITION - TIME RECORDS TEST D5

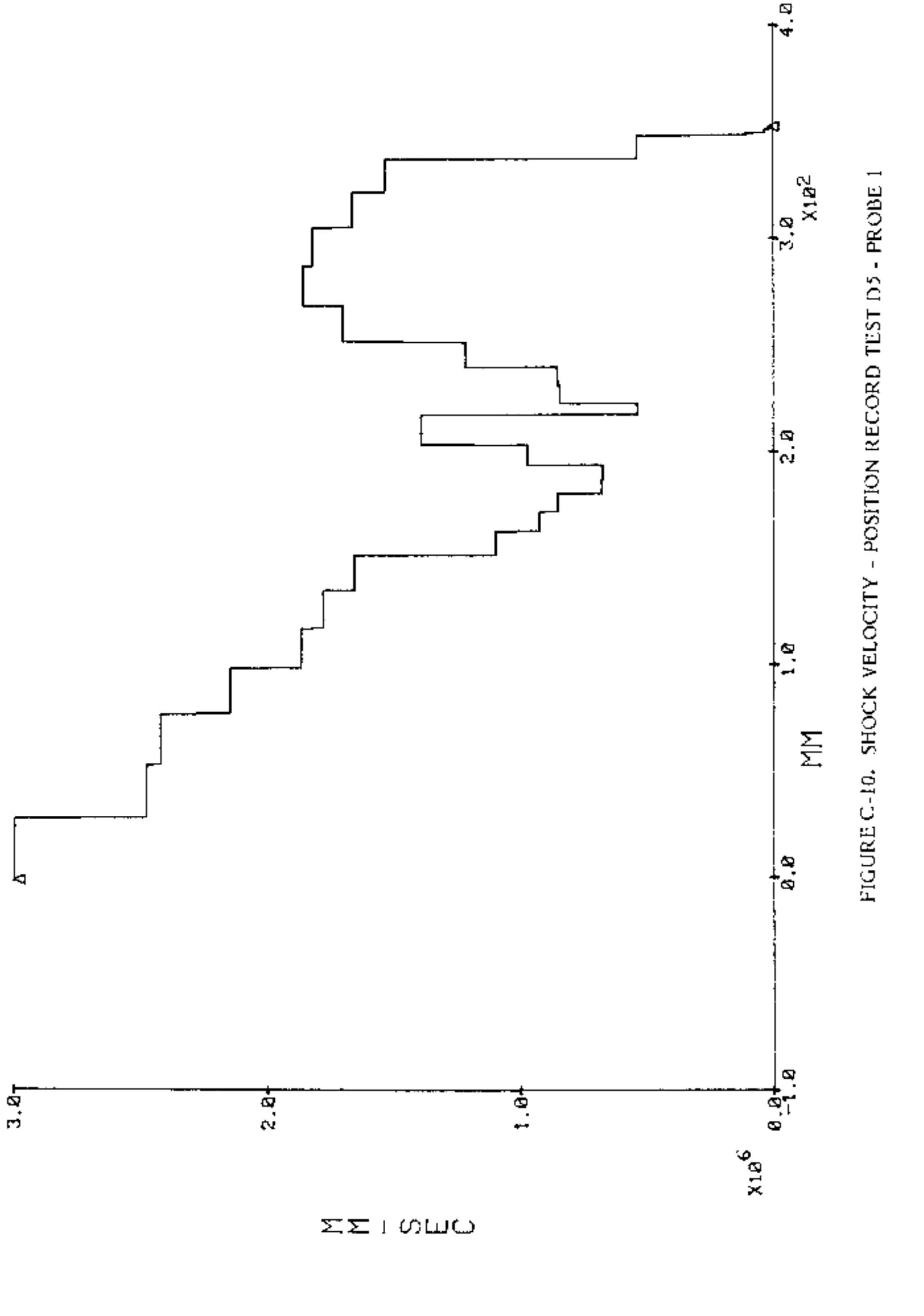

FIGURE C-10. SHOCK VELOCITY - POSITION RECORD TEST D5 - PROBE 1

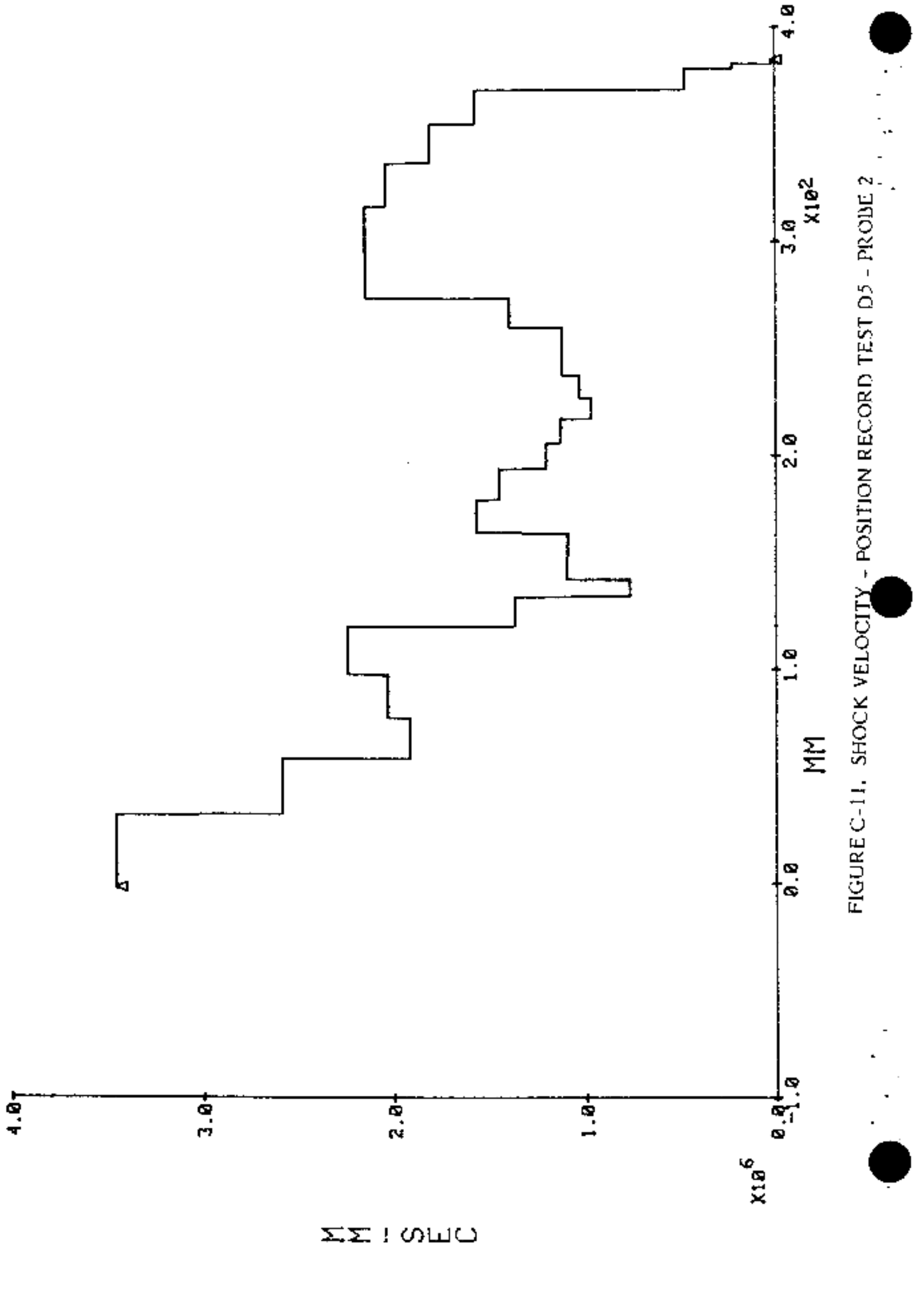

FIGURE C-11. SHOCK VELOCITY - POSITION RECORD TEST D5 - PROBE 2

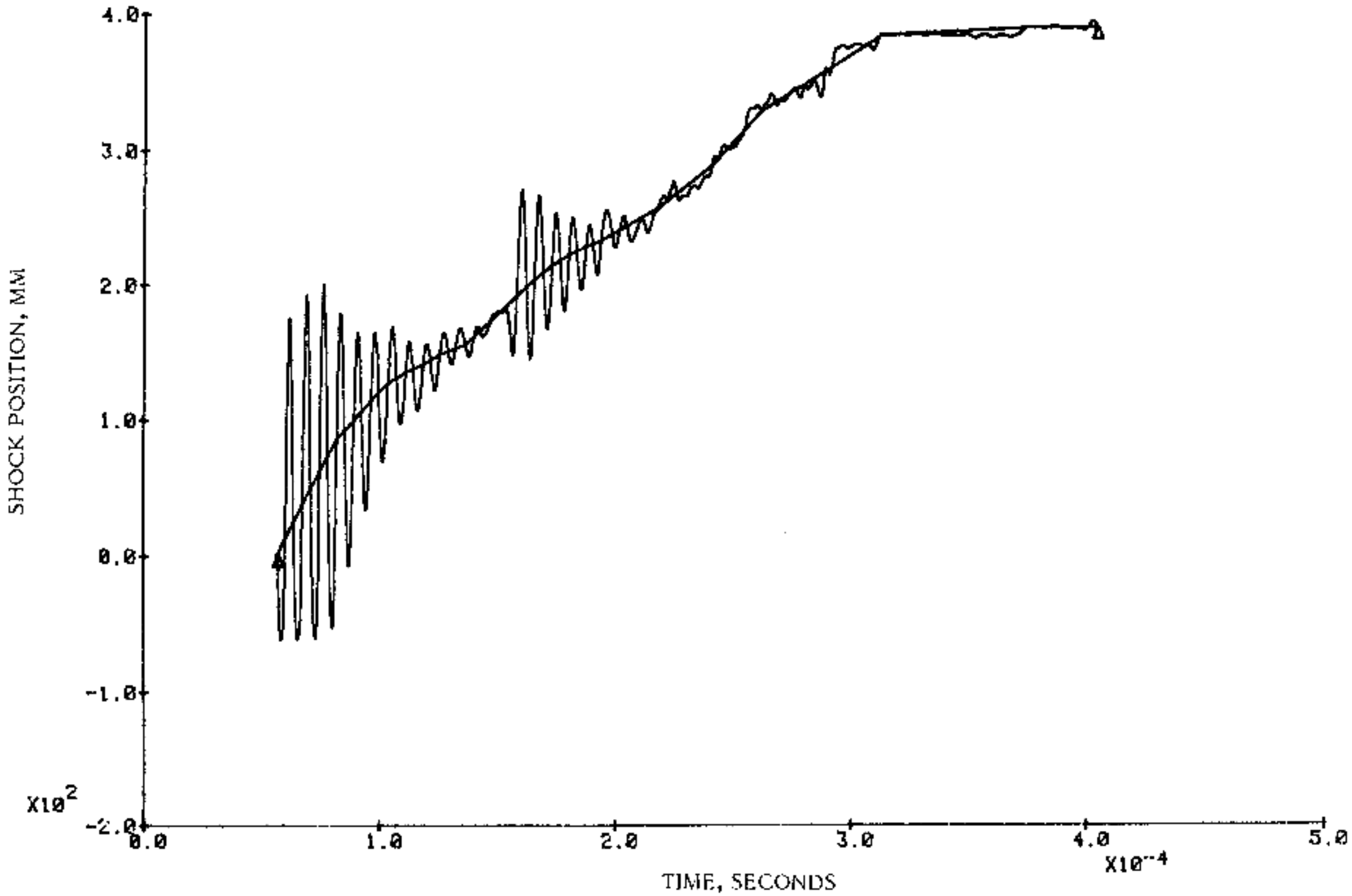

FIGURE C-12. RAW AND SMOOTHED POSITION-TIME RECORDS, TEST D6 PROBE 1

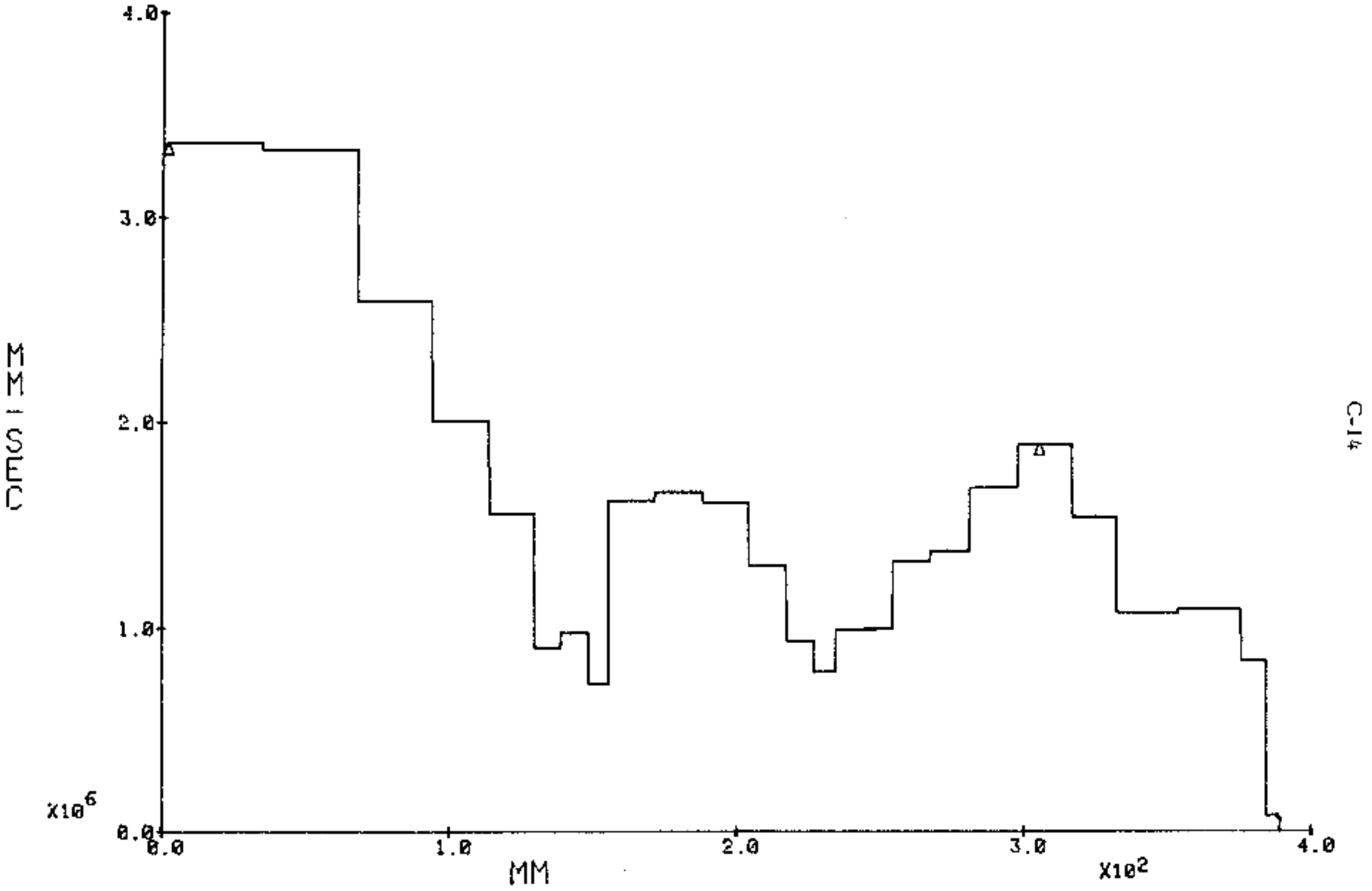

FIGURE C-13. SHOCK VELOCITY - POSITION RECORD, TEST D6 PROBE 1

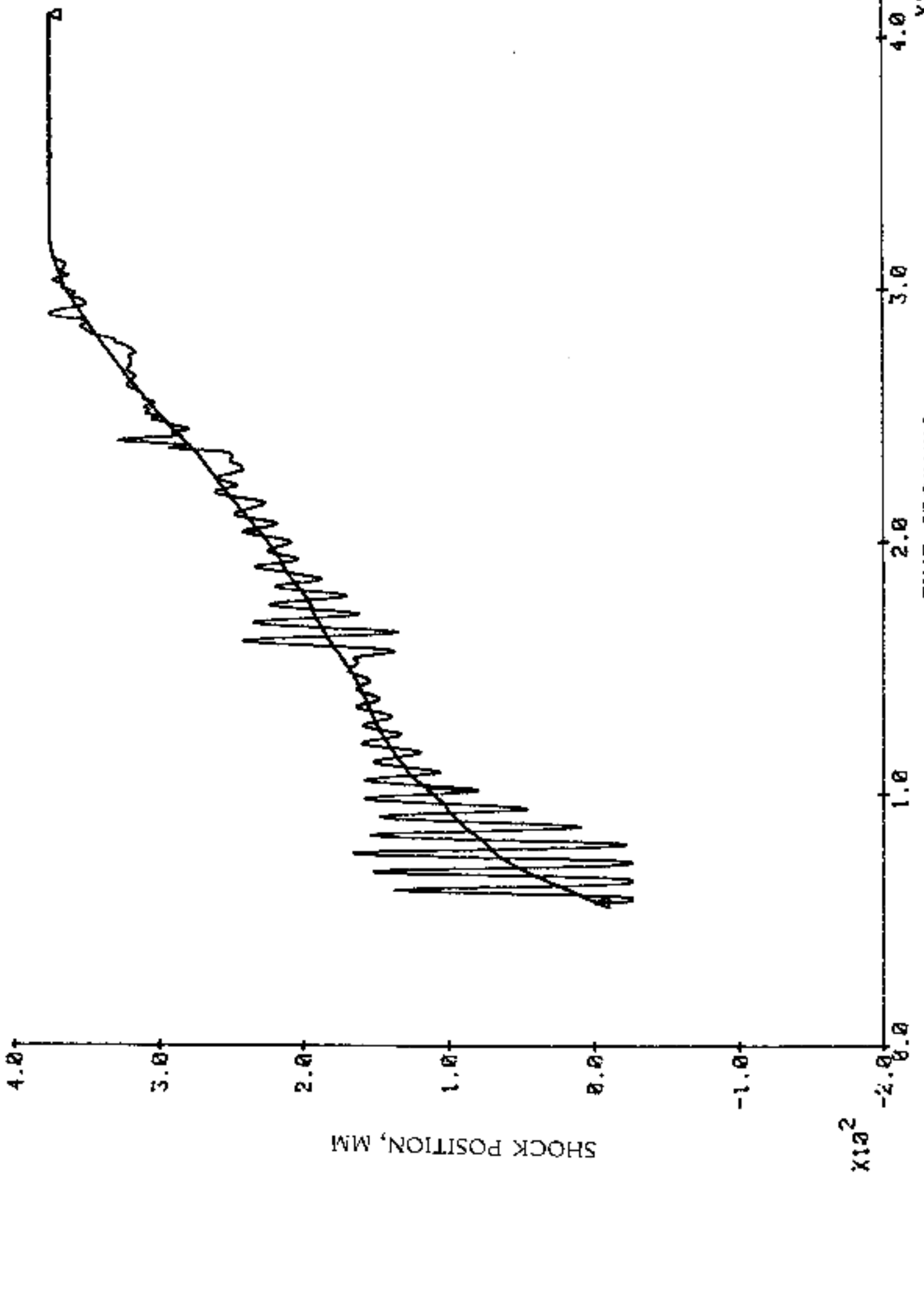

FIGURE C-14. RAW AND SMOOTHED POSITION-TIME RECORDS, TEST D6 PROBE 2

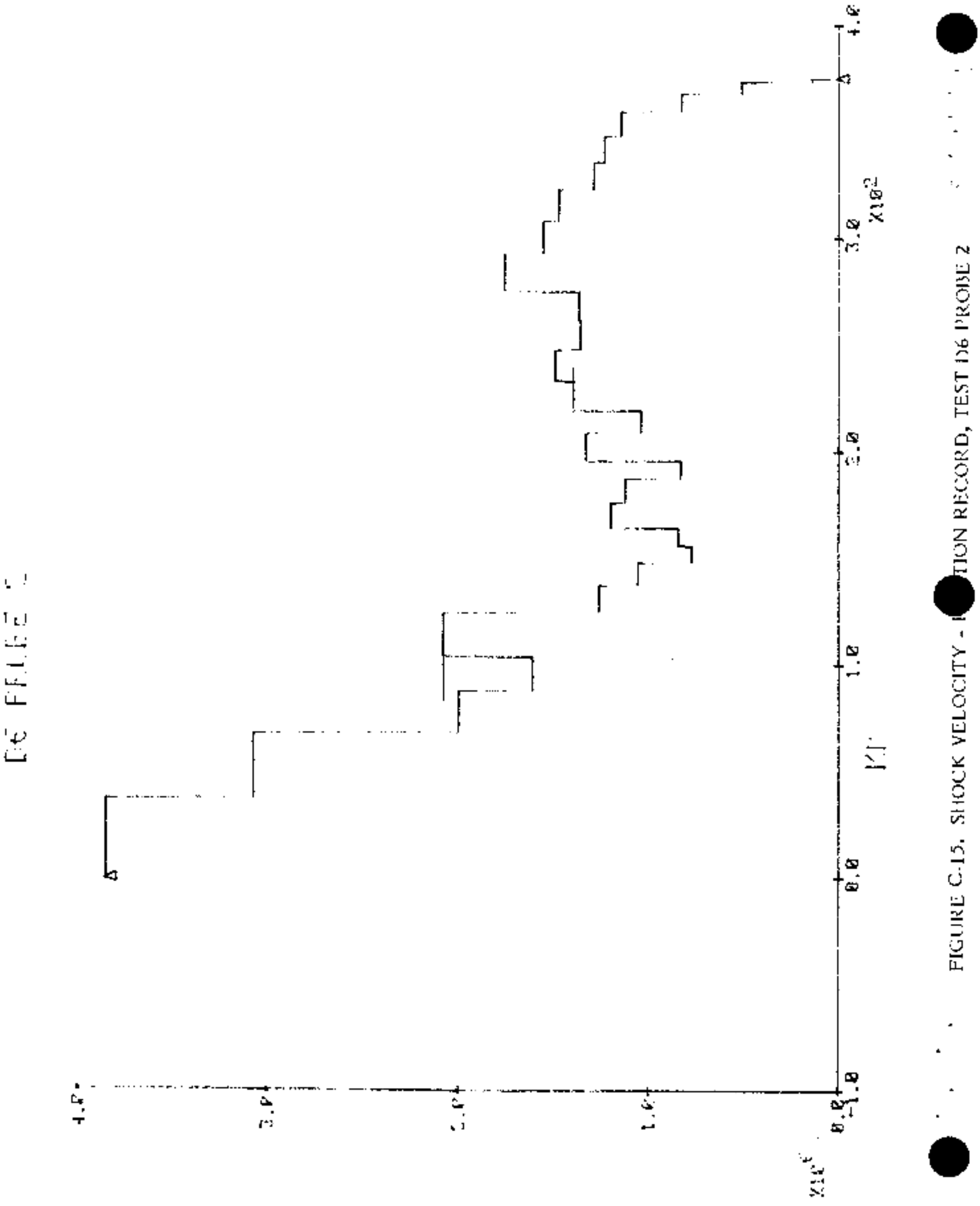

FIGURE C-15. SHOCK VELOCITY - PARTICLE VELOCITY RECORD, TEST 106 PROBE 2

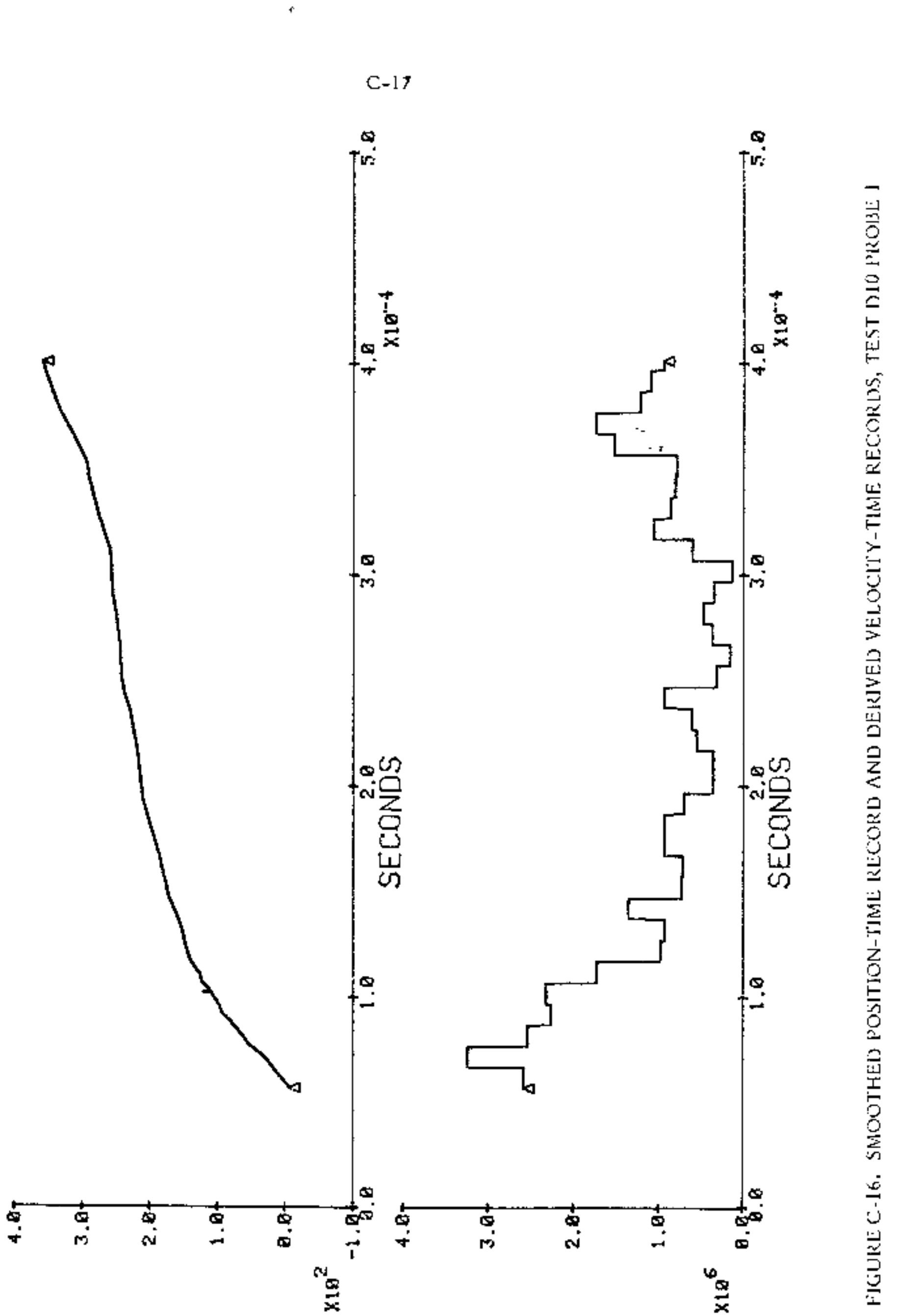

FIGURE C-16. SMOOTHED POSITION-TIME RECORD AND DERIVED VELOCITY-TIME RECORDS, TEST D10 PROBE 1

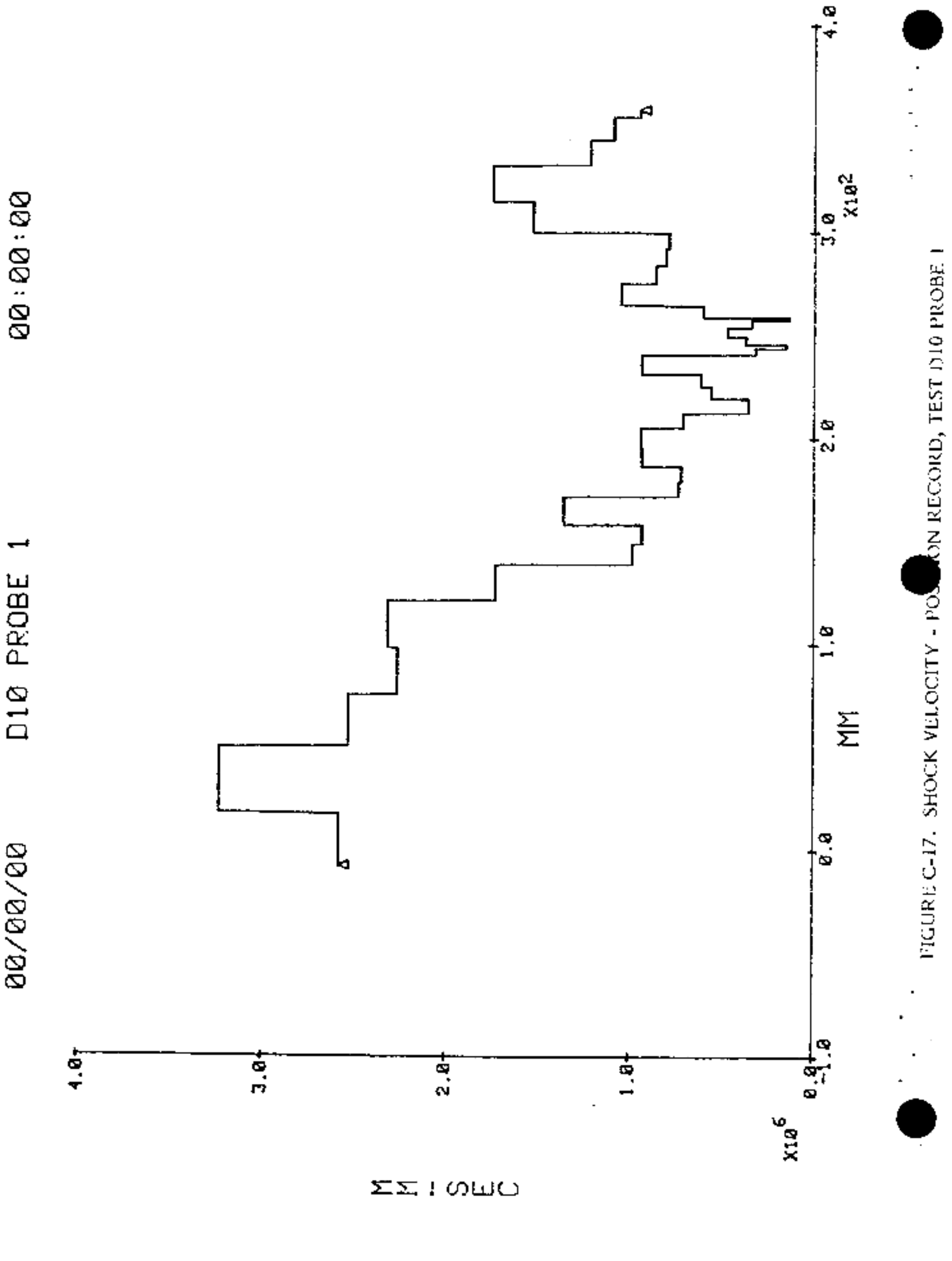

FIGURE C-17. SHOCK VELOCITY - POSITION RECORD, TEST D10 PROBE 1

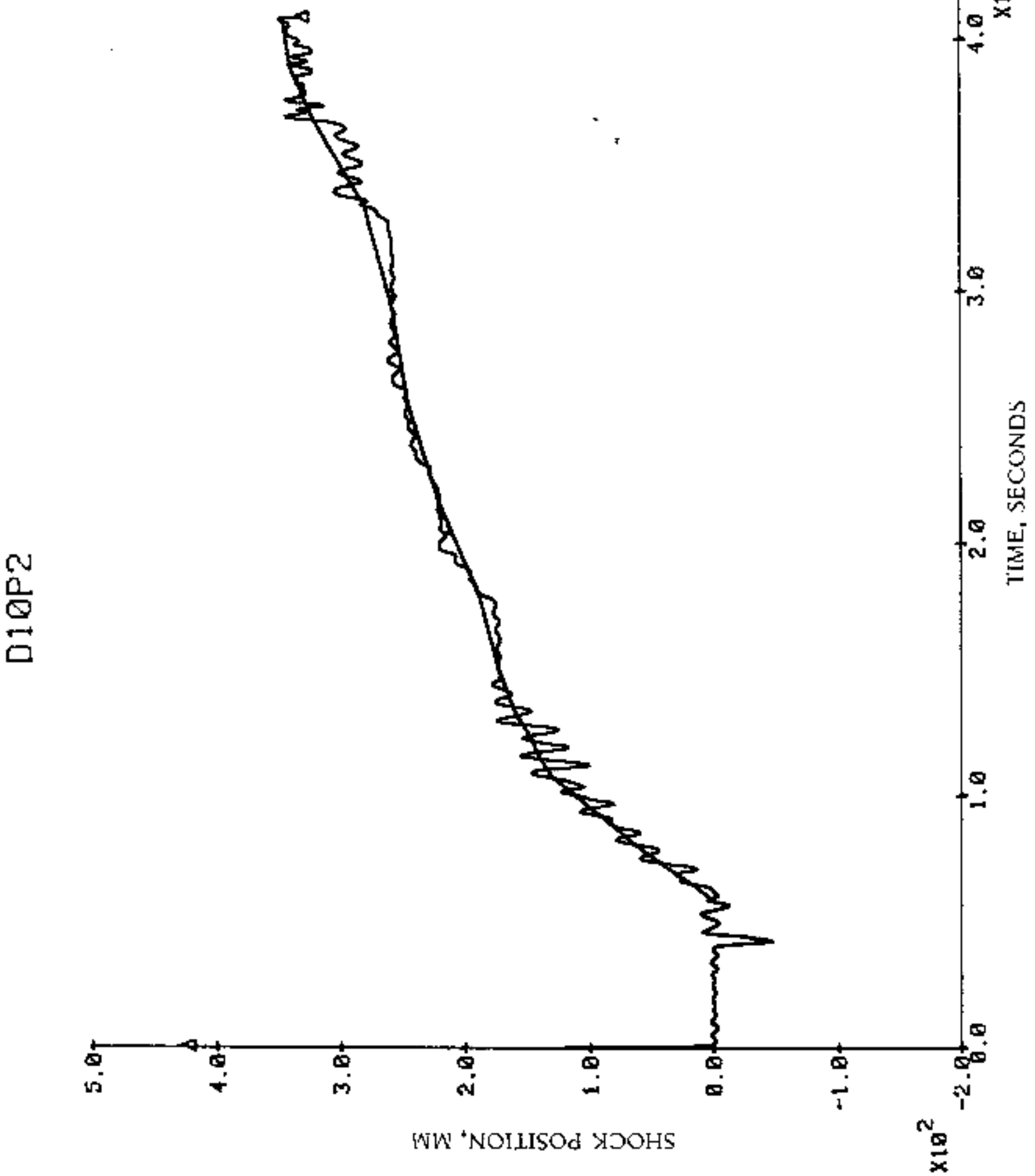

FIGURE C-18. RAW AND SMOOTHED POSITION-TIME RECORD, TEST D10 PROBE 2

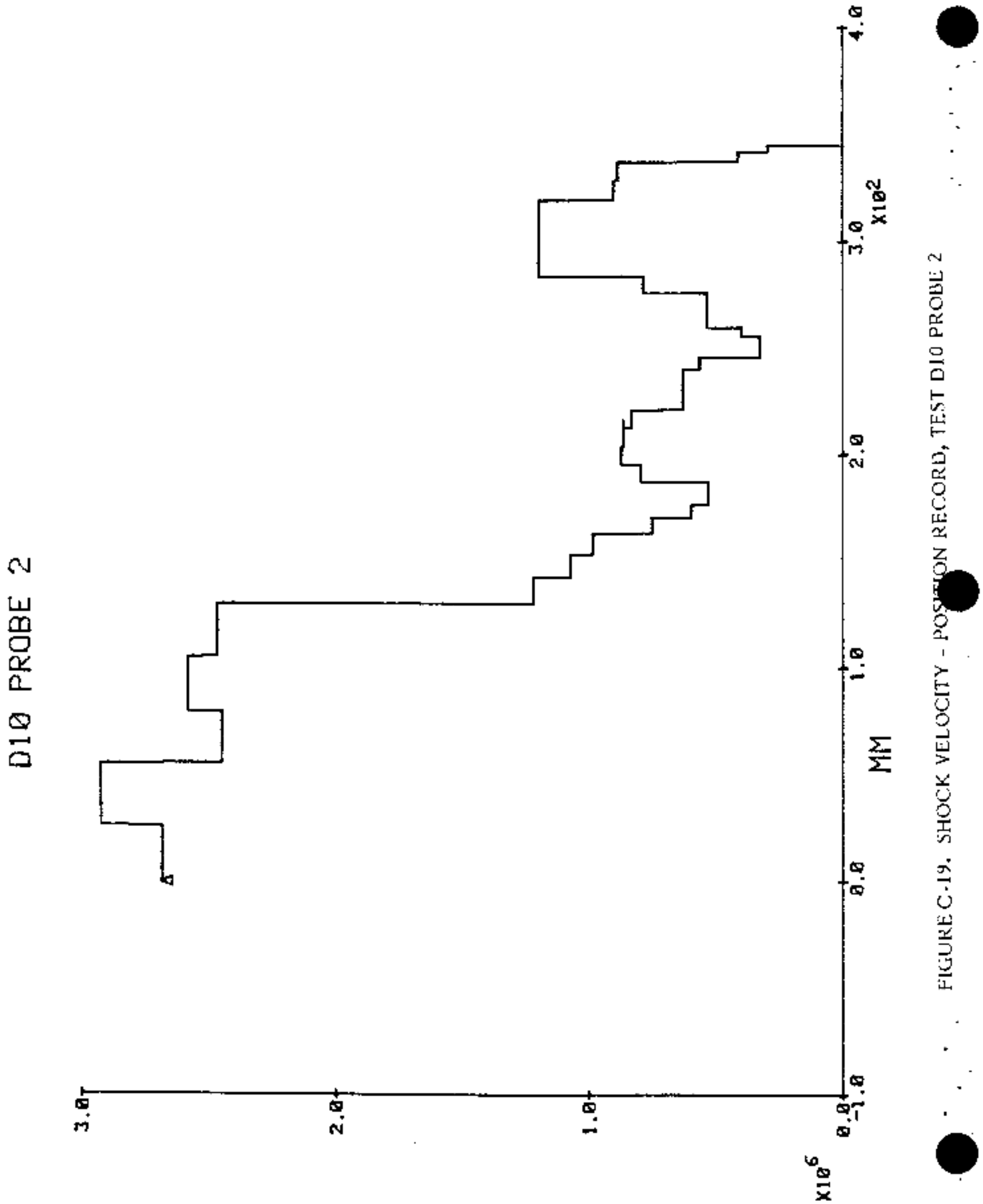

FIGURE C-19. SHOCK VELOCITY - POSITION RECORD, TEST D10 PROBE 2

FIGUREC-20. RAW AND SMOOTHED POSITION-TIME RECORD, TEST D11 PROBE 1

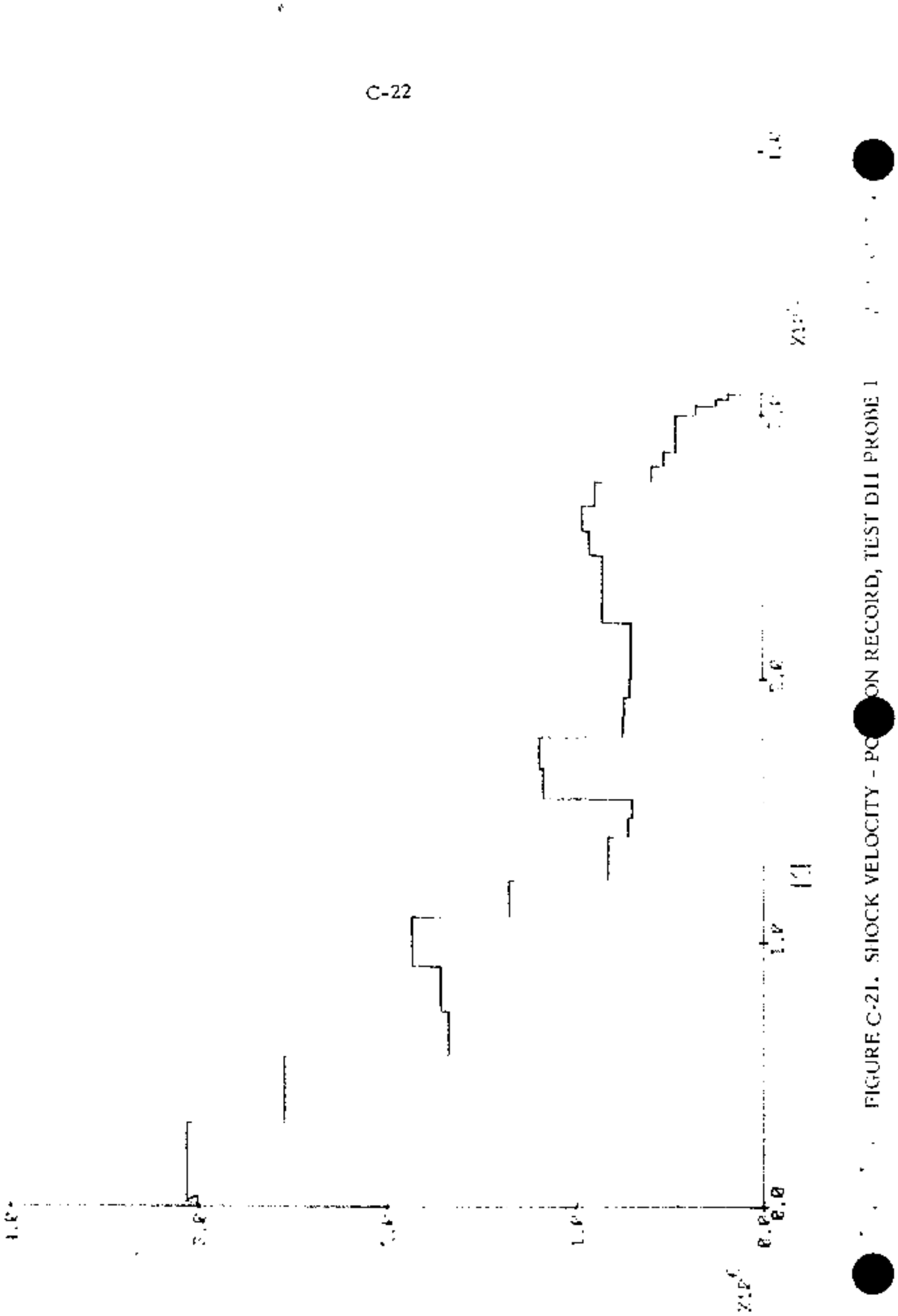

FIGURE C-21. SHOCK VELOCITY - PO[illegible]ON RECORD, TEST D11 PROBE 1

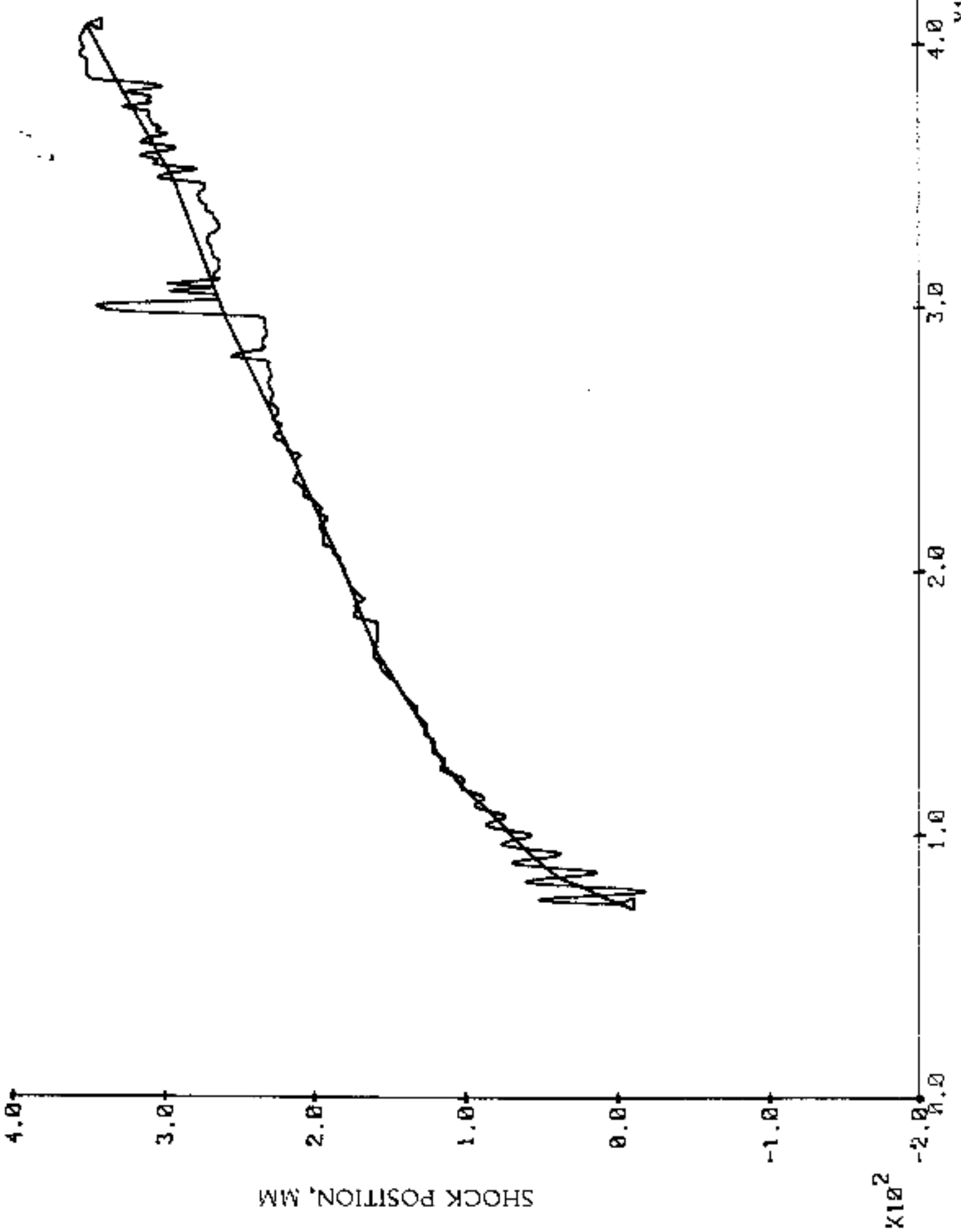

FIGURE C-22. RAW AND SMOOTHED POSITION-TIME RECORD, TEST D11 PROBE 2

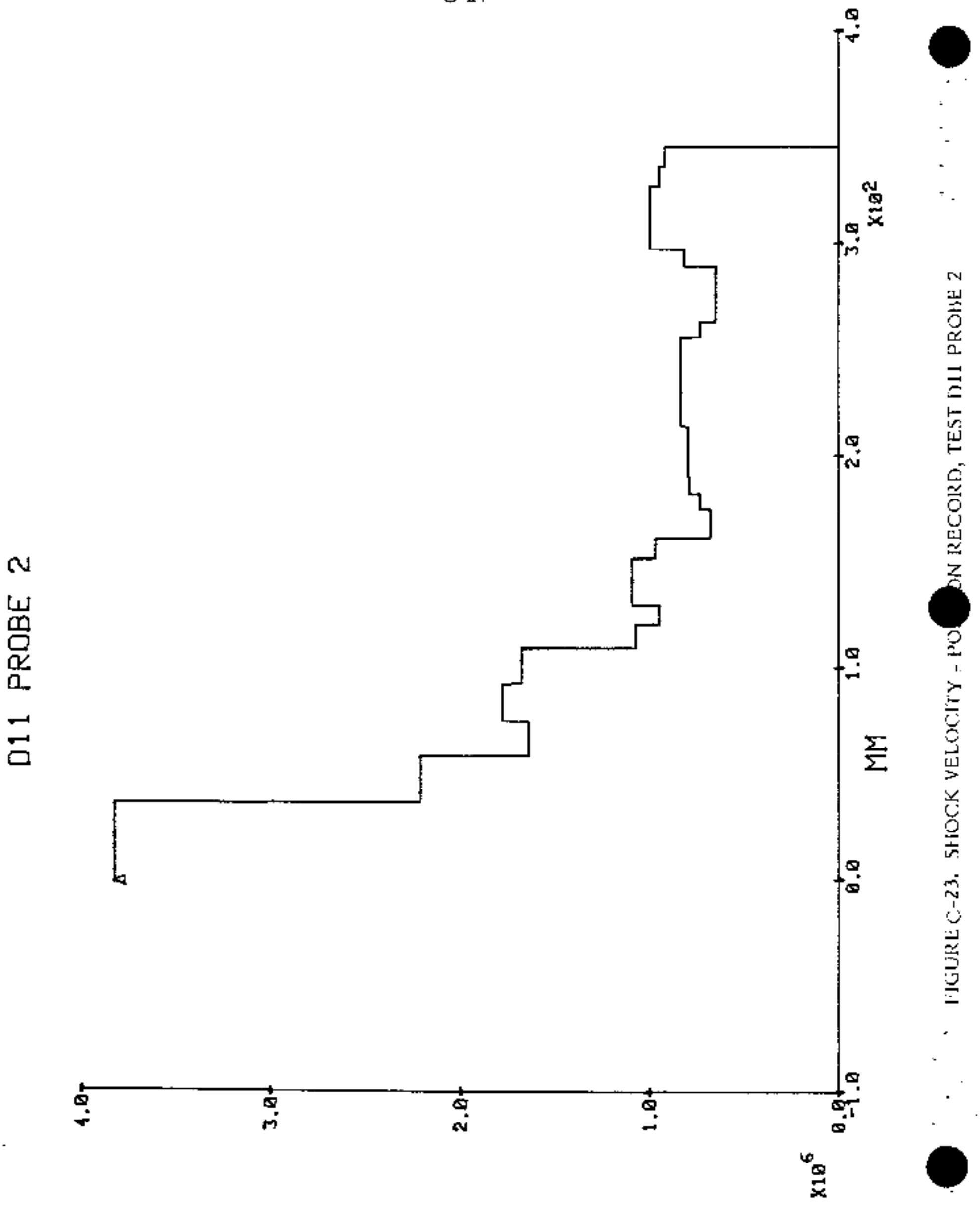

FIGURE C-23. SHOCK VELOCITY - POSITION RECORD, TEST D11 PROBE 2

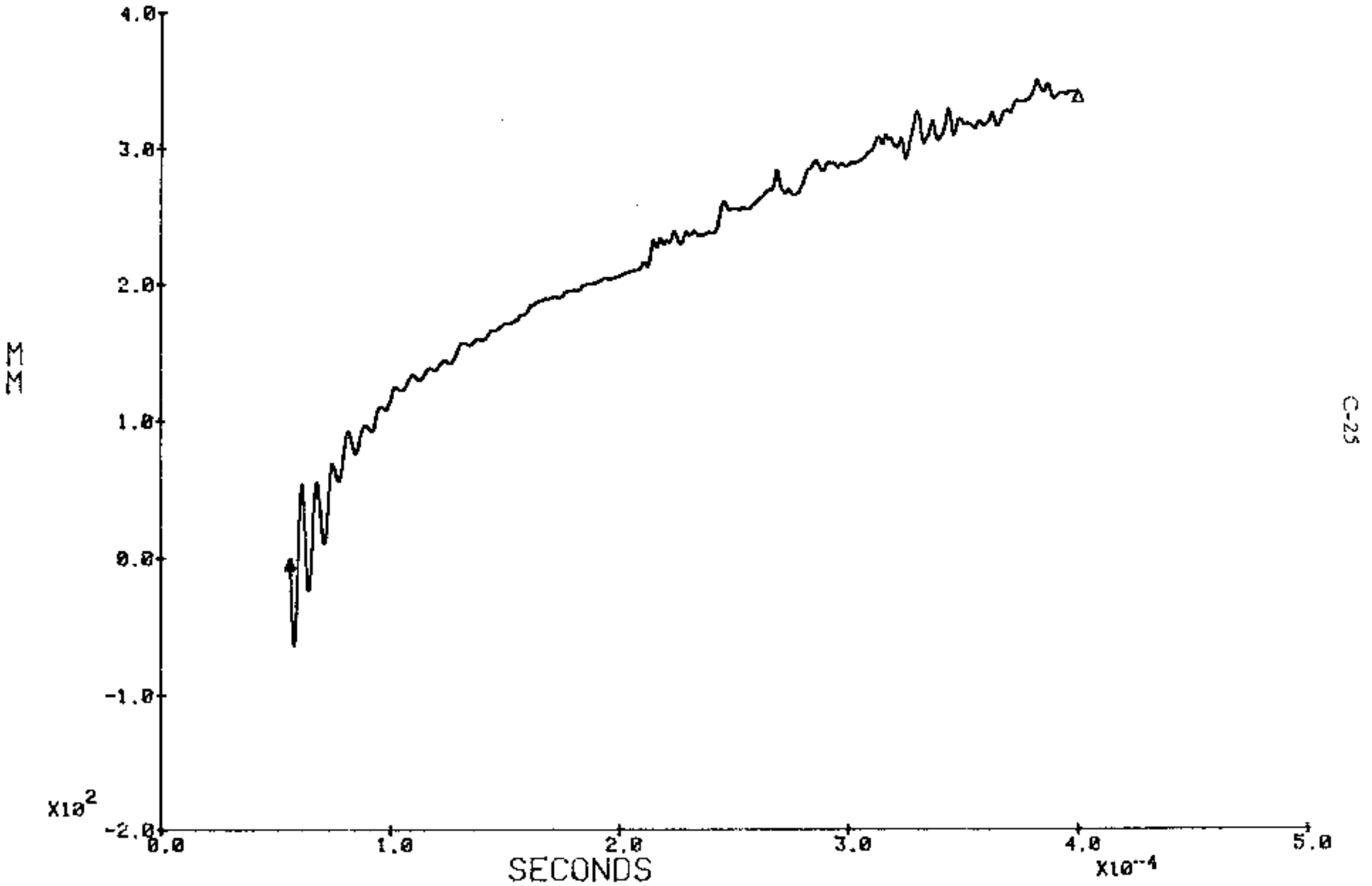

FIGURE C-24. RAW POSITION-TIME RECORD, TEST D12 PROBE 1

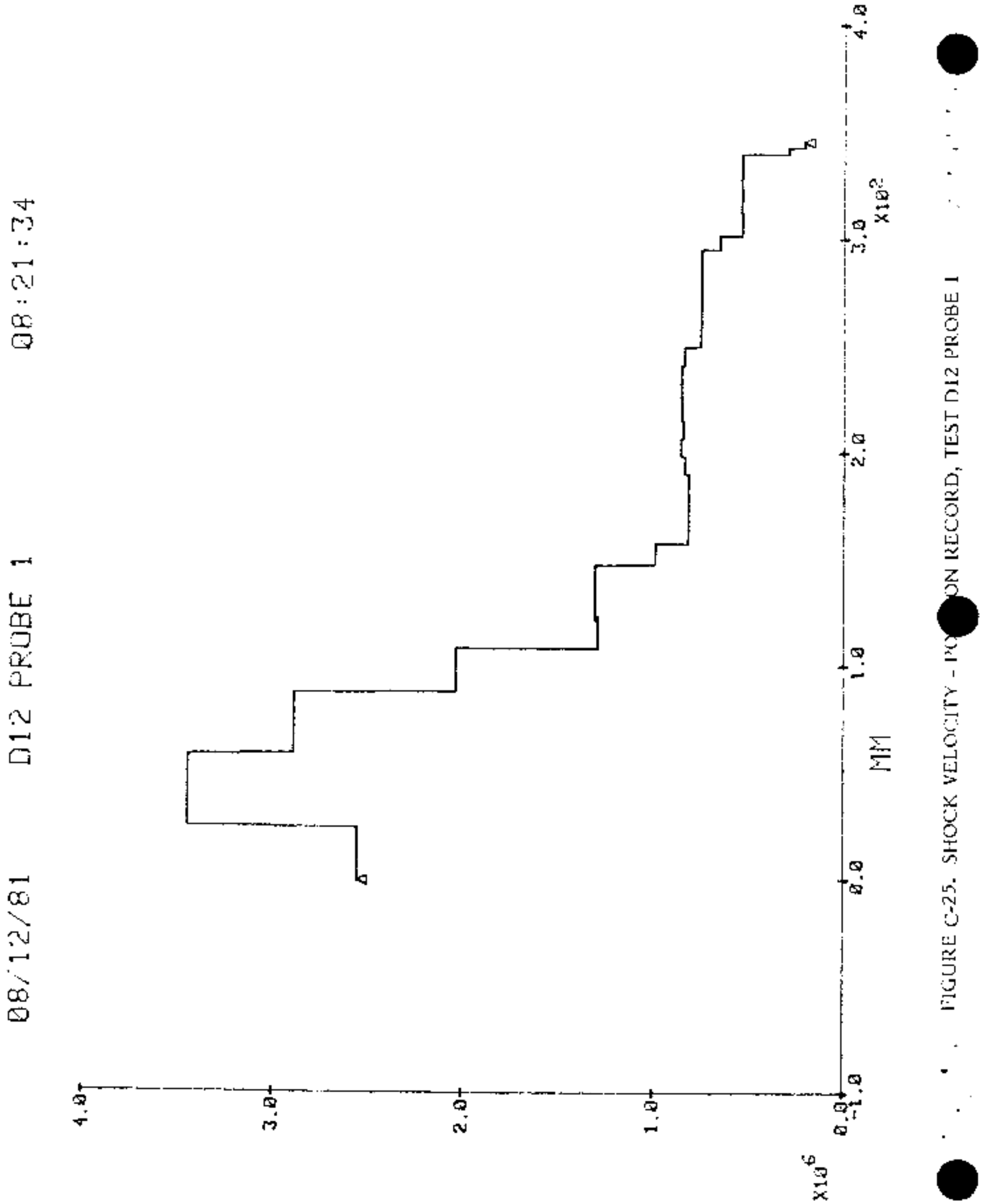

FIGURE C-25. SHOCK VELOCITY - PO[illegible]ON RECORD, TEST D12 PROBE 1

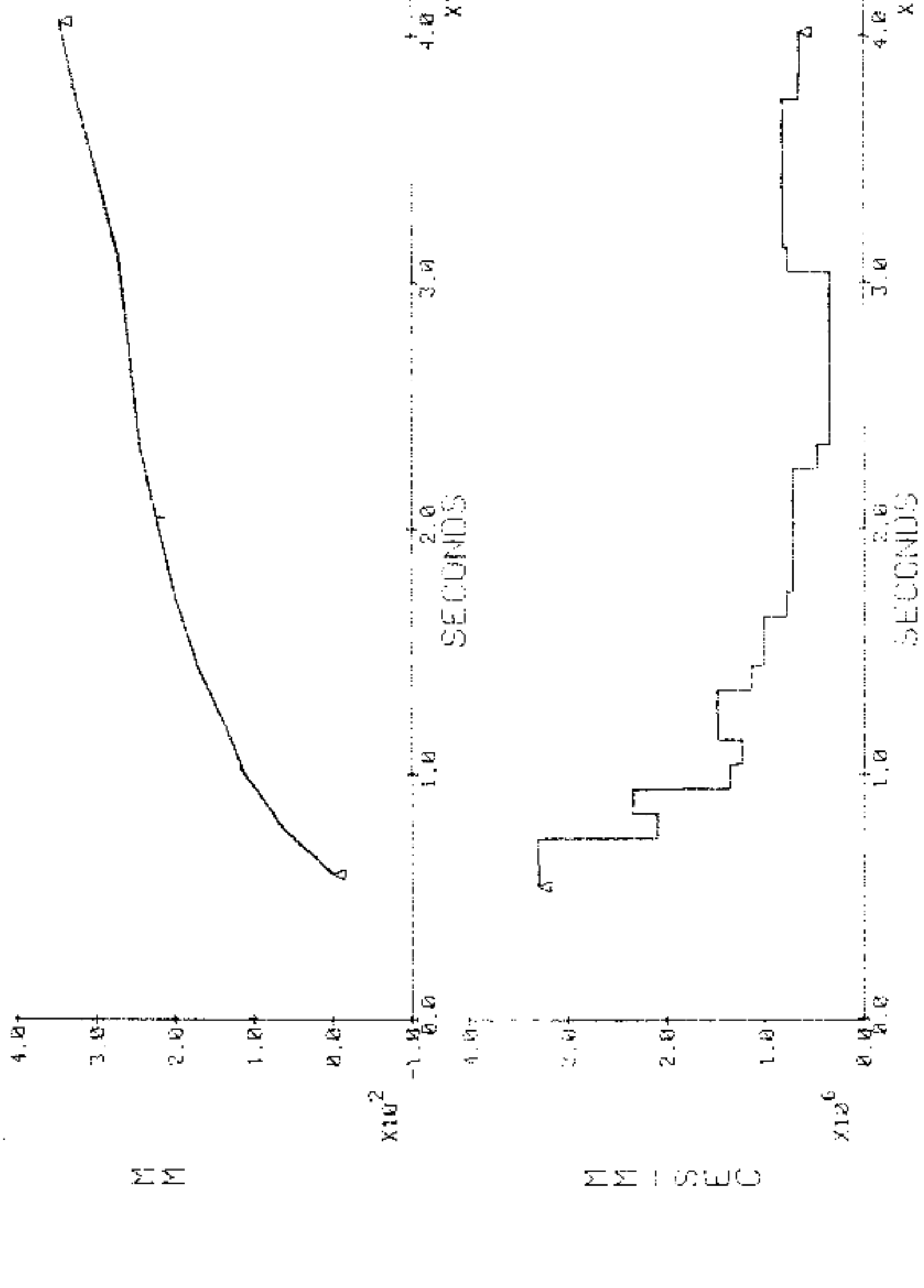

FIGURE C-26. SMOOTHED POSITION-TIME RECORD AND DERIVED VELOCITY-TIME RECORDS, TEST D13 PROBE 1

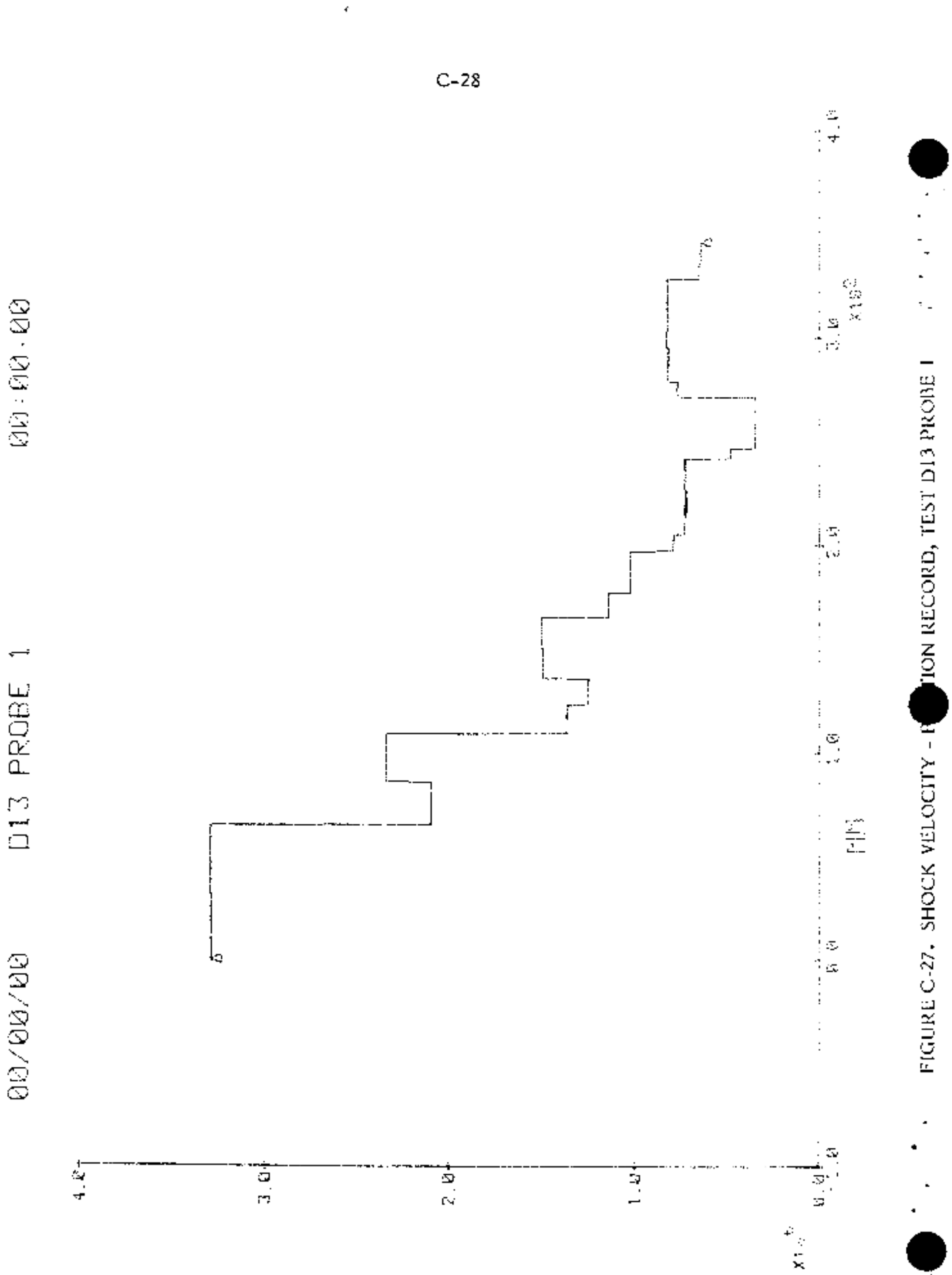

FIGURE C-27. SHOCK VELOCITY - PENETRATION RECORD, TEST D13 PROBE 1

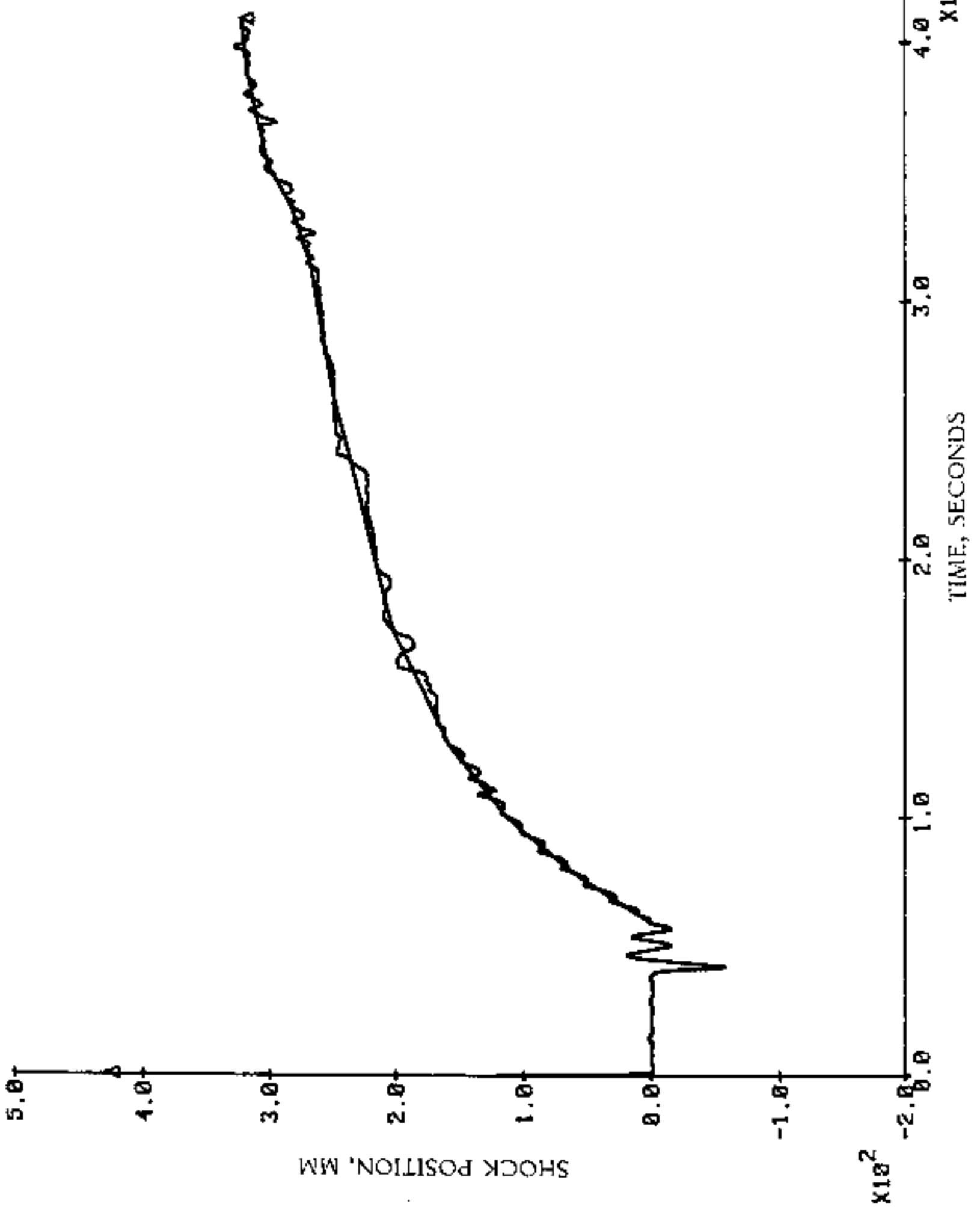

FIGURE C-28. RAW AND SMOOTHED POSITION-TIME RECORDS, TEST D13 PROBE 2

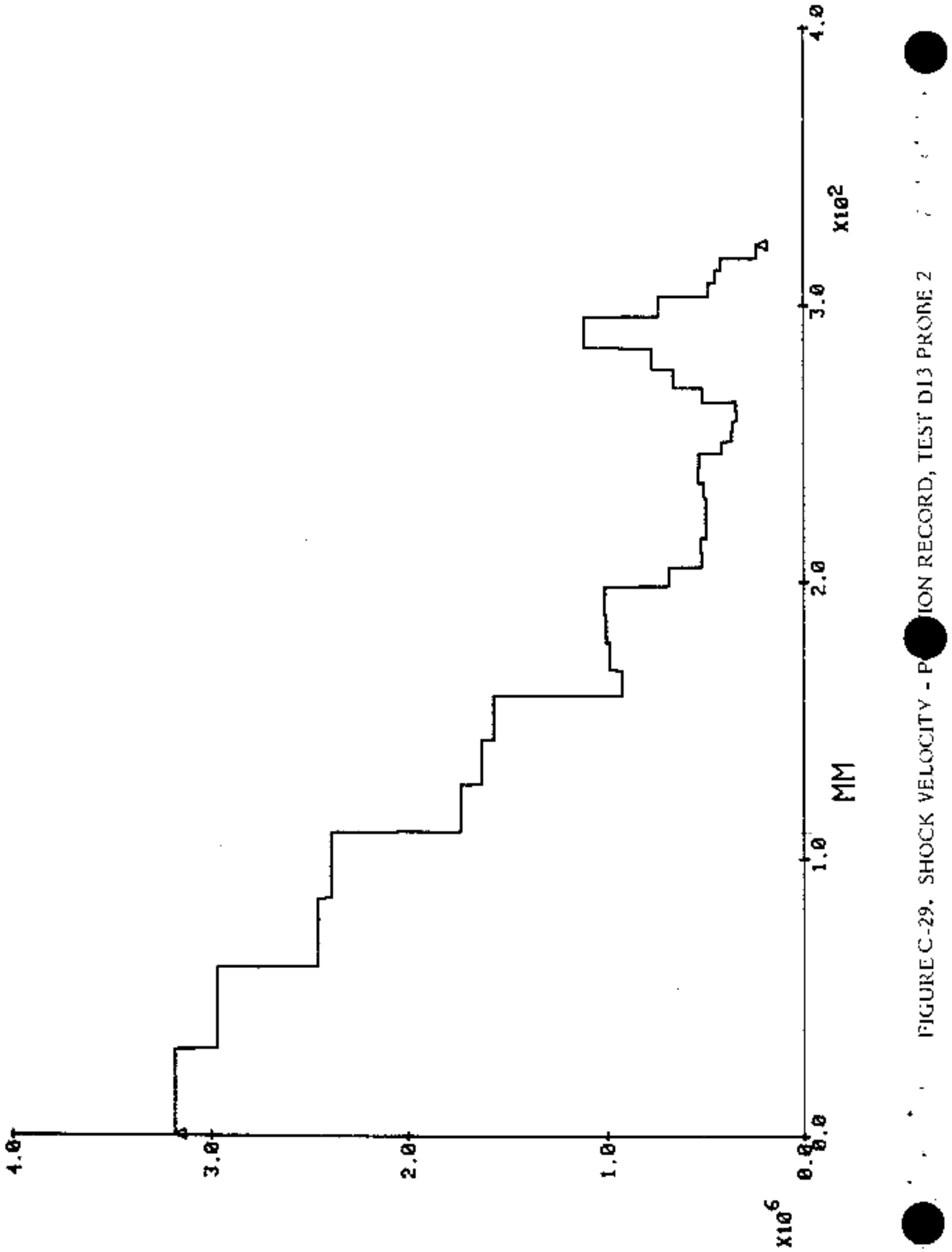

FIGURE C-29. SHOCK VELOCITY - PRESSION RECORD, TEST D13 PROBE 2

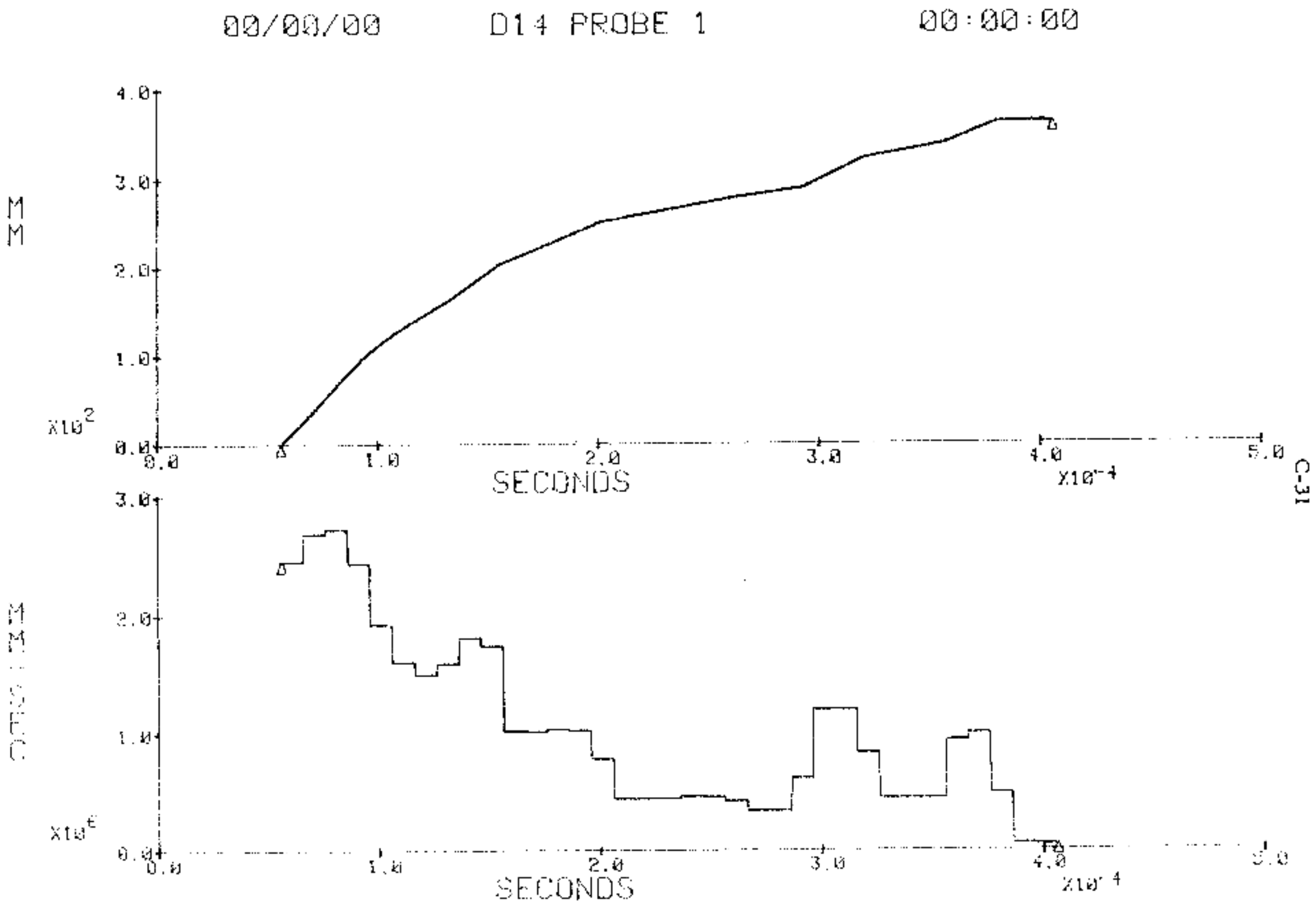

FIGURE C-30. SMOOTHED POSITION-TIME RECORD AND DERIVED VELOCITY-TIME RECORDS, TEST D14 PROBE 1

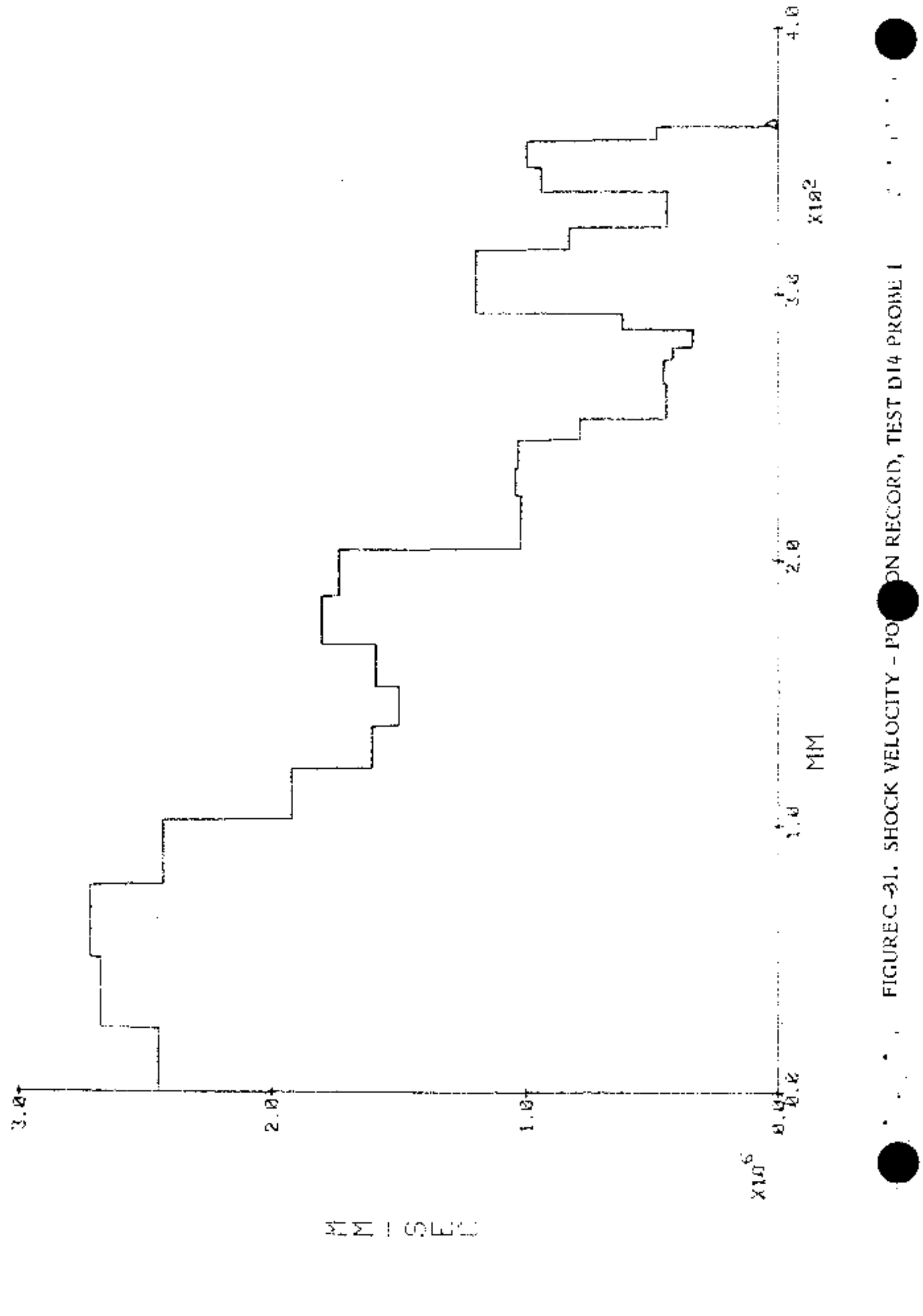

FIGUREC-31. SHOCK VELOCITY - PO[illegible]ON R[illegible]

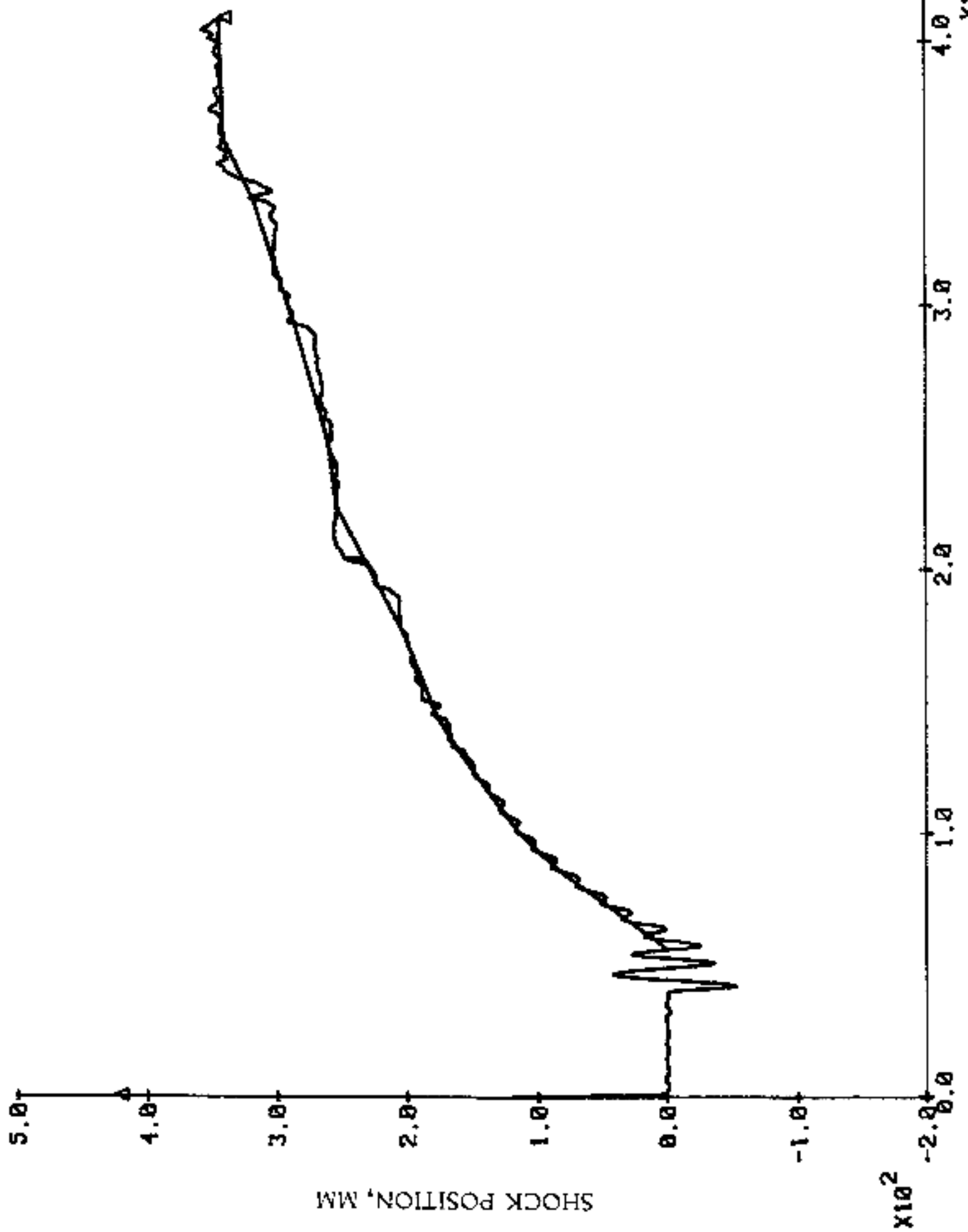

FIGURE C-32. RAW AND SMOOTHED POSITION-TIME RECORDS, TEST D14 PROBE 2

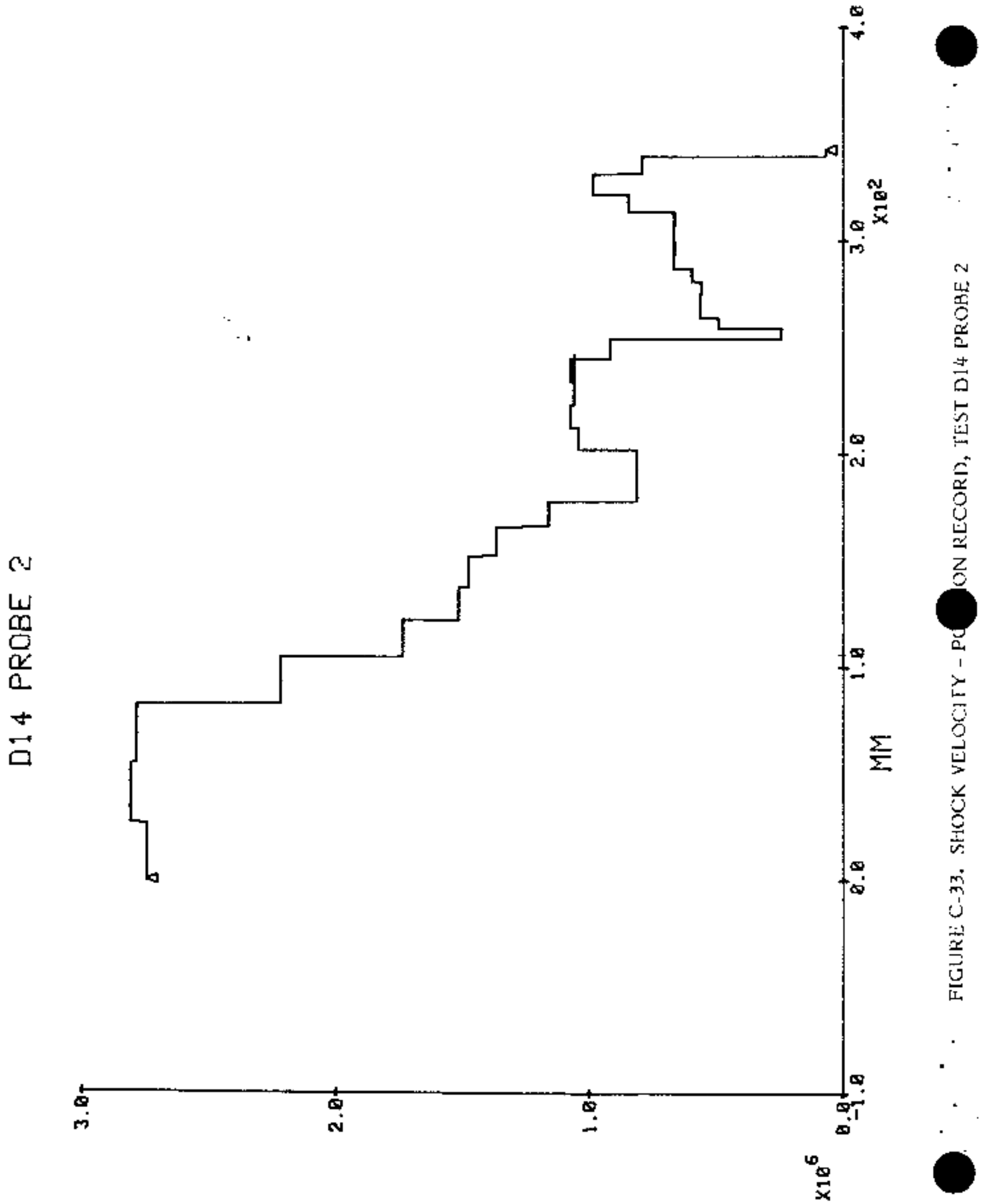

FIGURE C-33. SHOCK VELOCITY - PO[illegible]ON RECORD, TEST D14 PROBE 2

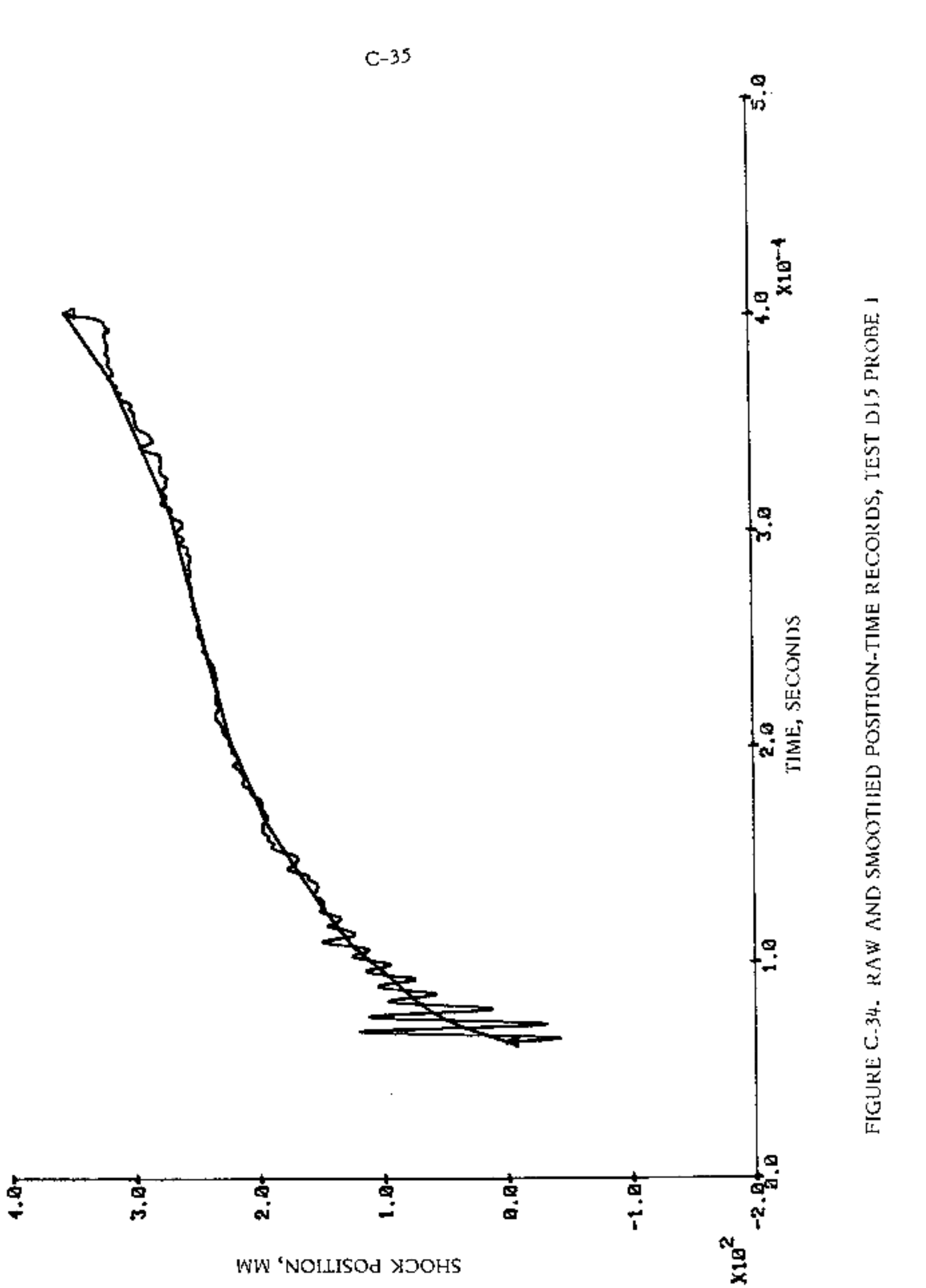

FIGURE C-34. RAW AND SMOOTHED POSITION-TIME RECORDS, TEST D15 PROBE 1

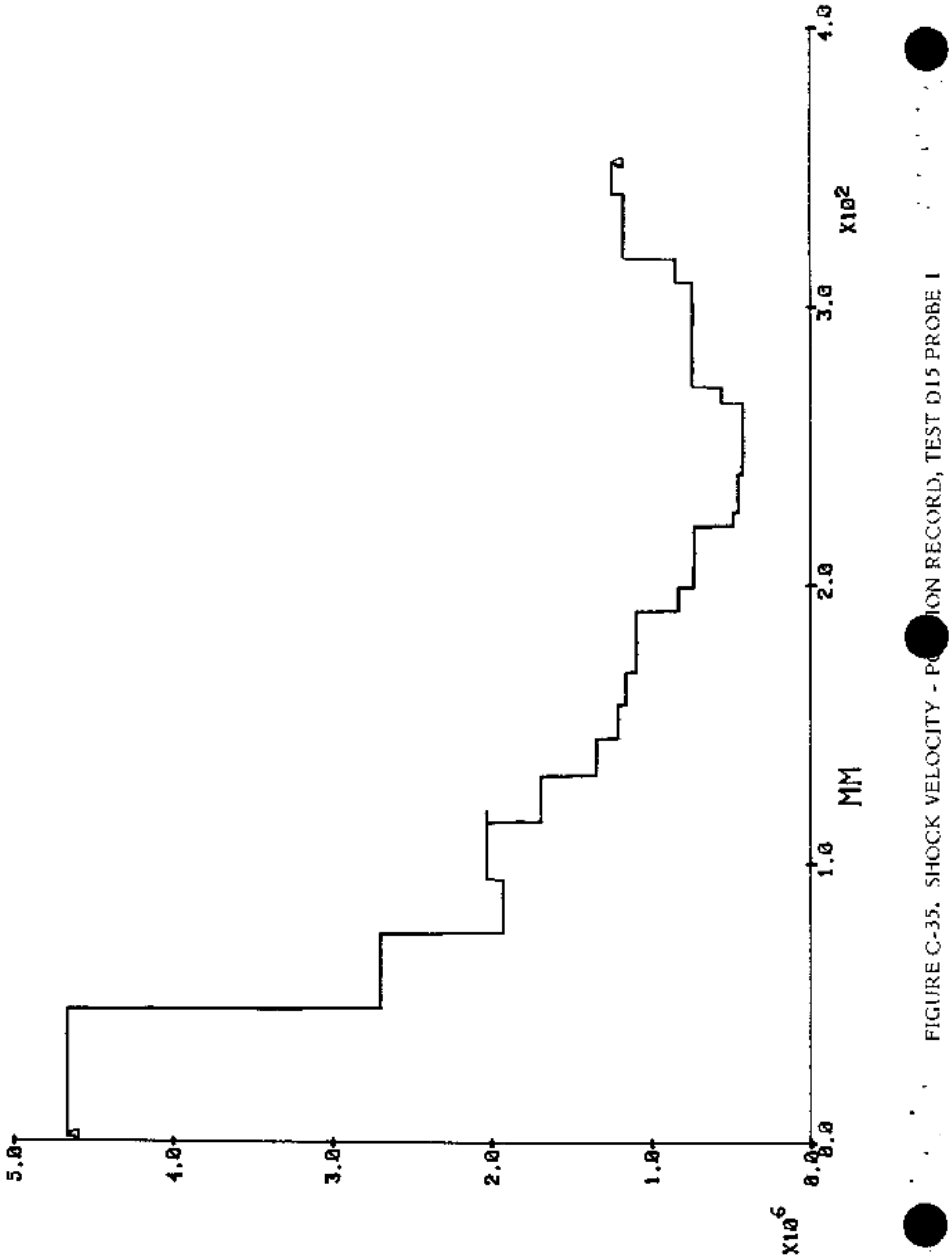

FIGURE C-35. SHOCK VELOCITY - PO ION RECORD, TEST D15 PROBE 1

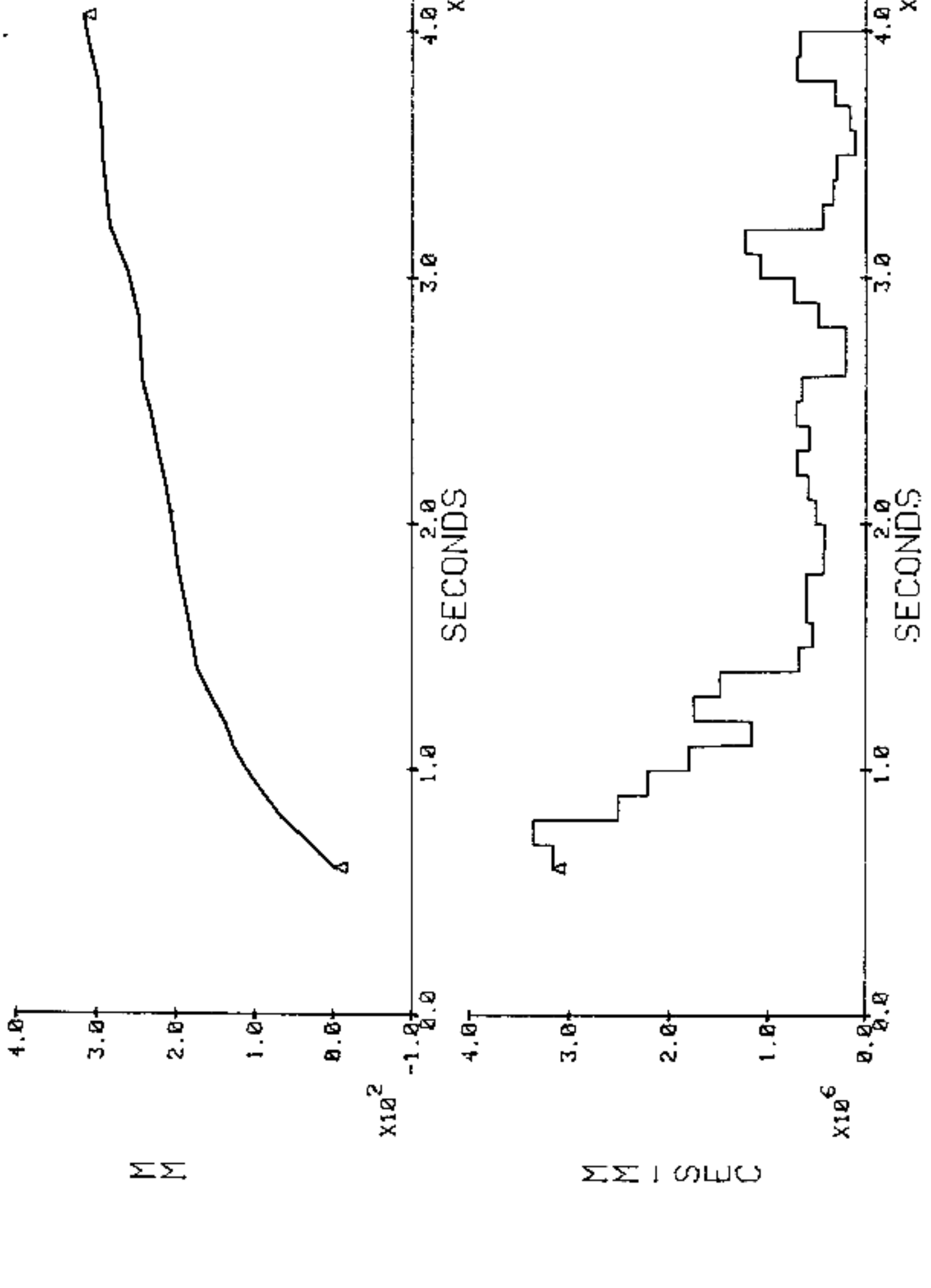

FIGURE C-36. SMOOTHED POSITION-TIME AND DERIVED VELOCITY-TIME RECORDS, TEST D16 PROBE 1

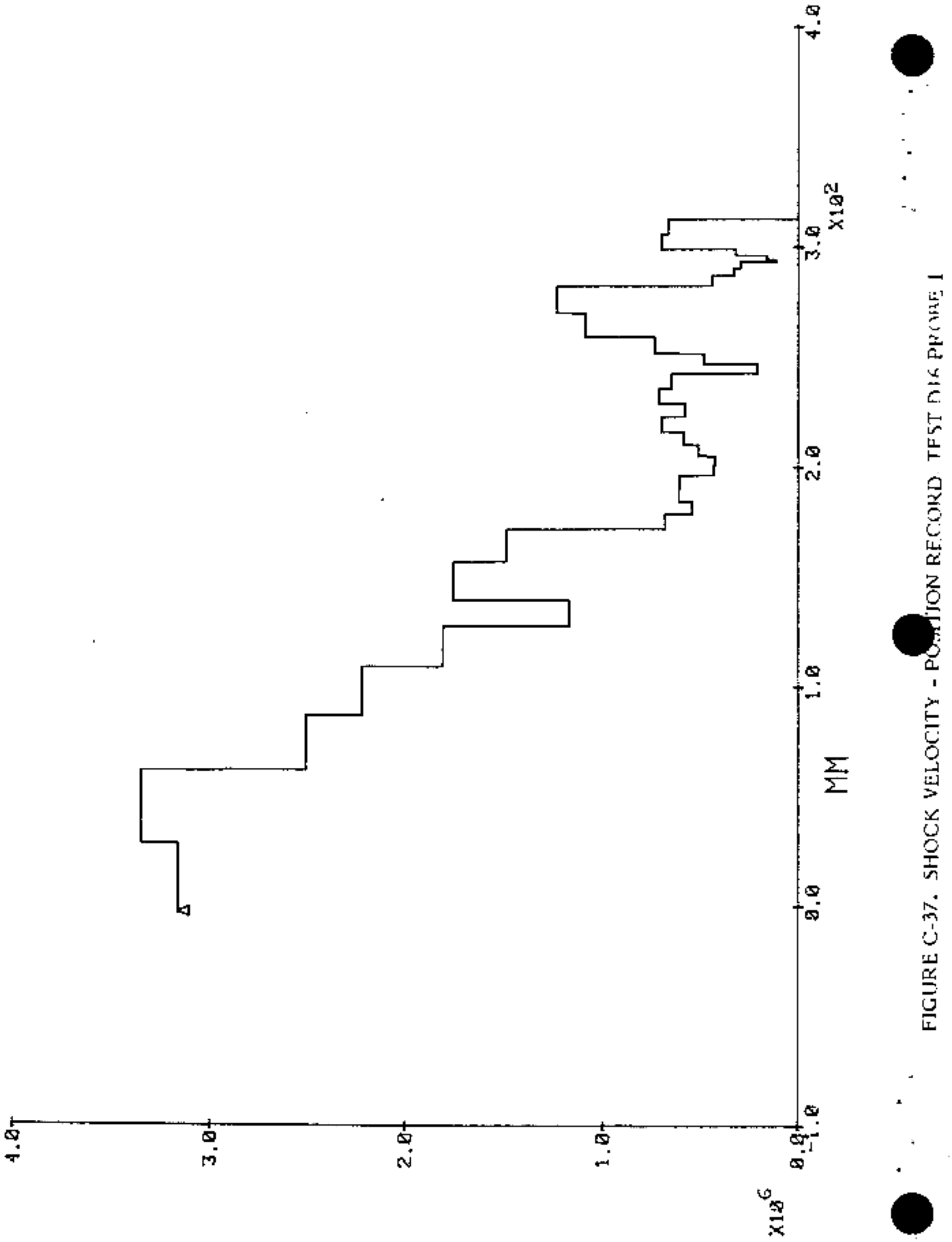

FIGURE C-37. SHOCK VELOCITY - POSITION RECORD, TEST DIG PROBE 1

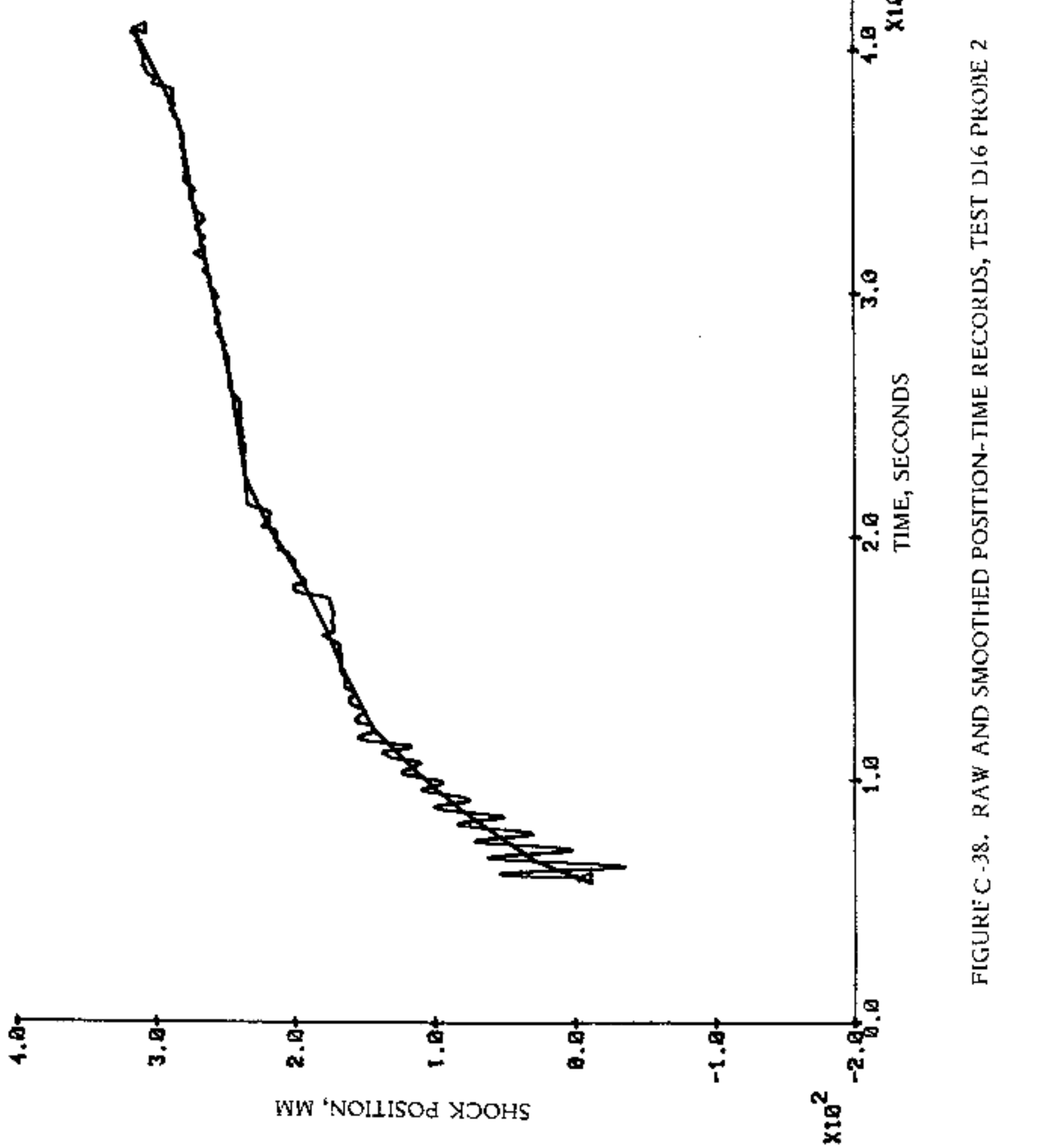

FIGURE C-38. RAW AND SMOOTHED POSITION-TIME RECORDS, TEST D16 PROBE 2

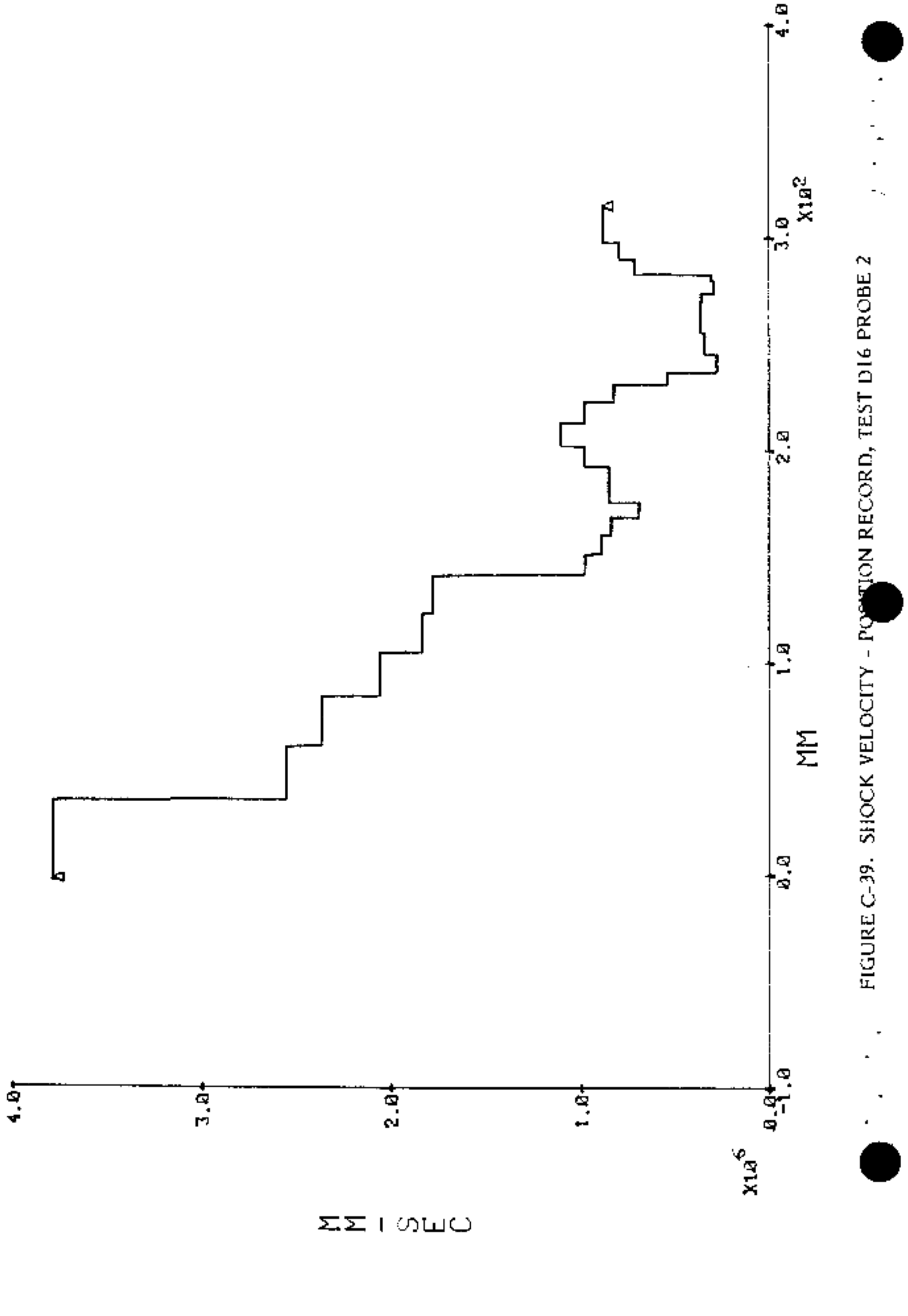

FIGURE C-39. SHOCK VELOCITY - POSITION RECORD, TEST D16 PROBE 2

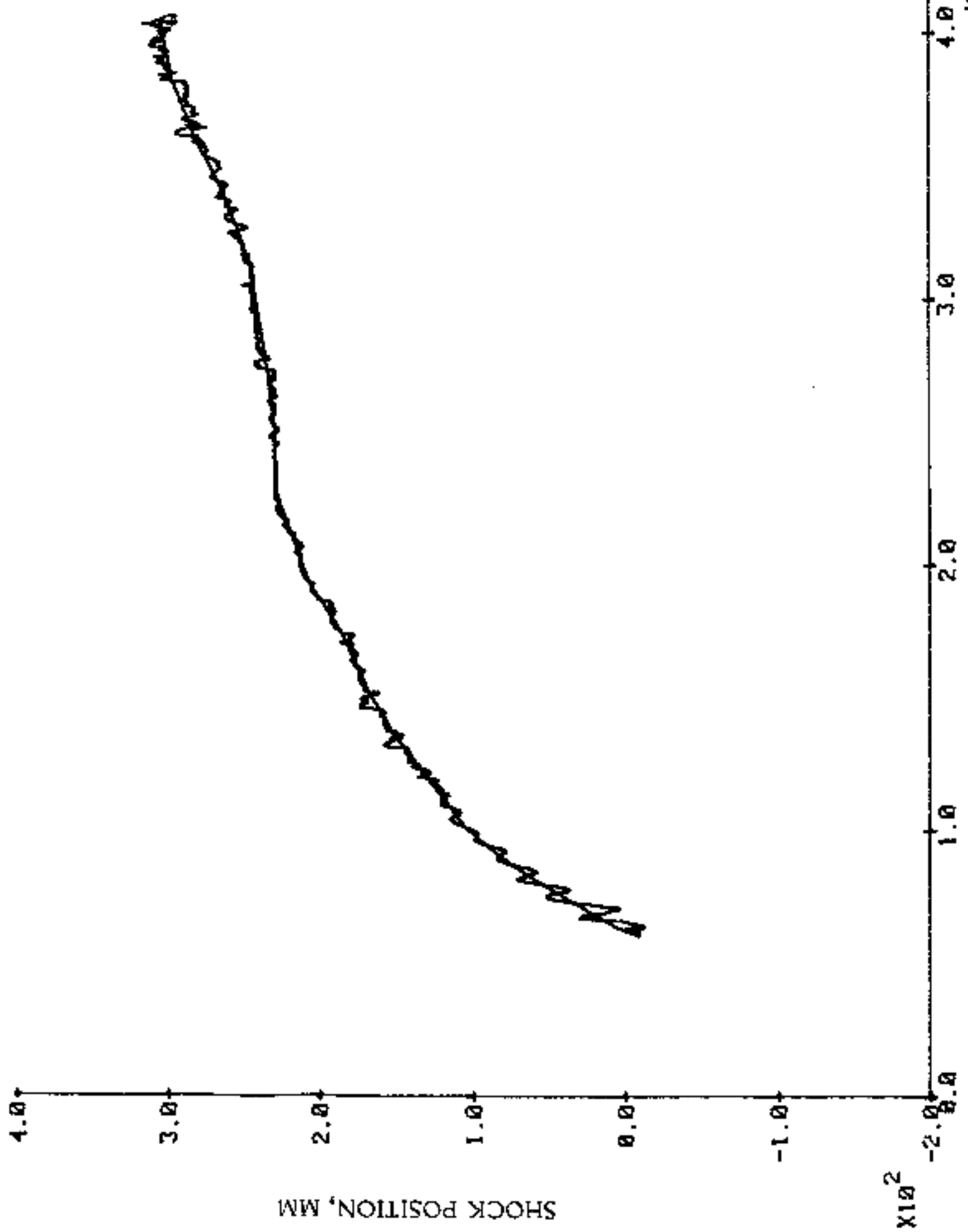

FIGURE C-40. RAW AND SMOOTHED POSITION-TIME RECORDS, TEST D17 PROBE 1

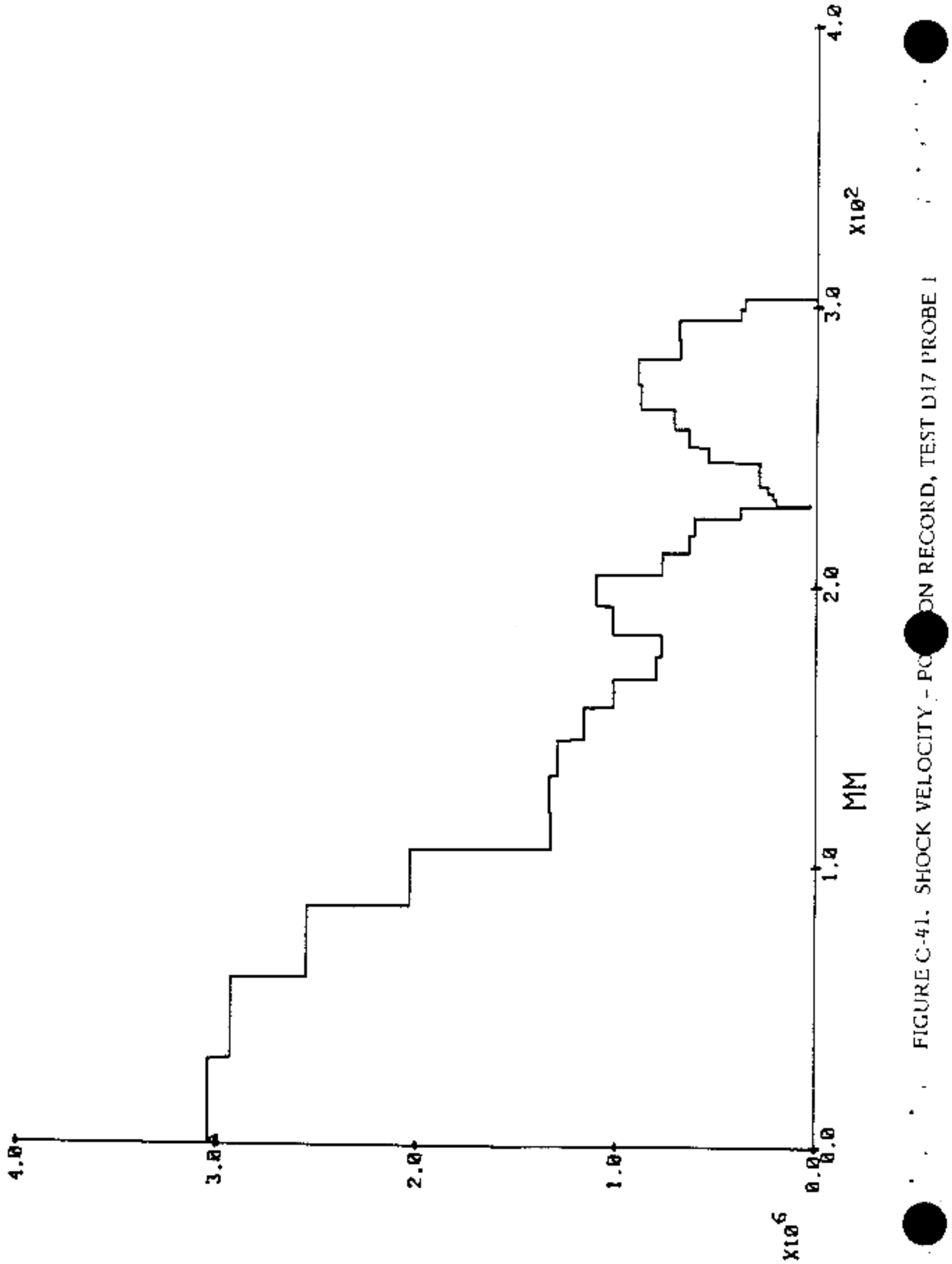

FIGURE C-41. SHOCK VELOCITY - PO[illegible]ON RECORD, TEST D17 PROBE 1

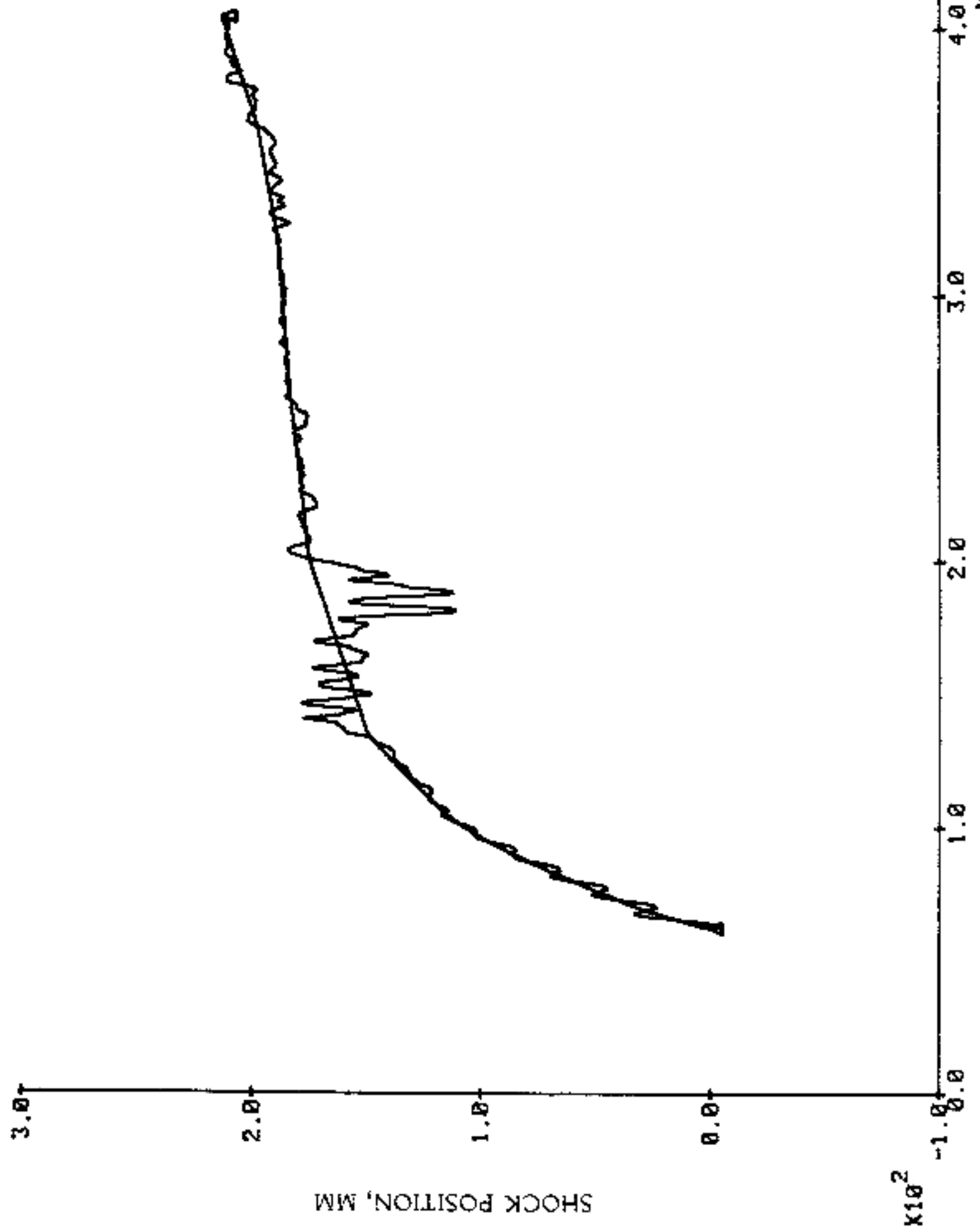

FIGURE C-42. RAW AND SMOOTHED POSITION-TIME RECORDS, TEST D17 PROBE 2

D17 PROBE 2

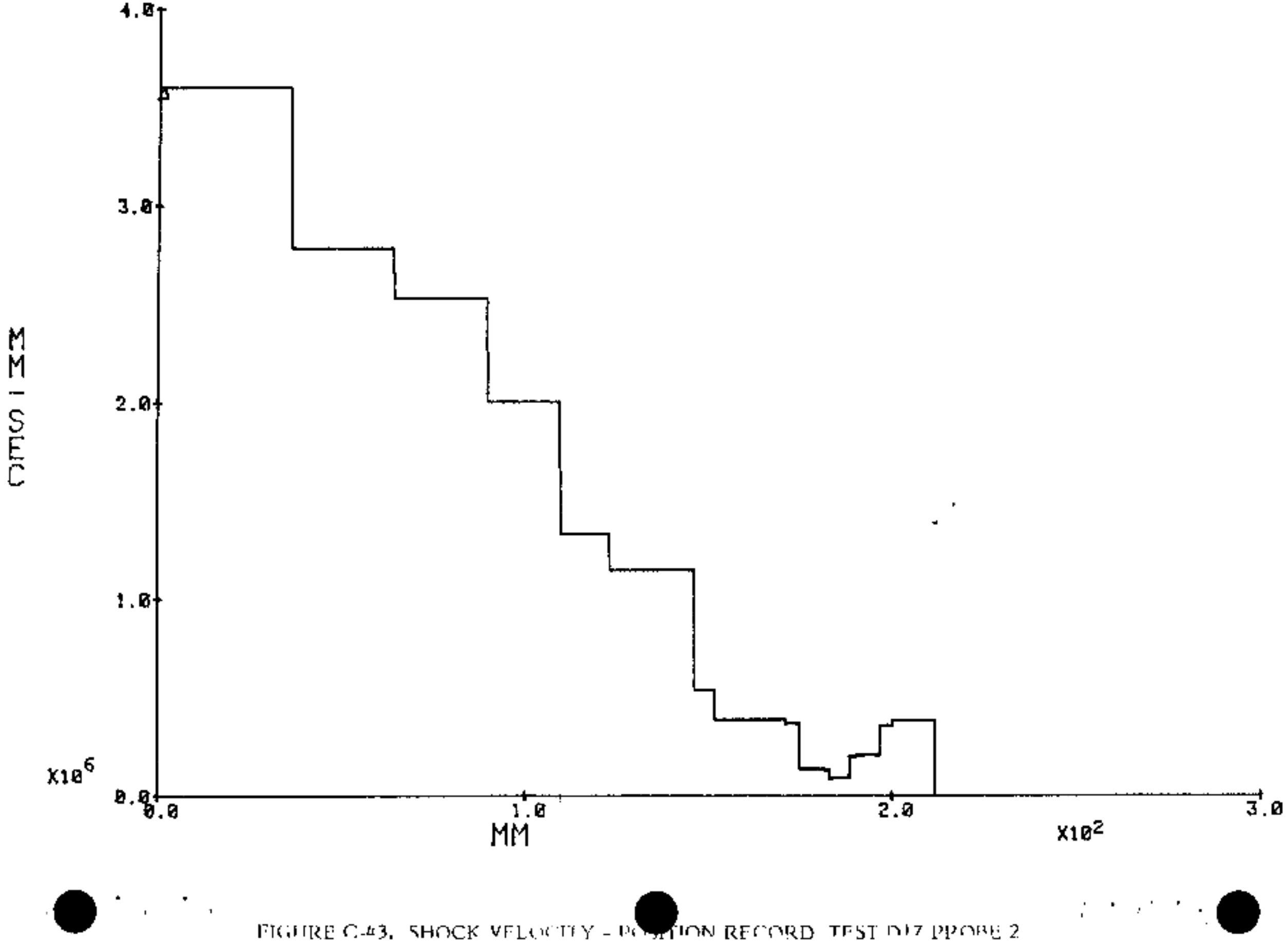

FIGURE C-43. SHOCK VELOCITY - POSITION RECORD TEST D17 PROBE 2

APPENDIX D

PRESSURE RECORDS

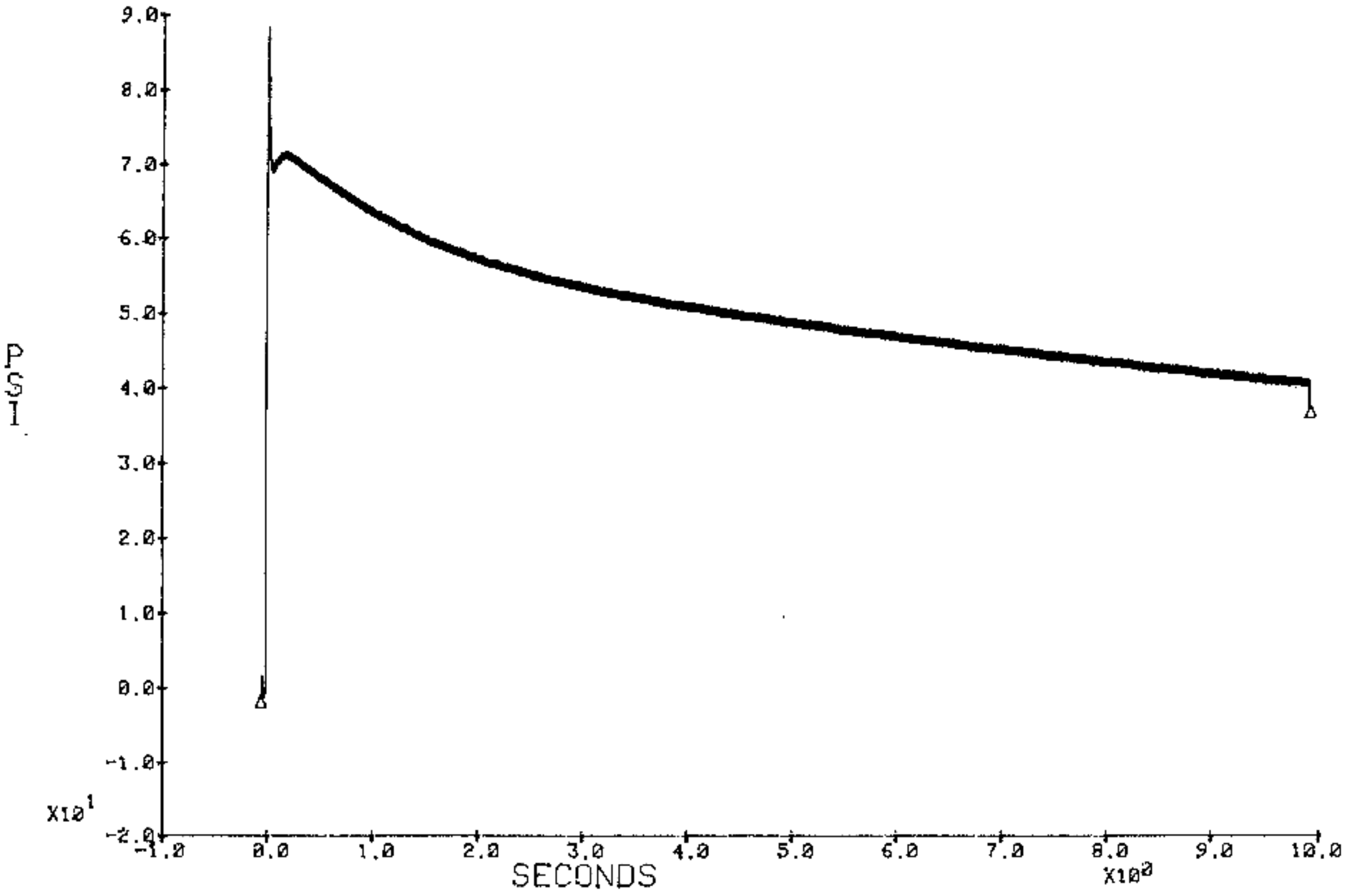

FIGURE D-1. PRESSURE-TIME RECORD FOR TEST D1

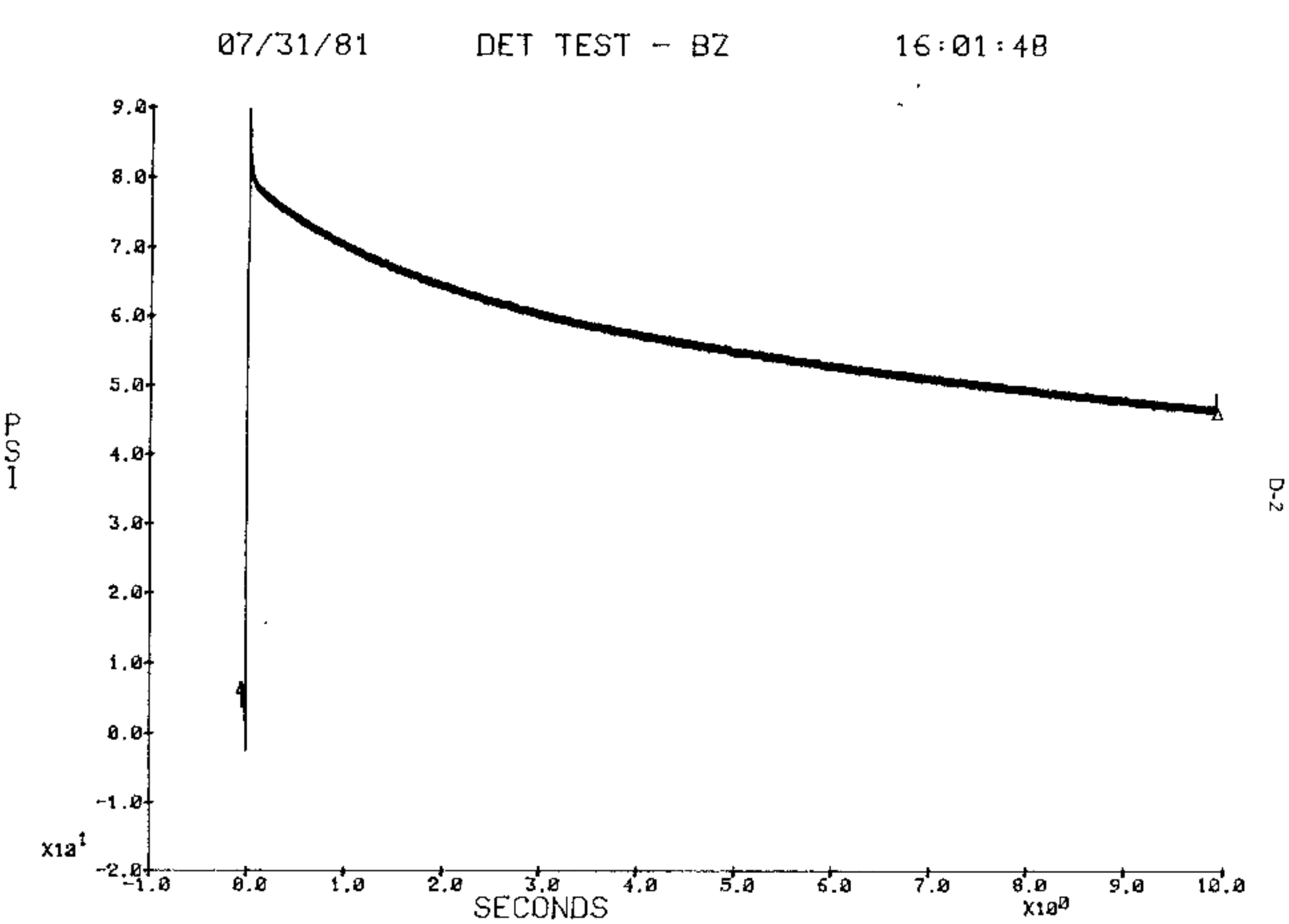

FIGURE D-2. PRESSURE-TIME RECORD FOR TEST D2

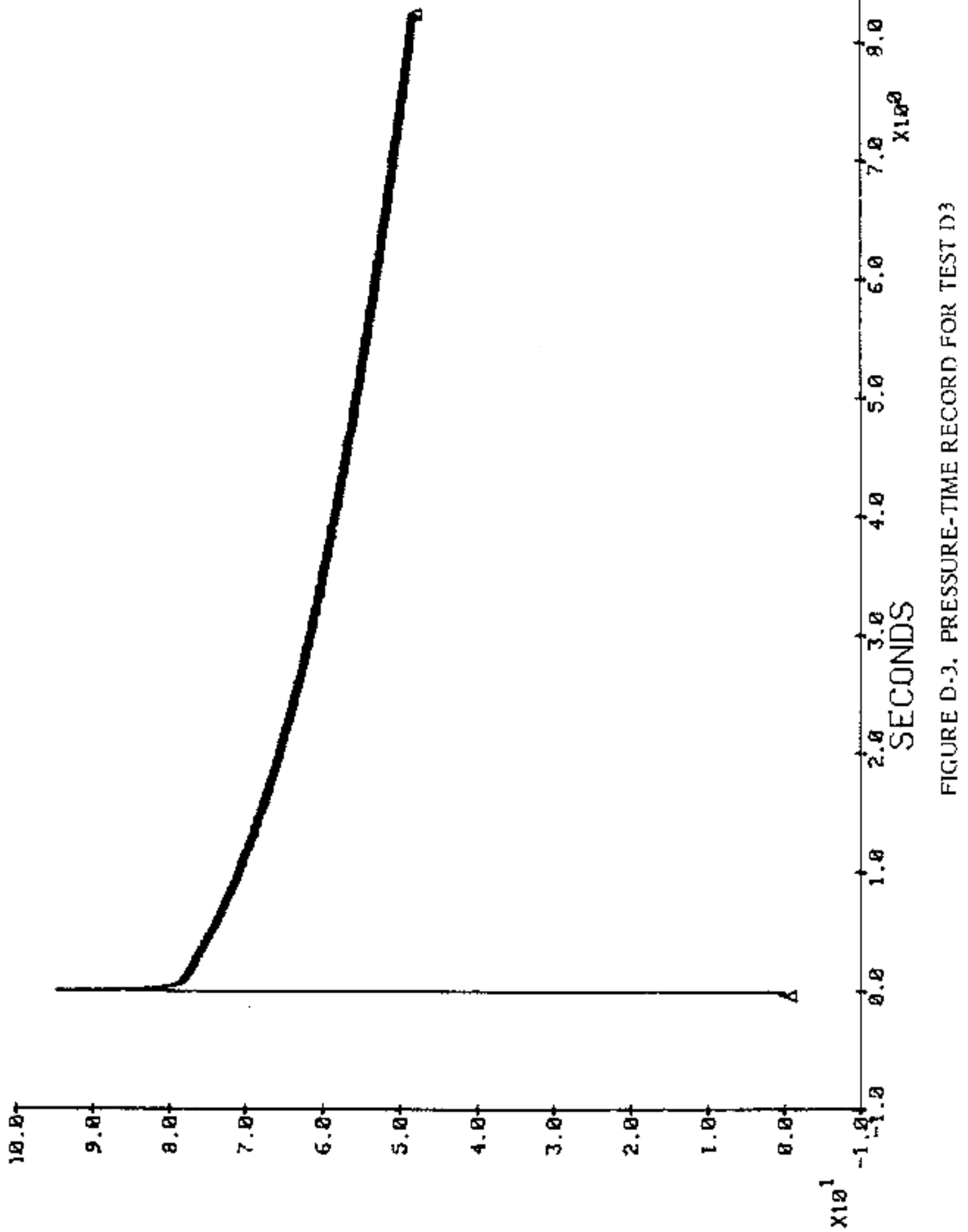

FIGURE D-3. PRESSURE-TIME RECORD FOR TEST D3

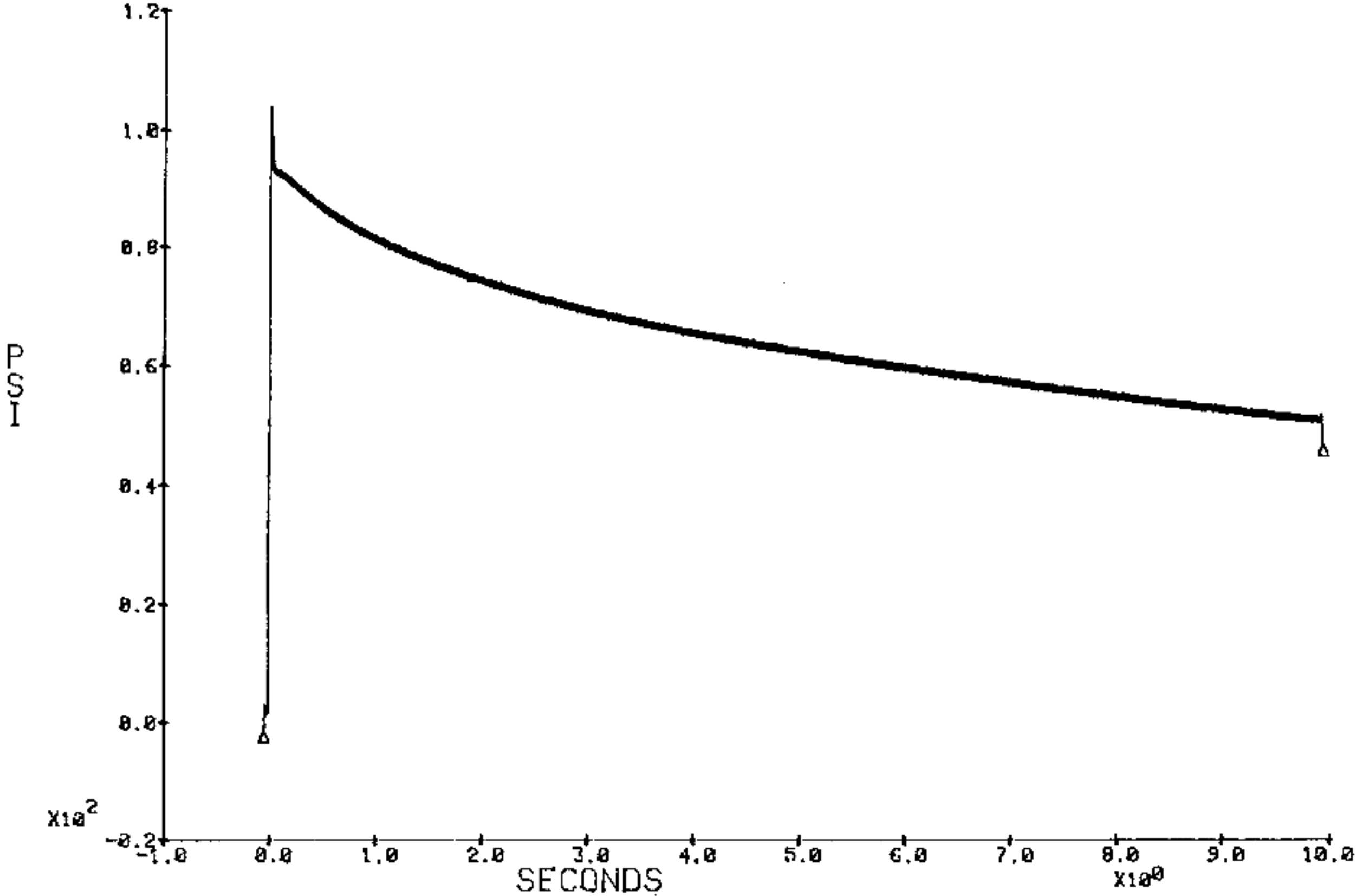

FIGURE D-4. PRESSURE-TIME RECORD FOR TEST D4

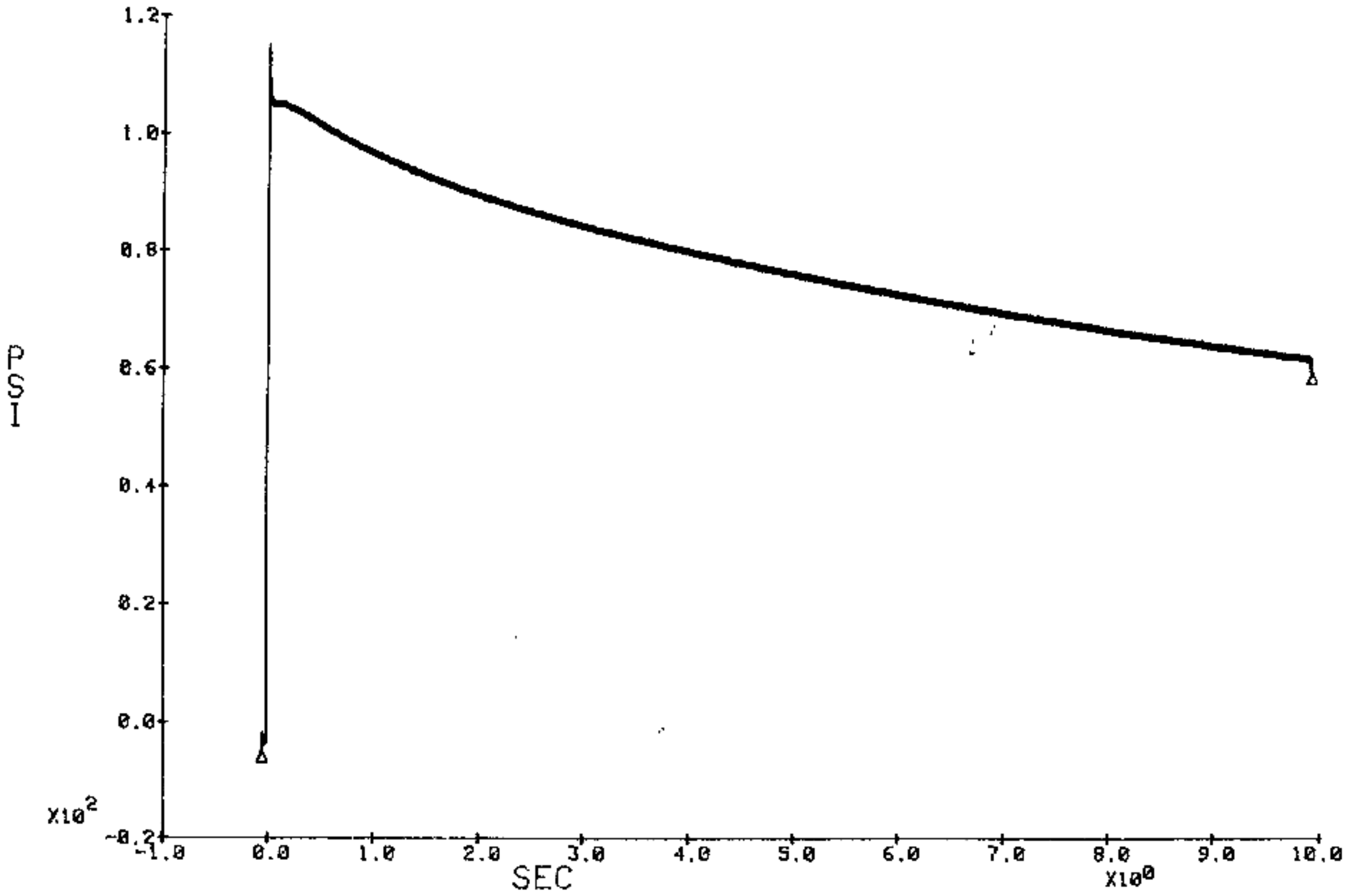

FIGURE D-5. PRESSURE-TIME RECORD FOR TEST D5

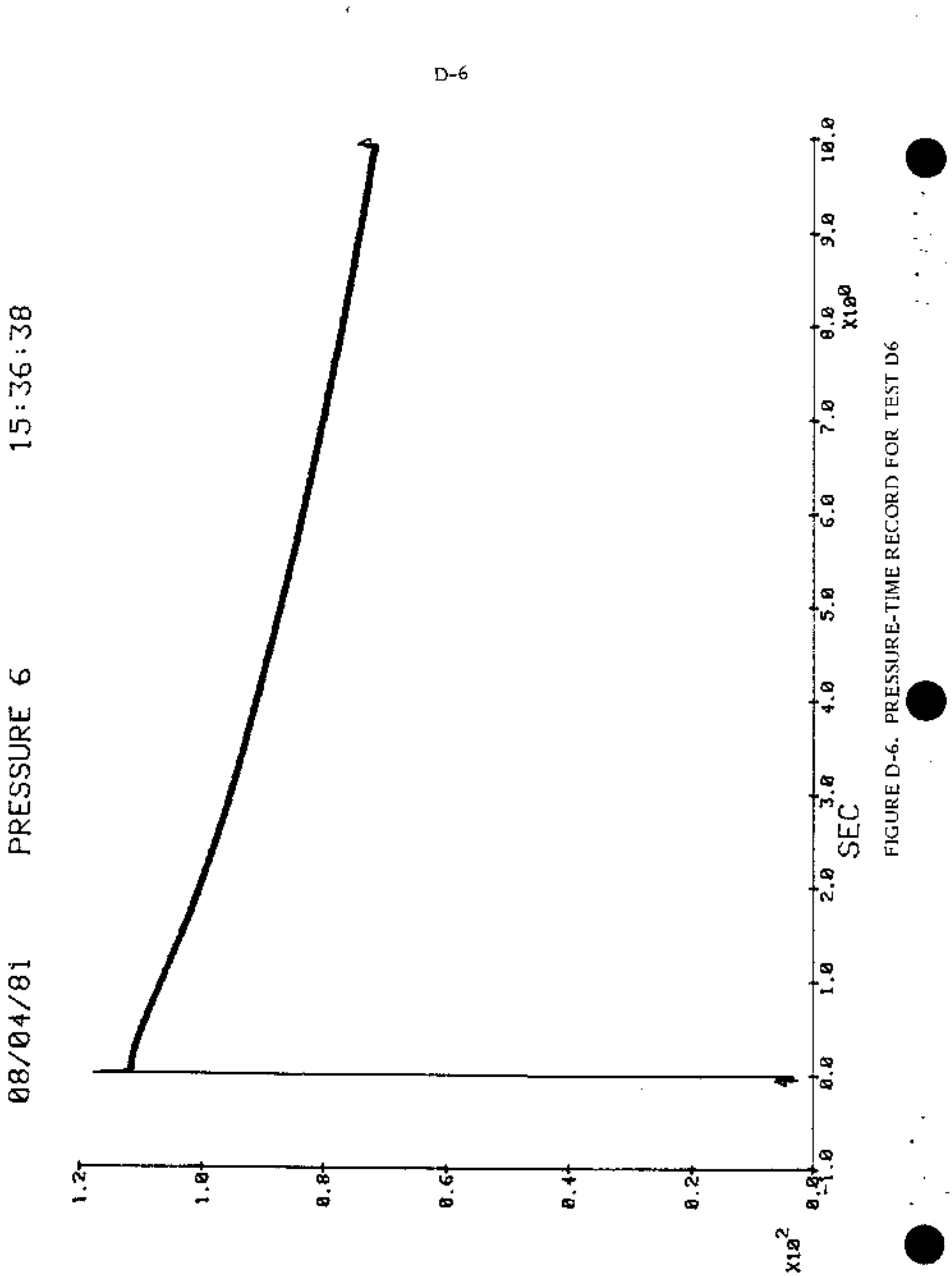

FIGURE D-6. PRESSURE-TIME RECORD FOR TEST D6

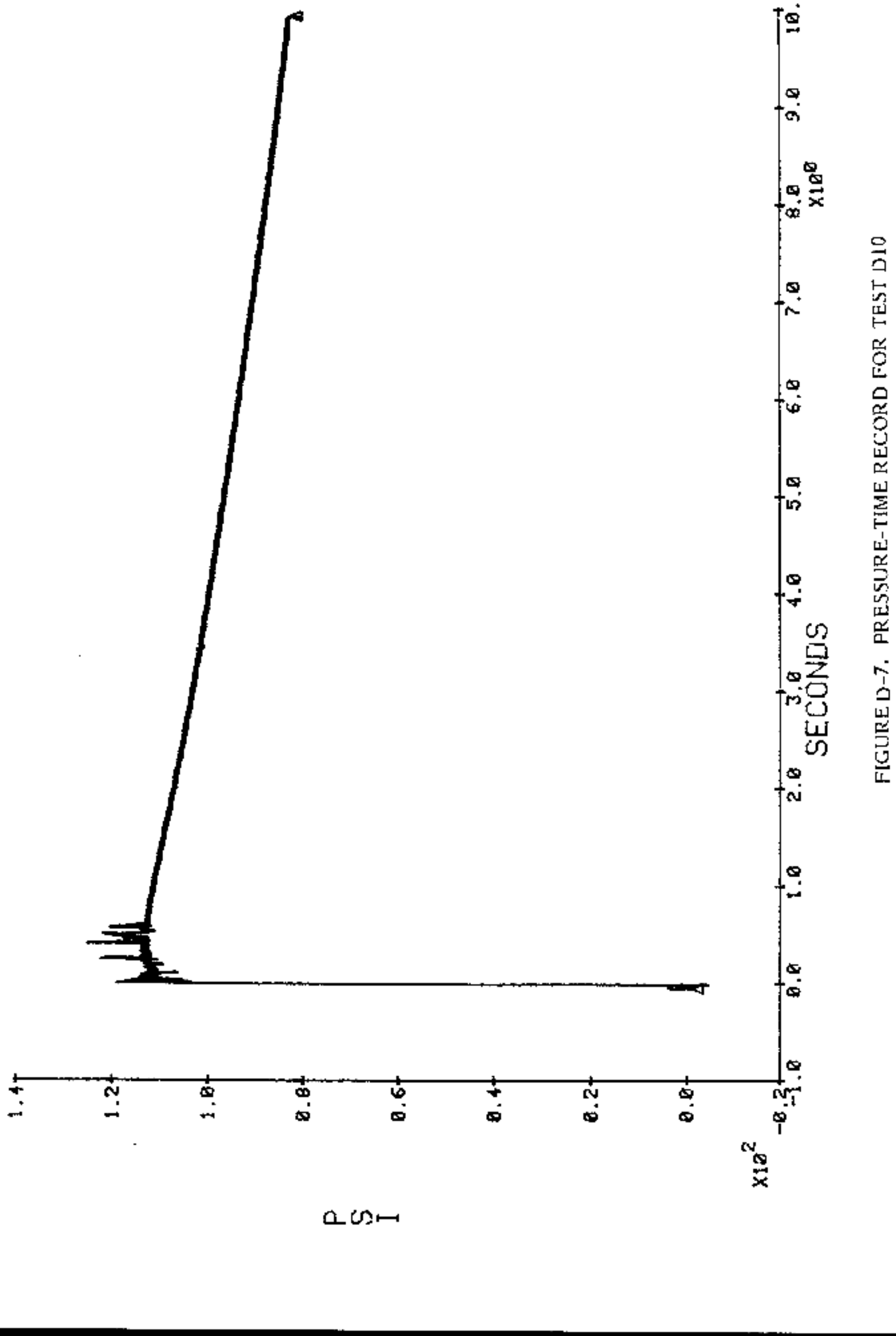

FIGURE D-7. PRESSURE-TIME RECORD FOR TEST D10

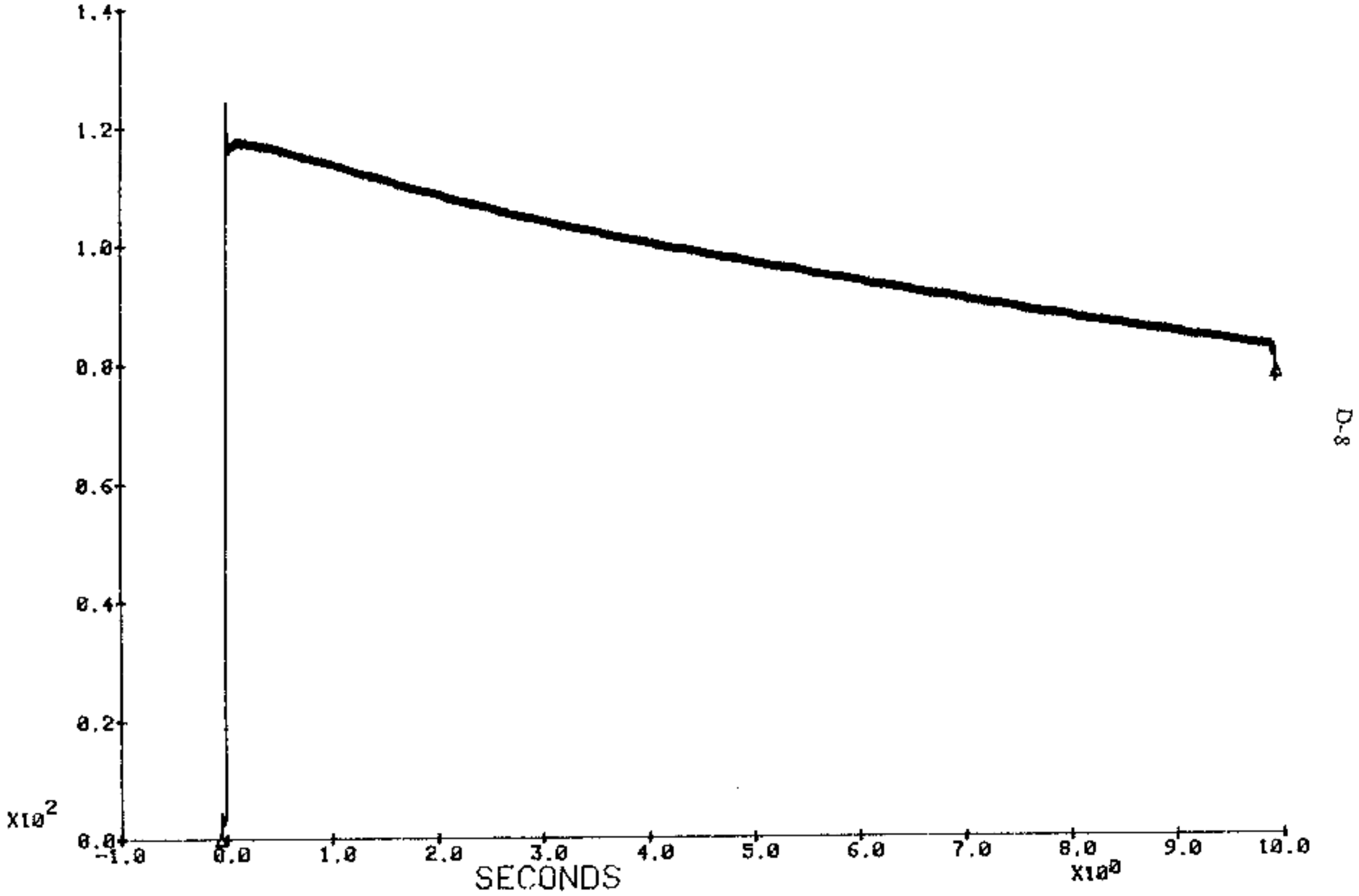

FIGURE D-8 PRESSURE-TIME RECORD FOR TEST D11

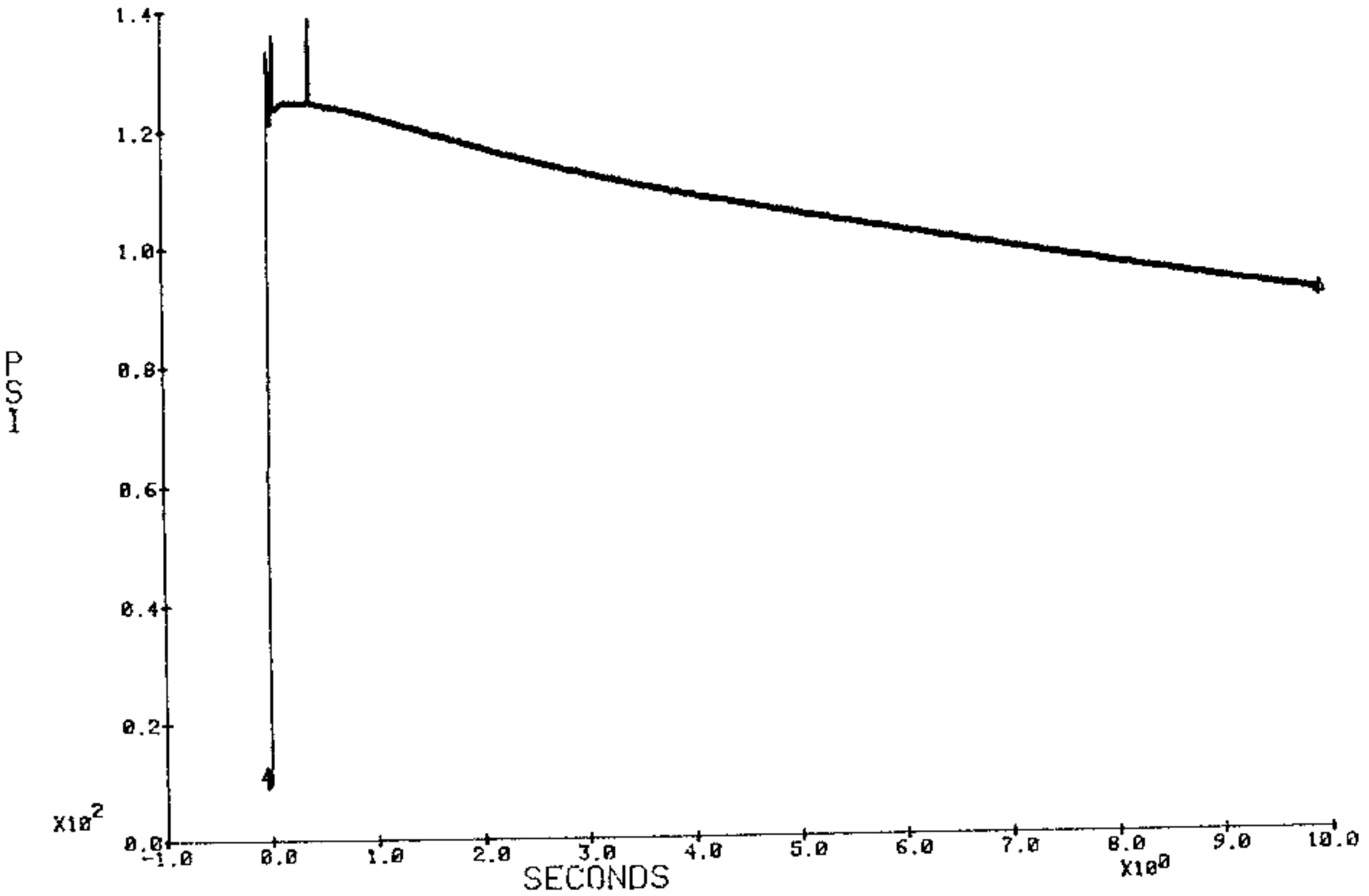

FIGURE D-9. PRESSURE-TIME RECORD FOR TEST D12

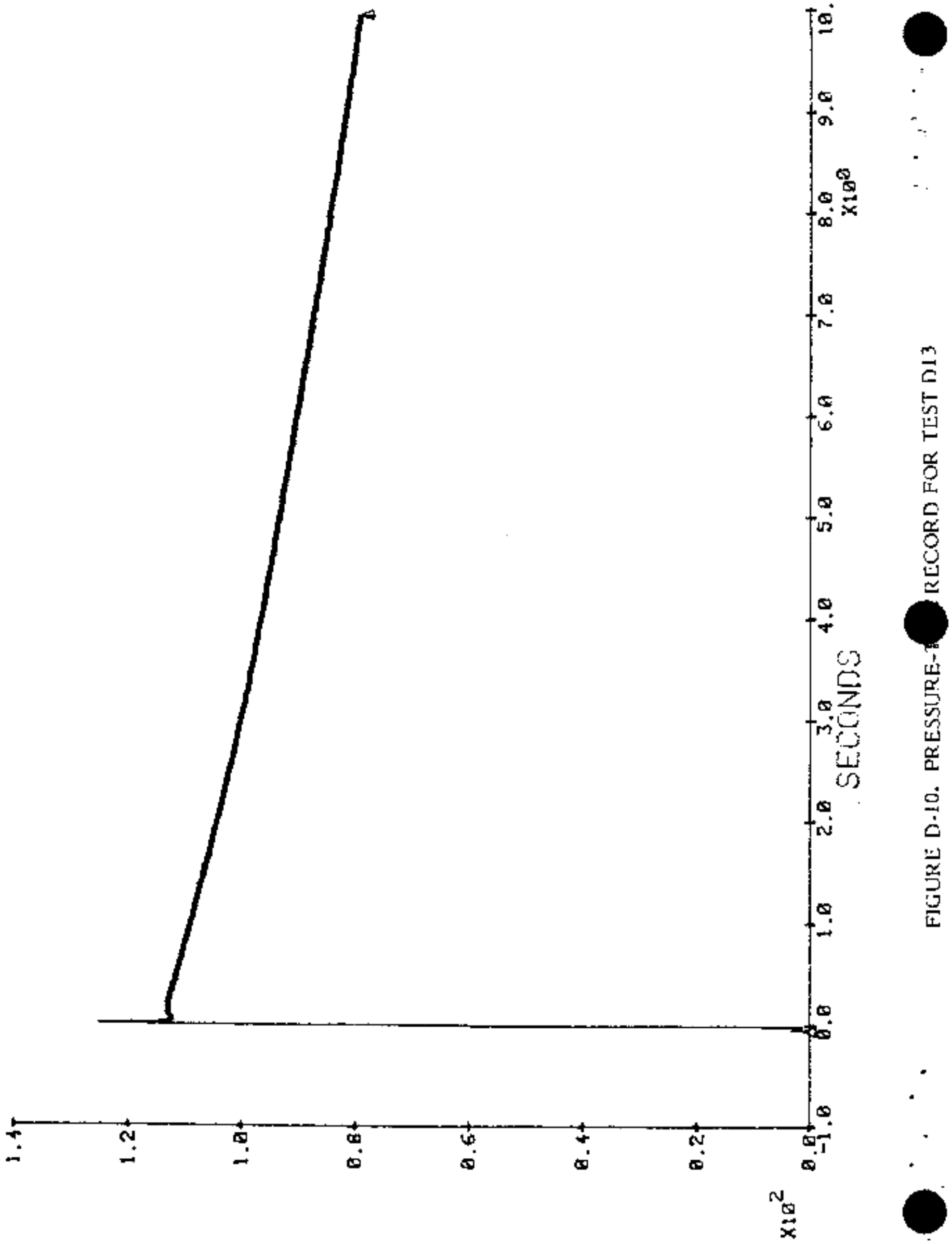

FIGURE D-10. PRESSURE-TIME RECORD FOR TEST D13

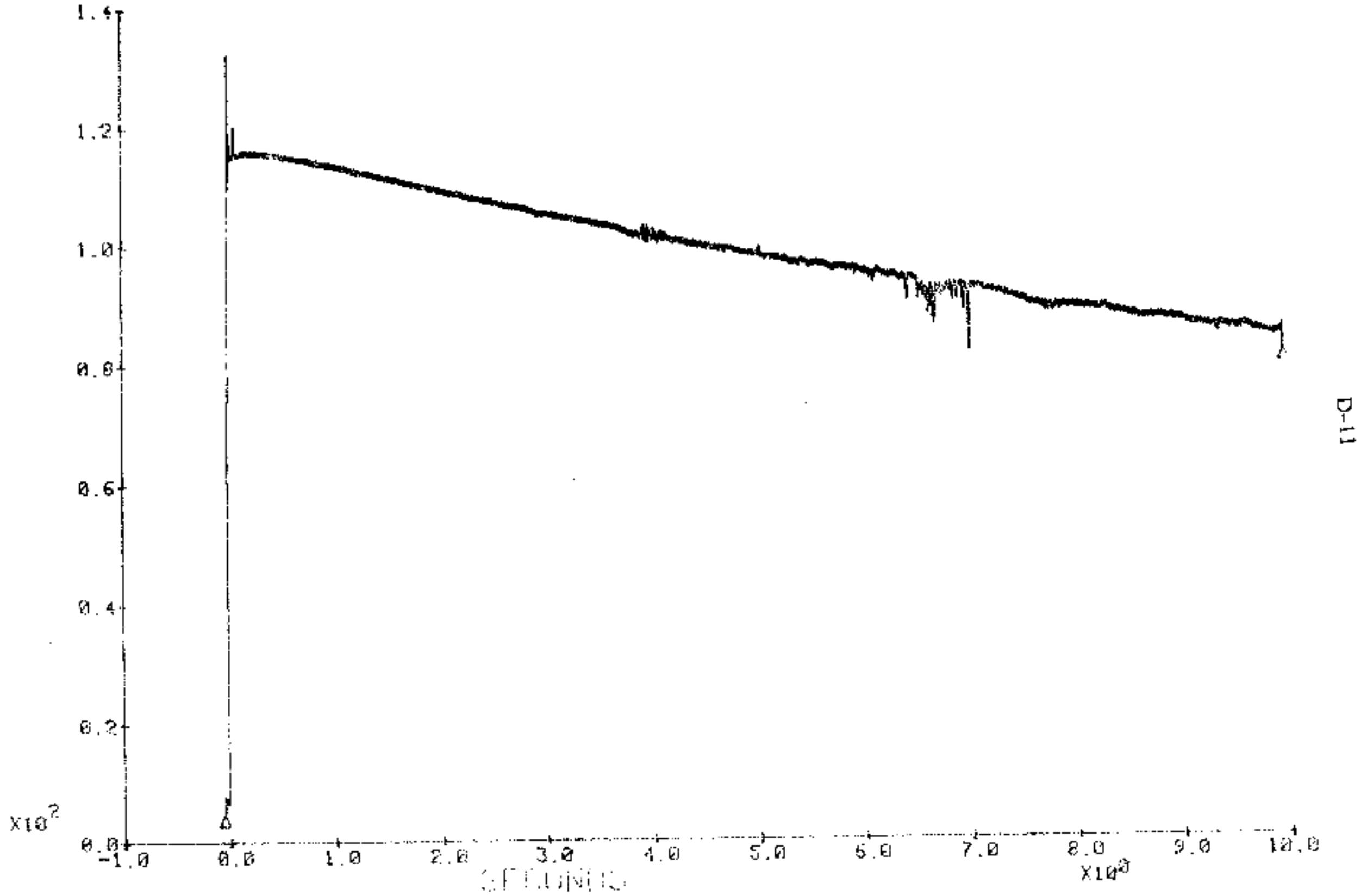

FIGURE D-11. PRESSURE-TIME RECORD FOR TEST D14

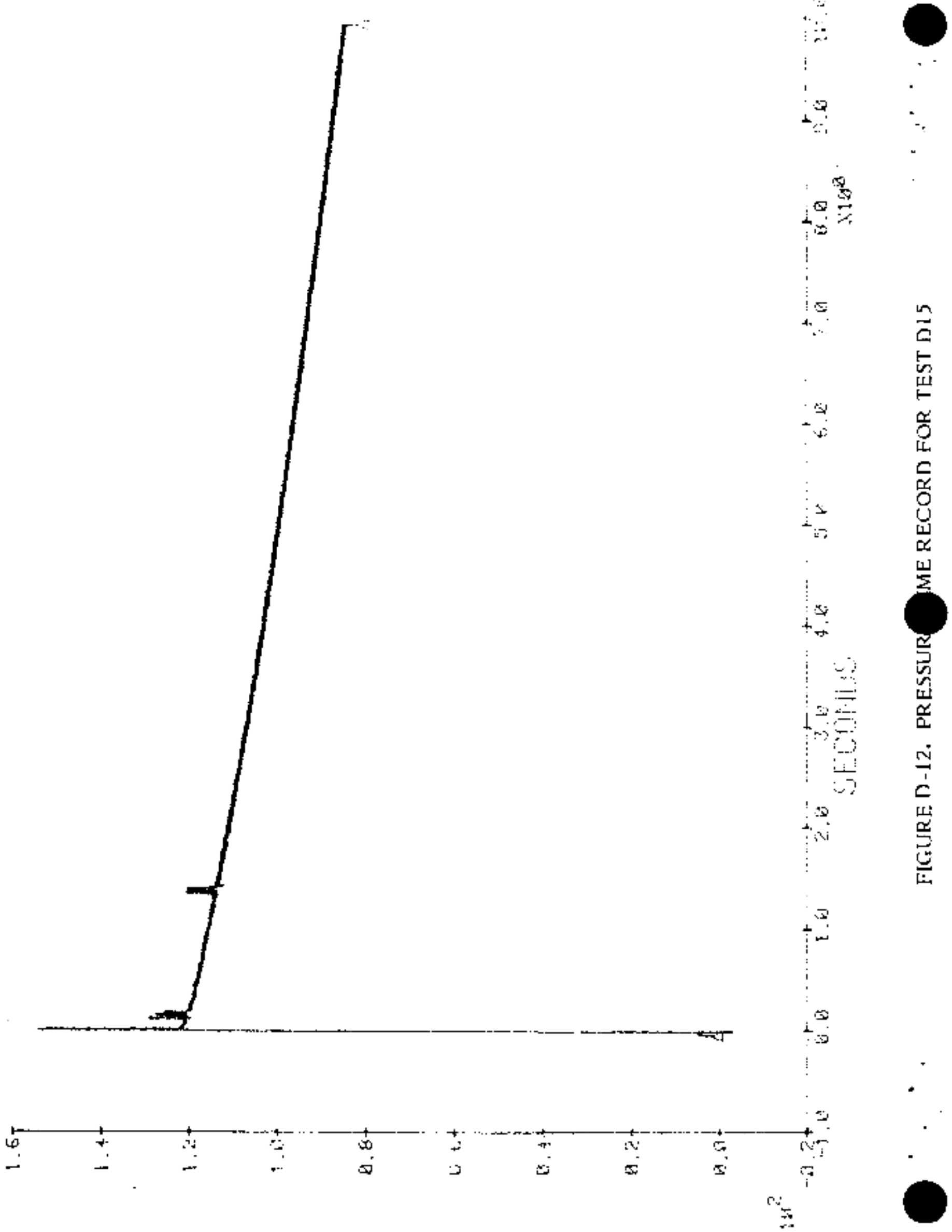

FIGURE D-12. PRESSURE-TIME RECORD FOR TEST D15

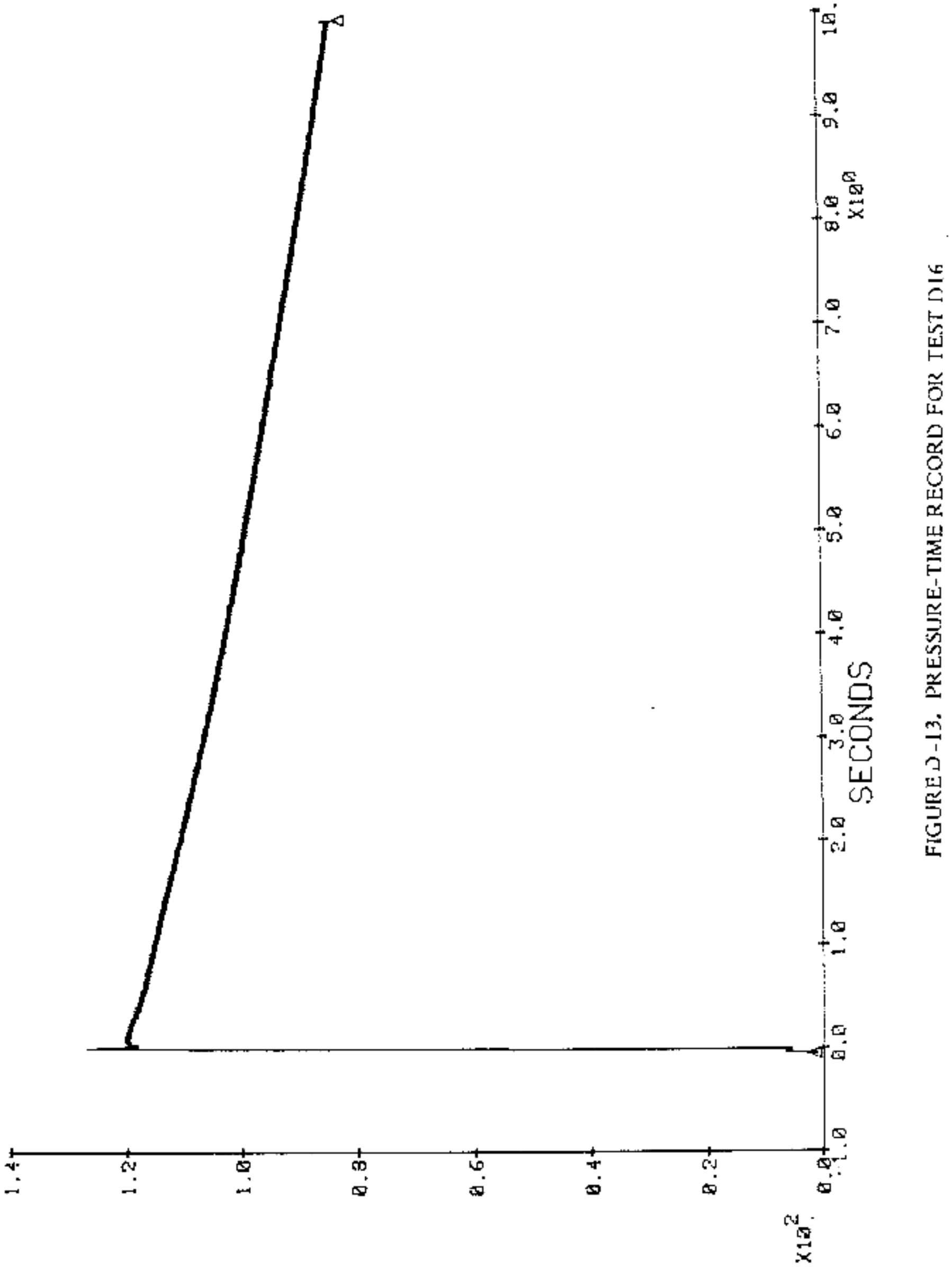

FIGURE D-13. PRESSURE-TIME RECORD FOR TEST D16

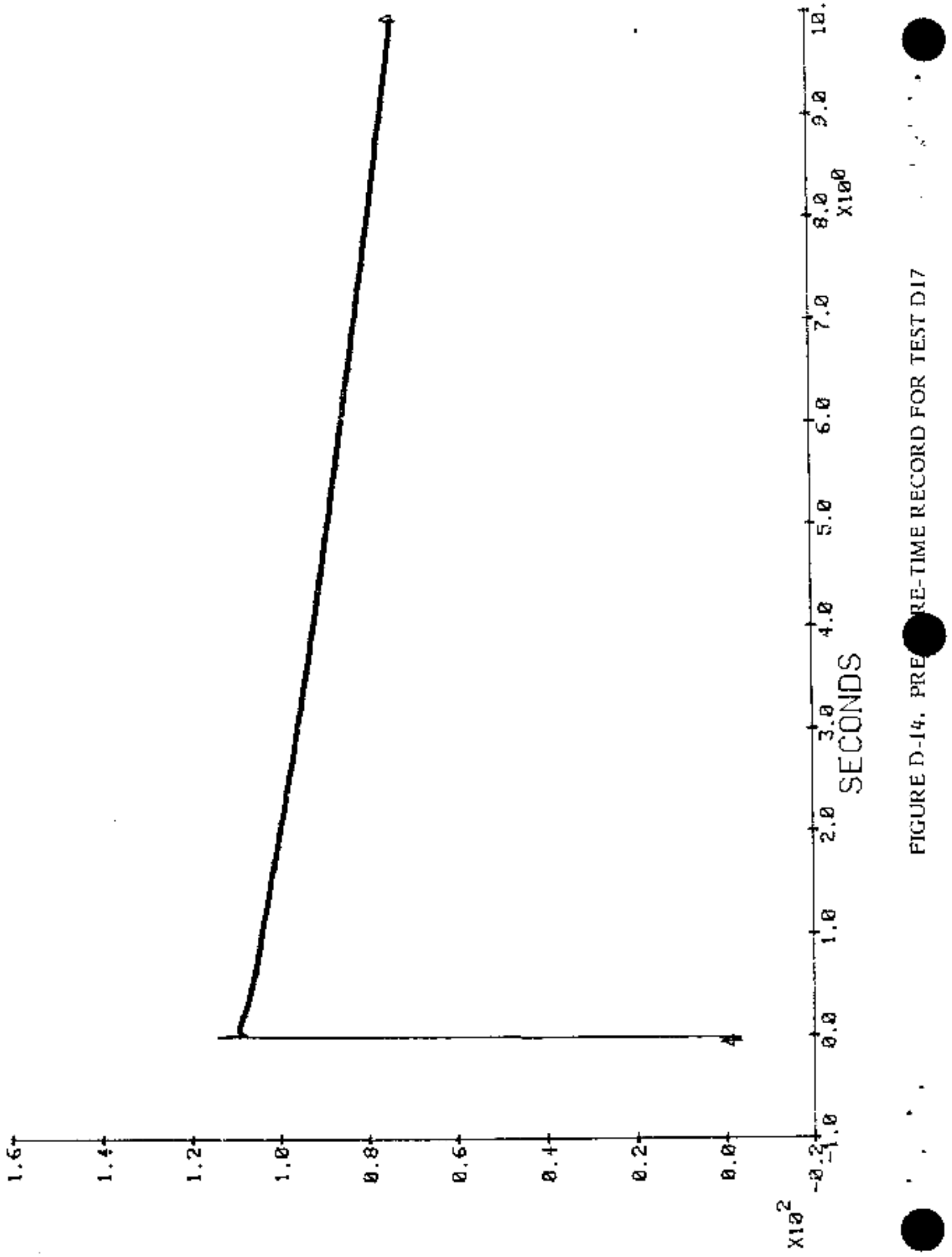

FIGURE D-14. PRESSURE-TIME RECORD FOR TEST D17

DISTRIBUTION LIST

No. of Copies	
12	Defense Documentation Center ATTN: DDC-PCA Alexandria, VA 22314
2	Defense Logistics Studies Information Center US Army Logistics Management Center Fort Lee, VA 23801
2	Chemical Systems Laboratory ARRADCOM ATTN: DRDAR-CLJ-L Aberdeen Proving Ground, MD 21010
2	Commander Pine Bluff Arsenal ATTN: SARPB-CO Pine Bluff, AR 71611
5	Commander US Army Toxic and Hazardous Materials Agency ATTN: DRXTH-IS Aberdeen Proving Ground, MD 21010
2	Commander US Army Toxic and Hazardous Materials Agency ATTN: DRXTH-ES Aberdeen Proving Ground, MD 21010
1	Commander ARRADCOM Procurement Directorate ATTN: DRDAR-PRB-S Aberdeen Proving Ground, MD 21010